Diss. ETH No. 14101

COMPETITIVE SORPTION AND TRANSPORT OF HEAVY METAL CATIONS IN SOILS

A dissertation submitted to the
SWISS FEDERAL INSTITUTE OF TECHNOLOGY ZÜRICH
for the degree of
DOCTOR OF NATURAL SCIENCES

presented by

ANDREAS VOEGELIN
Dipl. Natw., Swiss Federal Institute of Technology Zürich
born June 10, 1971
citizen of Reigoldswil BL

accepted on the recommendation of

Prof. Ruben Kretzschmar, examiner
Prof. Rainer Schulin, co-examiner
Prof. Willem H. van Riemsdijk, co-examiner

2001

To my parents

CONTENTS

ABSTRACT

Heavy metals in contaminated soils may deteriorate soil fertility, may have negative effects on crop yield, or may pollute the ground water. Ultimately, they pose a risk to human health. Risk assessment and remediation planning require knowledge of the processes that control heavy metal behavior. Adsorption and precipitation reactions play a key role in heavy metal mobility and bioavailability, and have been extensively studied in model systems with pure minerals and humic substances. However, the complexity of soils makes direct quantitative application of results from such idealized systems difficult, if not impossible. Therefore, sorption processes must also be studied and quantified in complex soil materials. Models are needed, that can appropriately describe such systems.

The objectives of this work were i) to investigate adsorption and immobilization of heavy metal cations (Cd^{2+}, Zn^{2+}, Ni^{2+}, Co^{2+}) in uncontaminated soil materials, ii) to study the mobilization of heavy metal cations from contaminated soil materials as a result of cation exchange and acidification processes, and, iii) to develop adsorption models that can accurately describe heavy metal adsorption in these systems. Experiments were conducted using batch, flow-through reactor, and packed column techniques.

Major cations compete with heavy metals for adsorption sites. A one-site exchange model was shown to adequately describe the adsorption and transport of Ca^{2+}, Mg^{2+}, and Na^{+} at environmentally relevant concentrations. To model specific metal adsorption on sites with high affinity for heavy metals, a second type of sorption sites was introduced. With this two-site cation exchange-specific adsorption model, Cd adsorption to a silt-loam soil material was accurately described. The experimental data covered a wide range of Cd solution concentrations (10^{-8} to 10^{-2} M), background electrolyte compositions (10^{-4} to 10^{-2} M $CaCl_2$ or $MgCl_2$ and 0.05 to 0.5 M NaCl), and pH levels (4.6 to 6.5). Extended to Zn^{2+} and Ni^{2+} adsorption, the two-site model correctly described coupled Cd-Ca, Cd-Zn-Ca and Cd-Zn-Ni-Ca transport experiments at pH 4.6. Cd^{2+}, Zn^{2+}, and Ni^{2+} exhibited similar and reversible adsorption behavior.

When the same soil material was equilibrated at pH 6.4 with a solution containing Cd^{2+}, Co^{2+}, Ni^{2+}, and Zn^{2+} (~0.1 mM each), a slow sorption process was observed in addition to adsorption. The extent of slow retention decreased in the order Zn > Ni > Co > Cd. Zn K-edge X-ray absorption spectroscopy (XAS) analysis showed that Zn had been incorporated into a Zn-Al layered double hydroxide (LDH). This likely also applies for Ni^{2+} and Co^{2+}. While precipitated metals were not Ca^{2+}-exchangeable, leaching with an acidified solution (pH 3.0) released more than 90% of the precipitated metals.

Contaminated soil materials were leached with 10 mM $CaCl_2$ to assess the reactivity of mobile metal pools. In acidic soils, Zn^{2+} and Cd^{2+} were highly mobile (40 to 70% Ca^{2+} exchangeable Zn and Cd) and showed similar adsorption behavior. In neutral soils, both Zn^{2+} and Cd^{2+} were less mobile, but the effect of soil pH was more pronounced for Zn^{2+}. These findings compare to the results of above column transport experiments at pH 4.6 and pH 6.4. By subsequent leaching with a dilute acidic solution (pH 3.0), the effects of acidification processes on non-exchangeable metal pools were assessed. Effluent patterns reflected the coupling of proton induced metal release, proton buffering reactions, $CaCO_3$ dissolution, advective transport and metal readsorption. By leaching the contaminated soils with Ca^{2+} and subsequently dilute acidic solution (pH 3.0), 65 to 90% of total Zn and Cd were released.

To describe Zn and Cd adsorption in a wide variety of soils, a generalized adsorption model based on scaled exchange coefficients was developed. Generalized model parameters were calibrated on Cd and Zn adsorption data compiled from the literature. The data covered a wide range of Cd or Zn concentrations (10^{-8} to 10^{-2} M) and soil materials (pH 4 -7, organic carbon 2 - 150 g/kg, clay 10 - 550 g/kg). Based on generalized model parameters, bulk soil properties, and mobilizable pools of Cd and Zn determined from a batch extraction, Cd^{2+} and Zn^{2+} effluent concentrations from Ca^{2+} leaching experiments with contaminated soils were adequately predicted. In the most acidic soil, the model gave an excellent prediction of the coupled effluent patterns of Zn^{2+}, Cd^{2+}, Mg^{2+}, and Ca^{2+}.

In conclusion, empirical adsorption models for Cd^{2+} and Zn^{2+} were developed and shown to adequately describe experimental data obtained under a variety of

conditions. Hence, these models may be useful for risk assessment, remediation design, and transport modeling. Analogous model approaches might also apply for cations such as Co^{2+}, Ni^{2+}, and Sr^{2+}. Immobilization of Zn^{2+}, Ni^{2+}, and Co^{2+} in metal bearing precipitates may represent an important sink in contaminated neutral soils. However, the leaching experiments show that in the long term, soil acidification processes might lead to metal remobilization.

ZUSAMMENFASSUNG

Schwermetalle in kontaminierten Böden können die Bodenfruchtbarkeit und den Ernteertrag beeinträchtigen oder das Grundwasser kontaminieren. Schliesslich stellen sie auch eine Gefahr für den Menschen dar. Zur Risikoabschätzung und für die Planung von Sanierungsmassnahmen ist ein Verständnis der Prozesse erforderlich, die das Verhalten von Schwermetallen kontrollieren. Adsorptions- und Ausfällungsreaktionen spielen eine Schlüsselrolle bezüglich der Mobilität und der Bioverfügbarkeit von Schwermetallen, und wurden in Modellsystemen mit reinen Mineralphasen oder Huminstoffen ausführlich untersucht. Eine direkte quantitative Anwendung der Resultate aus solchen idealisierten Systemen wird jedoch durch die Komplexität des Bodens erschwert, wenn nicht verunmöglicht. Daher müssen Sorptionsprozesse auch in komplexen Bodenmaterialien untersucht und quantifiziert werden. Dazu werden Modelle benötigt, die solche Systeme angemessen beschreiben können.

Die Ziele dieser Arbeit waren i) die Adsorption und Immobilisierung von Schwermetallkationen (Cd^{2+}, Zn^{2+}, Ni^{2+}, Co^{2+}) in unkontaminierten Böden und ii) die Mobilisierung von Schwermetallkationen aus kontaminierten Böden infolge von Kationenaustausch- und Versauerungsprozessen zu untersuchen, sowie iii) Adsorptionsmodelle zu entwickeln, die die Adsorption von Metallen in diesen Systemen angemessen beschreiben können. Experimente wurden im Batch, in Durchflussreaktoren, und in gepackten Bodensäulen durchgeführt.

Hauptkationen konkurrieren mit Schwermetallen um Bindungsplätze. Es wurde gezeigt, dass ein einfaches Austauschmodell genügt, um die Adsorption und den Transport von Ca^{2+}, Mg^{2+} und Na^{+} in umweltrelevanten Konzentrationsbereichen beschreiben zu können. Um die spezifische Adsorption von Metallen an Oberflächenplätzen mit einer hohen Affinität für Schwermetalle zu modellieren, wurde ein zweiter Typ von Sorptionsplätzen eingeführt. Mit diesem kombinierten Modell für Kationenaustausch und spezifische Adsorption wurde die Adsorption von Cd an einem siltig-lehmigen Bodenmaterial sehr gut beschrieben. Die experimentellen Daten umfassten einen weiten Bereich an Lösungskonzentrationen von Cd (10^{-8} bis 10^{-2} M), an

Zusammensetzungen des Hintergrundelektrolyten (10^{-4} bis 10^{-2} M $CaCl_2$ oder $MgCl_2$ und 0.05 bis 0.5 M NaCl) und an pH Werten (4.6 bis 6.5). Erweitert um die Adsorption von Zn^{2+} und Ni^{2+} konnte dieses Modell auch den gekoppelten Cd-Ca-, Cd-Zn-Ca- und Cd-Zn-Ni-Ca-Transport bei pH 4.6 beschreiben. Cd^{2+}, Zn^{2+} und Ni^{2+} zeigten ein ähnliches und reversibles Adsorptionsverhalten.

Wurde das gleiche Bodenmaterial bei pH 6.4 mit einer Cd^{2+}, Co^{2+}, Ni^{2+}, und Zn^{2+} haltigen (je ~0.1 mM) Lösung gespült, dann konnte zusätzlich zur Adsorption auch ein langsamer Sorptionsprozess beobachtet werden. Das Ausmass dieser langsamen Retention nahm in Reihenfolge Zn > Ni > Co > Cd ab. Die Analyse von Röntgenabsorptionsspektren zeigte, dass Zn in ein Zn-Al 2-Schicht Hydroxid (LDH) eingebunden worden war. Dies trifft wahrscheinlich auch für Ni^{2+} und Co^{2+} zu. Während die ausgefällten Metalle nicht Ca^{2+}-austauschbar waren, führte das Spülen mit einer angesäuerten Lösung (pH 3.0) zu einer Freisetzung von mehr als 90% der ausgefällten Metalle.

Kontaminierte Bodenmaterialien wurden mit 10 mM $CaCl_2$ gespült, um die Reaktivität des mobilen Schwermetallanteils zu bestimmen. In sauren Böden waren Zn^{2+} und Cd^{2+} sehr mobil (40 bis 70% Ca^{2+} austauschbares Zn und Cd) und zeigten ein ähnliches Adsorptionsverhalten. In neutralen Böden waren sowohl Zn^{2+} als auch Cd^{2+} weniger mobil, allerdings war der Einfluss des pH Wertes im Falle von Zn^{2+} wesentlich stärker ausgeprägt. Dieses Verhalten stimmt mit den Resultaten der obigen Transportexperimente bei pH 4.6 und pH 6.4 überein. Anschliessend wurden die Bodenmaterialien mit einer angesäuerten Lösung (pH 3.0) gespült, um den Einfluss von Bodenversaurungsprozessen auf den nicht-kationenaustauschbaren Anteil der Schwermetalle zu untersuchen. Die Konzentrationsmuster im Säulenausfluss widerspiegelten die miteinander verbundenen Prozesse der protoneninduzierten Schwermetallfreisetzung, der Protonenpufferung, der $CaCO_3$ Auflösung, des advektiven Transportes und der Readsorption der Metalle. Durch Spülen der kontaminierten Bodenmaterialien mit Ca^{2+} und anschliessend mit angesäuerter Lösung (pH 3.0) wurden 65 bis 90% der Totalgehalte an Zn und Cd freigesetzt.

Um die Adsorption von Zn und Cd an einer Vielzahl veschiedener Böden beschreiben zu können wurde ein verallgemeinertes Adsorptionsmodell basierend auf

skalierten Austauschkoeffizienten entwickelt. Modellparameter wurden an Adsorptionsdaten für Cd und Zn kalibriert, die aus der Literatur zusammengetragen wurden. Diese Daten umfassten einen weiten Bereich an Lösungskonzentrationen von Cd oder Zn (10^{-8} bis 10^{-2} M) und an Bodenzusammensetzungen (pH 4 -7, organischer Kohlenstoff 2 - 150 g/kg, Tongehalt 10 - 550 g/kg). Basierend auf der Bodenzusammensetzung und auf mobilen Gehalten an Cd und Zn, die mittels eines Batchexktraktes ermittelt wurden, konnte das Modell die Säulenausflusskonzentrationen von Cd^{2+} und Zn^{2+} angemessen voraussagen, die in den Mobilisierungversuchen mit 10 mM Ca^{2+} beobachtet worden waren. Im sauersten Boden wurde eine hervorragende Voraussage der gekoppelten Konzentrationsmuster von Zn^{2+}, Cd^{2+}, Mg^{2+} und Ca^{2+} erzielt.

In dieser Arbeit wurden empirische Adsorptionsmodelle für Cd^{2+} und Zn^{2+} entwickelt, und es wurde gezeigt, dass diese Modelle experimentelle Daten, die unter verschiedensten Bedingungen ermittelt wurden, angemessen beschreiben können. Diese Modelle könnten daher für Risikoabschätzungen, für die Planung von Sanierungsmassnahmen und für die Transportmodellierung von Nutzen sein. Analoge Modellansätze könnten wahrscheinlich auch für Kationen wie Co^{2+}, Ni^{2+} und Sr^{2+} angewendet werden. Die Immobilisierung von Zn^{2+}, Ni^{2+} und Co^{2+} in metallhaltigen Ausfällungen könnte eine wichtige Senke in kontaminierten neutralen Böden darstellen. Wie allerdings die Säulenexperimente gezeigt haben, könnten längerfristig Versauerungsprozesse diese Schwermetalle wieder freisetzen.

INTRODUCTION

Soil pollution with heavy metals is caused by human activities such as metal mining and smelting, fuel combustion, industrial and energy production, waste disposal, military activities, or agricultural application of pesticides, fertilizers, and sewage sludge. Some heavy metals, e.g. Cu, Zn, and Co, are essential for organisms and may be deficient in some soils. However, at elevated concentrations most heavy metals are toxic. Zn for instance can be phytotoxic and may severely affect soil fertility and crop yield. Cd is toxic even at trace concentrations, and following uptake by plants, may be a threat to animal and human health (Alloway, 1995; McGrath, 1994; Martin and Bullock, 1994). Soils act as filters and retain heavy metal inputs. Over time, however, heavy metals may be leached through the soil profile. Accumulated heavy metals in soils hence represent a potential risk for groundwater and drinking water contamination. Changes in soil chemistry, e.g. due to acid deposition or reforestation of arable land, might also cause an increase in metal bioavailability and mobility. The prediction of metal fate, the risk assessment of heavy metal contaminated soils and the evaluation of remediation strategies requires knowledge about the relevant metal retention processes in a specific soil material (Bolt and Van Riemsdijk, 1987).

A large body of literature exists on metal retention in soils. Over wide ranges of soil and solution composition, adsorption processes on soil surfaces have a dominant influence on metal solubility (McBride, 1989; Hayes and Traina, 1998). Most important sorbents for heavy metals in soils are Fe, Mn, and Al oxide and hydroxide minerals, clay minerals, and soil organic matter. At acidic conditions, non-specific reversible cation exchange reactions may significantly contribute to the adsorption of heavy metal cations such as Zn^{2+}, Ni^{2+}, Co^{2+}, and Cd^{2+}, and major cations effectively compete with heavy metal cations for exchange sites. With increasing pH, heavy metal cation adsorption strongly increases and becomes more specific. Surfaces of Fe, Mn, and Al (hydr)oxides, variable charge sites on clay edges, and high-affinity sorption sites on soil organic matter strongly retain heavy metals. Specific adsorption may go along with precipitation or coprecipitation reactions. Kinetic adsorption, (co)precipitation, and diffusion of

metals into soil particles may lead to slowly decreasing heavy metal availability over time (McBride, 1999; Sparks, 1998). Metal adsorption in soils is often described by empirical isotherm equations such as the Freundlich isotherm. Isotherm parameters can be related to soil and solution properties. However, such relations are purely empirical and restricted to the systems derived from (Jenne, 1998). Metal retention studies on soil materials yield only limited information on fundamental retention processes such as metal adsorption behavior on different sorbent phases or surface metal precipitation, because the process of interest may be combined with or even overshadowed by numerous other simultaneous processes. To elucidate fundamental aspects of metal sorption, studies are therefore conducted in simplified model systems such as pure oxide or clay suspensions.

Metal cation adsorption on model sorbents such as different clay minerals, Fe, Al, and Mn oxides, and soil humic and fulvic acids is well studied. Numerous equilibrium models were developed to describe metal adsorption to these phases over wide conditions in solution composition. Model assumptions can be based on spectroscopic results on the effective type of metal binding (Hayes and Traina, 1998). Spectroscopy is also used to study the slow formation of heavy metal bearing precipitates upon metal adsorption on inorganic soil compounds at neutral to alkaline pH (Sparks, 1998). Besides adsorption/desorption and precipitation reactions, also the diffusion of heavy metals into microporous oxide phases may be an important process in metal retention (Axe and Anderson, 1998).

Detailed knowledge gained from model systems helps in qualitatively rationalizing observations from studies on metal retention in soils. However, quantitative predictions on metal behavior in real soil systems based on these findings are connected with considerable uncertainty, due to the inherent heterogeneity of natural materials and the complexity of the solid matrix consisting of a multitude of intimately associated sorbent phases (Zachara and Westall, 1998). Uncertainty further increases if kinetic processes, and hence time, are to be considered (Sparks, 1998). Description of experimental metal adsorption data in soil materials based on such models may be questionable, as it is often impossible to properly define all necessary model input parameters. Therefore the complexity of real soil systems still requires the application of

empirical model approaches for accurate quantitative purposes such as metal transport modeling (Zachara and Westall, 1998; Sparks, 1998; McBride, 1999). Such models should account for the central aspects of metal retention in a given system, e.g. competition among heavy metal and major cations for sorption sites (Bolt and Van Riemsdijk, 1987). However, they should also be simple to adjust to a specific soil material, based on the information available.

Accurate determination of metal behavior in a specific system can only be based on experiments with the respective soil material. In general, metal adsorption to uncontaminated soils or desorption / extraction of metals from contaminated soils is studied in batch experiments. Packed soil columns represent a further technique to study metal behavior in soil materials (Selim and Amacher, 1996). The column setup is often used to test adsorption models obtained from batch adsorption or extraction data (Kretzschmar and Voegelin, 2001). Column leaching studies with contaminated materials may be carried out to assess metal reactivity or to test potential remediation strategies. Packing homogeneous columns with high chromatographic resolution, effects arising from heterogeneous flow paths can be minimized. The resulting elution curves can be interpreted with respect to the underlying chemical processes. While batch and column techniques allow to assess heavy metal reactivity in contaminated soils, direct evidence on the types of metal binding can only be obtained by spectroscopic techniques (Hayes and Traina, 1998; Manceau *et al.*, 2000).

In this work, heavy metal sorption, mobilization, and transport processes in soil materials were investigated using the flow-through reactor and packed column technique. The overall objectives were i) to study the adsorption and immobilization of heavy metal cations (Cd^{2+}, Zn^{2+}, Ni^{2+}, Co^{2+}) in uncontaminated soil materials, ii) to study the mobilization of heavy metal cations from contaminated soil materials as a result of cation exchange and acidification processes, and, iii) to develop adsorption models that can accurately describe heavy metal adsorption in these systems.

Major cations (Ca^{2+}, Mg^{2+}, K^{+}, Na^{+}) compete with heavy metal cations for adsorption sites. The first chapter therefore deals with the modeling of the adsorption and transport of Ca^{2+}, Mg^{2+}, and Na^{+} in a silt-loam soil material. Various exchange

models are compared in their performance in describing the experimental adsorption and transport data.

In the second chapter, column Cd^{2+} and Ni^{2+} transport experiments taken from the literature are reanalyzed and modeled with an equilibrium exchange model. The exchange model approach and the Freundlich isotherm approach, which is widely used to describe heavy metal adsorption to soil materials, are compared in their ability to describe the transport experiments.

A two-site model accounting for non-specific cation exchange and specific adsorption reactions of Cd is presented in the third chapter. The model is applied to an extensive dataset on Cd adsorption to an acidic silt-loam soil material. Extended for Zn and Ni, the performance of the model with respect to the description of transport experiments involving Cd^{2+}, Zn^{2+}, Ni^{2+}, and Ca^{2+} is assessed.

The formation of metal bearing precipitates might present an important sink for heavy metals in contaminated soils. Therefore, the fourth chapter is concerned with slow sorption processes of Cd, Co, Ni, and Zn in a silt-loam soil material. A combined approach based on column experiments and X-ray absorption spectroscopy is used to elucidate the extent of slow sorption processes and to study the underlying binding mechanism.

Risk assessment and remediation design for contaminated soils requires information on the mobility and reactivity of the heavy metals. In the fifth chapter, the mobilization potential of heavy metals (Cd, Zn, Pb, Cu) from four contaminated soils of different composition and contamination history as a result of cation exchange and acidification processes is assessed using column leaching experiments.

In the sixth chapter, a generalized model for Cd and Zn adsorption in soils is developed. The model is calibrated on a compilation of Cd and Zn adsorption data taken from the literature. The model is tested on Cd and Zn adsorption and on Cd transport data. To assess the performance of the model in contaminated soils, predictions of the Ca induced mobilization of Cd and Zn from contaminated soil materials are compared with the respective experimental results.

References

Alloway, B.J., ed., *Heavy Metals in Soils.* Chapman & Hall, London, 1995.

Axe, L., Anderson, P.R., *Intraparticle diffusion of metal contaminants in amorphous oxide minerals.* In: *Adsorption of Metals by Geomedia.* Jenne, E.A., ed., Academic Press, 427-443, **1998.**

Bolt, G.H., Van Riemsdijk, W.H., *Surface chemical processes in soil.* In: *Aquatic Surface Chemistry.* Stumm, W., ed., John Wiley & Sons, New York, 127-164, **1987.**

Hayes, K.F., Traina, S.J., *Metal ion speciation and its significance in ecosystem health.* In: *Soil Chemistry and Ecosystem Health.* Huang, P.M., ed., Soil Science Society of America, Inc., Madison, 45-84, **1998.**

Jenne, E.A., *Adsorption of metals by geomedia: data analysis, modeling, controlling factors, and related issues.* In: *Adsorption of Metals by Geomedia.* Jenne, E.A., ed., Academic Press, 427-443, **1998.**

Kretzschmar, R., Voegelin, A., *Modeling competitive sorption and release of heavy metals in soils.* In: *Heavy Metal Release in Soils.* Selim, H.M.,Sparks, D.L., eds., CRC Press, Boca Raton, (in press), **2001.**

Manceau, A., Lanson, B., Schlegel, M.L., Harge, J.C., Musso, M., Eybert-Berard, L., Hazemann, J.-L., Chateigner, D., Lamble, G.M., *Quantitative Zn speciation in smelter-contaminated soils by EXAFS spectroscopy.* American Journal of Science 300, 289-343, **2000**.

Martin, M.H., Bullock, R.J., *The impact and fate of heavy metals in an oak woodland ecosystem.* In: *Toxic Metal in Soil - Plant Systems.* Ross, S.M., ed., John Wiley & Sons Ltd, Chichester, 327-365, **1994.**

McBride, M.B., *Reactions Controlling Heavy Metal Solubility in Soils.* Advances in Soil Science 10, 1-56, **1989**.

McBride, M.B., *Chemisorption and precipitation reactions.* In: *Handbook of Soil Science.* Sumner, M.E., ed., CRC Press, Boca Raton, B/265-B/302, **1999.**

McGrath, S.P., *Effects of heavy metals from sewage sludge on soil microbes in agricultural ecosystems.* In: *Toxic Metal in Soil - Plant Systems.* Ross, S.M., ed., John Wiley & Sons Ltd, Chichester, 247-274, **1994.**

Selim, H.M., Amacher, M.C., *Reactivity and Transport of Heavy Metals in Soils.* CRC Press, Boca Raton, **1996**.

Sparks, D.L., *Kinetics and mechanisms of chemical reactions at the soil mineral/water interface*. In: *Soil Physical Chemistry.* Sparks, D.L., ed., CRC Press, Boca Raton, 135-191, **1998.**

Zachara, J.M., Westall, J.C., *Chemical modeling of ion adsorption in soils*. In: *Soil Physical Chemistry.* Sparks, D.L., ed., CRC Press, Boca Raton, 47-95, **1998.**

CHAPTER 1

MULTICOMPONENT TRANSPORT OF MAJOR CATIONS PREDICTED FROM BINARY ADSORPTION EXPERIMENTS

Abstract

Accurate modeling of multicomponent sorption and transport of major cations in subsurface porous media is a prerequisite for predicting complex environmental processes, such as the movement of trace metals in soils and aquifers. In this study, various cation exchange models were compared in their ability to predict ternary Ca-Mg-Na transport in an acidic soil from binary Ca, Mg, and Na adsorption data. A flow-through reactor technique was used to measure binary adsorption isotherms of Ca, Mg, and Na over wide concentration ranges of the adsorptive and the respective background cations. High-resolution transport experiments were conducted in water-saturated chromatographic glass columns. Three sorption models based on cation exchange equations were compared: a 1-site Gaines-Thomas (1-GT), a 1-site Rothmund-Kornfeld (1-RK), and a 3-site Gaines-Thomas (3-GT) model. Although the fit of adsorption data was clearly improved from the 1-GT to the 1-RK to the 3-GT model, transport predictions were overall not improved compared to the 1-GT model. While predictions by the 1-GT and the 3-GT model were virtually identical, predictions by the 1-RK model were partly improved and partly deteriorated. The most simple 1-GT model therefore seems to be adequate for predicting multicomponent transport phenomena involving major cations, however, multi-site models may be useful for predicting transport of trace metals in the presence of several major cations. Regardless of the model used, accurate determination of the cation exchange capacity at the pH conditions of interest is extremely critical in cation transport modeling.

Voegelin, A., Vulava, V. M., Kuhnen, F., Kretzschmar, R., *Multicomponent transport of major cations predicted from binary adsorption experiments.* Journal of Contaminant Hydrology 46, 319-338, **2000**.

1.1 Introduction

Understanding the reactive transport behavior of inorganic chemical species becomes necessary when dealing with environmental problems such as fresh- or seawater intrusions into aquifers, landfill leaching plumes, or transport of heavy metals in soils and aquifers. Predicting the transport of reactive solutes in porous media generally requires both an accurate description of sorption and an appropriate transport model (Jury and Flühler, 1992). In the case of a single component adsorbing to the soil matrix, retention can be estimated from a simple batch adsorption experiment. However, in the case of a multicomponent system with several interacting species, complex coupled breakthrough patterns can arise. Such multicomponent transport phenomena can only be described with models accounting for the underlying chemical reactions between the soil matrix and the interacting solute species. For practical reasons, it is infeasible to experimentally determine the partition behavior of all species in a multicomponent system at all possible solution compositions. Therefore, the complex multicomponent system must be predicted from a limited number of simplified adsorption experiments, e.g., binary adsorption experiments with only two interacting species present at a time.

One example for multicomponent behavior is the sorption and transport of major cations (e.g., Ca^{2+}, Mg^{2+}, Na^{+}, K^{+}) in natural subsurface environments. The classical way to treat the competitive sorption of major cations is the definition of cation exchange reactions with constant exchange stoichiometry based on charge equivalents, e.g., the Gaines-Thomas convention (McBride, 1994; Sparks, 1995). Complex breakthrough patterns are reported for laboratory column and field scale experiments (Cernik *et al.*, 1996; Appelo *et al.*, 1990; Beekman and Appelo, 1990; Valocchi *et al.*, 1981; Dance and Reardon, 1983; Bjerg and Christensen, 1993). Respective cation exchange coefficients were determined from binary column (Cernik *et al.*, 1996; Beekman and Appelo, 1990) or binary batch experiments (Bjerg and Christensen, 1993), from multicomponent batch experiments (Valocchi *et al.*, 1981), or from the composition of soil solution and exchanger phase in the field system (Dance and Reardon, 1983). However, problems can arise when using such exchange coefficients to predict cation behavior over a wide range in solution composition. Exchange coefficients may vary with solution and exchanger phase composition due to

dependence on pH, ionic strength, sorbent heterogeneity, specific adsorption, or variation of the activity of the adsorbed species (McBride, 1994; Sparks, 1995). One possible approach to handle the variability of exchange coefficients would be the use of a more flexible exchange convention such as the Rothmund-Kornfeld formulation of the Gaines-Thomas exchange equation (Bond, 1995; Bond and Verburg, 1997) or the introduction of concentration dependent acitivity coefficients for adsorbed species. An alternative approach is the introduction of additional sorption sites with different exchange coefficients, thereby accounting for chemical heterogeneity and specific adsorption in an empirical fashion (Cernik *et al.*, 1996). For a binary Ca-Na soil system, this multi-site approach was recently shown to improve the fits of adsorption data spanning over wide ranges in solution composition (Vulava *et al.*, 2000).

In the present study, a large set of binary adsorption data including all possible combinations within the ternary Ca-Mg-Na-soil system was measured using a flow-through reactor technique. A 1-site Gaines-Thomas (1-GT), a 1-site Rothmund-Kornfeld (1-RK), and a 3-site Gaines-Thomas (3-GT) model were compared in their ability to describe the entire dataset. All three models were then coupled to a mixing-cell transport code and ternary cation transport in packed soil columns was predicted. Predictions were compared with results from high-resolution column transport experiments.

1.2 Materials and Methods

1.2.1 Soil Material

The soil material used in the experiments was collected from the B-horizon (15-25 cm sampling depth) of an acidic soil in northern Switzerland (Riedhof soil, aquic dystric Eutrochrept, silt loam texture). The soil material was gently broken into small aggregates, dried at 40°C, and sieved to various fractions smaller than 2 mm. For all adsorption and column experiments, the sieve fraction 63-400 μm was used. This fraction consisted of 37% sand, 47% silt, and 16% clay. It contained 6 g/kg organic carbon, and had pH 4.1 when suspended in deionized water. Exchangeable cations were determined from an unbuffered 0.1 M $BaCl_2$ extraction (Hendershot and Duquette, 1986). A potassium chloride method (Thomas, 1982) was used to measure the exchangeable acidity. From these results, a cation exchange capacity (CEC) of 0.060

$mol_c/kg \pm 0.002$ mol_c/kg (base saturation ~20%) was calculated. From a 0.01 M $Ca(NO_3)_2$-$Mg(NO_3)_2$ column exchange experiment at pH 4.6, the same CEC was obtained.

1.2.2 Binary Cation Adsorption Experiments

Competitive adsorption experiments were conducted in binary cation systems (Ca/Na; Mg/Na; Mg/Ca) at pH near 4.6. The solution concentrations of the respective *adsorptive cation* ranged from 10^{-7} to 10^{-1} M, while the concentrations of the respective *background cation* ranged from 0.02 to 0.5 M for Na and from 10^{-4} to 10^{-2} M for Ca and Mg. The experiments were carried out using a flow-through reactor technique (Grolimund *et al.*, 1995). Briefly, pre-weighed soil samples were placed on cellulose-acetate membrane filters (0.45 µm, Schleicher & Schuell) in flow-through reactor cells consisting of slightly modified air monitoring cassettes. All cells were connected to a 24-channel peristaltic pump and the soil samples were extensively pre-conditioned by leaching with 500 mL/g soil of 0.5 M $CaCl_2$, 0.5 M $MgCl_2$ or 1.0 M NaCl at a rate of 3 mL/min. The pH value of all influent solutions was adjusted to pH 4.6 by addition of HCl. Following this first pre-washing step, during which the soil was completely saturated with the respective background cation, the influent electrolyte concentration was reduced to the desired background cation concentration. After equilibrium was reached, the reactors were drained and weighed to determine the amounts of entrapped electrolyte solution. The reactors were then refilled with a solution containing the same background electrolyte plus a known amount of the desired adsorptive cation (Ca, Mg, or Na). In this adsorption step, the cell outflow was connected back to the inflow (closed-loop arrangement) and the solution was re-circulated through the reactor cells for 24 h. After equilibration, cation concentrations were measured in initial and final solutions by atomic absorption (Varian SpectrAA 400 Flame-AAS) and emission (Varian Liberty 200 ICP-AES) spectroscopy. The adsorbed amounts were calculated from differences between initial and final solution concentrations and soil weights. In order to be able to accurately measure adsorption isotherms over several orders of magnitude in adsorptive cation concentration, the soil-to-solution ratio in each reactor had to be varied from 50 to 1000 g/L. Thereby, distribution fractions of the adsorptive

cation between 0.2 and 0.8 were obtained, allowing reliable estimates of the adsorbed amounts as a function of adsorptive cation in solution. Note, that varying the ratio between the soil in the reactor and the circulating solution does not alter the soil-to-solution ratio in the reactor itself, where the cation exchange reactions take place. Changing the soil-to-solution ratio in the flow-though reactor technique therefore should not affect the experimental results.

1.2.3 Ternary Cation Transport Experiments

Transport experiments were conducted in ternary cation systems (Ca/Mg/Na) using a packed soil column technique. Chromatographic glass columns (Omni) were uniformly packed with the dry soil material and flushed for several minutes with CO_2 gas to displace the air from the pore space. The columns were then connected to a HPLC pump (Jasco PU-980) and pre-conditioned by leaching with several hundred pore volumes of 0.5 M $CaCl_2$ solution adjusted to pH 4.6. Solutions were first passed through a degasser (Gastorr GT-103) and then through the soil columns in the upward direction. Due to rapid dissolution of CO_2 gas, complete water saturation was achieved within a few pore volumes. Two different column dimensions were used for transport experiments. The first column (C1) was 48.1 cm long and had 0.3 cm inner diameter, while the second column (C2) was 19.1 cm long and had 0.66 cm inner diameter. These dimensions were chosen for two reasons: (i) to maximize the column Péclet number resulting in high precision, high resolution breakthrough data with well-resolved cation transport fronts, (ii) column diameter was varied to increase the range in pore water velocities that could be achieved with the HPLC pump. To characterize the soil columns, a short nitrate pulse (0.1 mL) was injected and the resulting breakthrough peaks were monitored on-line using an UV-VIS detector. Pore volume, dispersivity, and column Péclet number were determined numerically from the flow rate and the first or second moments of the nitrate breakthrough curves. The column parameters are listed in Table 1.1.

Table 1.1: Properties of the two soil columns C1 and C2 used for ternary cation transport experiments.

Column	C1	C2
Diameter (cm)	0.3	0.66
Length (cm)	48.1	19.1
Volume (mL)	3.46	6.53
Mass of Soil (g)	4.10	7.47
Pore Volume (mL)	2.11	3.87
Bulk Density (g/mL)	1.94	1.93
Porosity (%)	61	59
Dispersivity (mm)	~1	~1
Péclet number	~450	~250

For cation transport experiments, sequences of electrolyte solutions of varying composition were passed through the soil columns and the effluent cation concentrations were monitored. The effluents were sampled in regular intervals using an automated fraction collector. Concentrations of Ca, Mg, and Na in the effluents were measured by atomic absorption spectrometry (Varian SpectrAA 400 Flame-AAS).

Six different transport experiments were conducted, for which the sequences of feed solutions, column dimensions, and flow velocity are given in Table 1.2. In Experiments 1 and 2, the same sequence of feed solutions was used, but the column dimensions and flow velocity were different. The feed solution was switched three times after steady state had been reached. In Experiment 3, the Na concentration in the feed solutions was increased about 20-fold compared to Experiments 1 and 2, resulting in higher Na saturation of the soil material. In Experiments 4 and 5, the feed solution was switched before steady state had been reached. To test for possible kinetic effects on cation breakthrough, Experiment 5 was run at about 30 times lower pore water velocity compared to Experiment 4. In Experiment 6, an exchange between seawater and freshwater was mimicked with respect to typical concentrations of Ca, Mg, and Na in sea- and freshwaters.

Table 1.2: Sequences of feed solutions and pore water velocities applied in the ternary cation transport experiments (Experiments 1 to 6).

Experiment Nr. column pore water velocity	Influent (pore volumes)	$CaCl_2$ (mM)	$MgCl_2$ (mM)	NaCl (mM)
Experiment 1	<0	5.2	4.55	4.65
column C1	0	5.3	—	—
v = 5.6 cm/min	20	—	2.4	4.6
	65	5.2	4.55	4.65
Experiment 2	<0	5.2	4.55	4.65
column C2	0	5.3	—	—
v = 2.2 cm/min	20	—	2.4	4.6
	65	5.2	4.55	4.65
Experiment 3	<0	5.4	5.0	95
column C1	0	5.0	—	—
v = 5.6 cm/min	20	—	2.6	95
	65	5.7	5.4	95
Experiment 4	<0	5.3	5.1	4.7
column C1	0	5.0	—	—
v = 5.6 cm/min	4.6	—	2.5	4.7
	22.8	5.3	5.1	4.7
Experiment 5	<0	5.2	5.4	4.7
column C2	0	5.0	—	—
v = 0.2 cm/min	4.4	—	2.5	4.7
	20.8	5.2	5.4	4.7
Experiment 6	<0	11.5	49	470
column C2	0	3.1	0.62	1.7
v = 4.9 cm/min	20	11.5	49	470

1.2.4 Modeling Cation Adsorption and Transport

The competitive sorption of major cations in soils is usually described by cation exchange reactions (McBride, 1994; Sparks, 1995). Several different conventions have been proposed in the past to formulate mass action laws for cation exchange. In this study, we use the well-known cation exchange convention of Gaines and Thomas (Gaines and Thomas, 1953). Exchange reactions in the ternary $Ca^{2+}/Mg^{2+}/Na^{+}$ system are written as

$$CaX_2 + 2Na^{+} \rightleftharpoons 2NaX + Ca^{2+} \quad (1.1)$$

$$CaX_2 + Mg^{2+} \rightleftharpoons MgX_2 + Ca^{2+} \quad (1.2)$$

where X denotes an exchange site with charge -1. The activities of adsorbed species are assumed to correspond to the charge equivalent fractions y_M

$$y_M = z_M q_M / CEC \quad (1.3)$$

where CEC is the cation exchange capacity of the adsorbent (in mol_c/kg), z_M is the charge of cation M, and q_M is the amount of cation M adsorbed (in mol/kg). For the ternary $Ca^{2+}/Mg^{2+}/Na^{+}$ system, CEC can be expressed as

$$CEC = 2q_{Ca} + 2q_{Mg} + q_{Na} \quad (1.4)$$

Having defined the activities of adsorbed species as the equivalent fractions y_M, the mass action laws corresponding to Equations 1.1 and 1.2 for the Gaines-Thomas convention can be written as

$$K_{NaCa}^{GT} = \frac{y_{Na}^2 (a_{Ca}/c_0)}{y_{Ca} (a_{Na}/c_0)^2} \quad (1.5)$$

$$K_{MgCa}^{GT} = \frac{y_{Mg}(a_{Ca}/c_0)}{y_{Ca}(a_{Mg}/c_0)} \tag{1.6}$$

where K^{GT} are the Gaines-Thomas exchange coefficients, a_M are the activities of the free metal ions in solution, and c_0 equals 1 mol/L.

Equations 1.5 and 1.6 always yield a slope of 1 in a log-log plot of the amount adsorbed versus activity in solution (Vulava *et al.*, 2000). However, experimental slopes are often close to but not equal to unity. In the Rothmund-Kornfeld formulation (Rothmund and Kornfeld, 1918; Sposito, 1981; Bond, 1995) of the Gaines-Thomas exchange convention, the activity of the exchanger species is assumed to be equal to the charge equivalent fraction raised to the power n^{-1}. This formulation offers the flexibility to adjust the slope and vertical displacement of the adsorption isotherms. While some researchers report different exponents for different binary systems (Bond and Verburg, 1997), others applied individual exponents to each cation in their system (Carlson and Buchanan, 1973). In this study, the most simple approach with a unique exponent n^{-1} is used. Raising the charge equivalent fractions to n^{-1} is equivalent to raising the ratio of the activities of the species in solution to the power n:

$$K_{NaCa}^{RK} = \frac{y_{Na}^2}{y_{Ca}}\left(\frac{(a_{Ca}/c_0)}{(a_{Na}/c_0)^2}\right)^n \tag{1.7}$$

$$K_{MgCa}^{RK} = \frac{y_{Mg}}{y_{Ca}}\left(\frac{(a_{Ca}/c_0)}{(a_{Mg}/c_0)}\right)^n \tag{1.8}$$

where K^{RK} are the Rothmund-Kornfeld exchange coefficients. For n=1, the Rothmund-Kornfeld formulation and the classical Gaines-Thomas convention are identical. Adsorption isotherm equations for each cation M can be derived by solving Equation 1.4 for the respective concentration of the adsorbed species, q_M. In a log-log plot, adsorption isotherms resulting from the Gaines-Thomas equation exhibit a slope equal to 1, while isotherms resulting from the Rothmund-Kornfeld equation have a slope equal to n.

The Gaines-Thomas equation is also used in a multi-site approach, in which experimental cation adsorption isotherms are modeled as a linear superposition of adsorption isotherms corresponding to several classes of binding sites with different exchange coefficients. Such a multi-site approach accounts for the heterogeneity of natural soil materials and the non-ideality of cation exchange behavior in an empirical fashion (Cernik *et al.*, 1996; Vulava *et al.*, 2000). In multi-site models, the total charge of the cation exchange sites equals the CEC:

$$\sum_i z_i S_i = CEC \tag{1.9}$$

where S_i and z_i are the concentration and the charge of site i, respectively.

Solution speciation was included in all model calculations according to the following reactions

$$Ca^{2+} + Cl^- \rightleftharpoons CaCl^+ \qquad \log K = 0.57 \tag{1.10}$$

$$Mg^{2+} + Cl^- \rightleftharpoons MgCl^+ \qquad \log K = 0.63 \tag{1.11}$$

$$Na^+ + Cl^- \rightleftharpoons NaCl^0 \qquad \log K = -0.19 \tag{1.12}$$

with thermodynamic stability constants K derived from conditional constants (Martell and Smith, 1982; Smith and Martell, 1989). The Davies equation was used for activity corrections (Sposito, 1981).

The amounts of cations adsorbed were related to the activities of free cations in solution, assuming that adsorption of chloride complexes of Ca and Mg is negligible. The entire ternary dataset was used to fit the 1-site Gaines-Thomas exchange model using a non-linear least squares procedure (Cernik and Borkovec, 1995). Subsequently, the 1-site Gaines-Thomas model was extended to the 1-site Rothmund-Kornfeld and the 3-site Gaines-Thomas model respectively. The fit was optimized by step-wise trial-and-error adjustment of the model parameters. The total charge concentration of exchange sites was set to equal the CEC. Fitting parameters in the 1-site Gaines-Thomas model

were the two exchange coefficients (Equations 1.5 and 1.6). In the 1-site Rothmund-Kornfeld model the parameter *n* (equaling 1 in Gaines-Thomas convention) was optimized and the exchange coefficients readjusted. In the case of the 3-site Gaines-Thomas model, two additional sites with very low concentrations were added to the 1-site Gaines-Thomas model in order to improve the fit of adsorption data in specific regions of the adsorption isotherms. Relative mean square errors (RMSE) were calculated for all fits using the equation

$$\mathrm{RMSE}=\sqrt{\frac{1}{n}\sum_{i=1}^{n}\left(\frac{\log(q_{i,exp}/q_0)-\log(q_{i,calc}/q_0)}{\log(q_{i,exp}/q_0)}\right)^2} \qquad (1.13)$$

where $q_{i,exp}$ and $q_{i,calc}$ are the measured and the calculated amounts adsorbed of datapoint *i* respectively, *n* is the total number of datapoints, and q_0 equals 1 mol/kg.

Transport was predicted using a continuous mixing-cell transport code based on a kinetic approach. Solution is assumed to constantly flow through a cascade of stirred mixing cells with instantaneous mixing in each cell. Transport and chemical reactions are directly coupled and the combined differential equations solved simultaneously. While the reactions follow stoichiometrically balanced reaction equations, the respective reaction rates can be defined as a function of activities in solution, i.e., they do not have to follow elementary mass law kinetics. This is necessary if Rothmund-Kornfeld exchange coefficients, which do not depend on the reaction stoichiometry, are used in transport modeling. However, as cation exchange reactions are very fast, reaction rates were chosen high enough to maintain local equilibrium. For the 1-GT model, the same predictions were obtained from the kinetic transport code and from the thermodynamic transport code ECOSAT (Keizer *et al.*, 1993). Input parameters for transport predictions were the sorption model parameters, the soil material packing density, and the column Peclet number.

1.3 Results and Discussion

1.3.1 Binary Cation Adsorption

The adsorption data for all binary cation systems are shown in Figure 1.1. The data are plotted as adsorbed cation concentrations q_M (in mol/kg) as a function of the concentration of free cations M in solution (mol/L). Each figure shows a set of adsorption isotherms in the presence of different total concentrations of the respective background cation. Several general features of the adsorption isotherms can be observed: At high adsorptive cation concentrations in solution, the adsorbed amounts approach a plateau value, which corresponds to the CEC of the soil material (0.060 mol_c/kg). At low adsorptive cation concentrations in solution, the experimental adsorption isotherms are linear with a slope near unity on a log-log plot. Due to cation exchange with the background cation, the adsorbed amounts generally decrease with increasing background cation concentration.

The solid lines in Figure 1.1 represent the best-fit description of the experimental data with the 1-site Gaines-Thomas cation exchange model. Model calculations are based on measured final adsorptive and background cation concentrations. The small wiggles in the calculated lines are due to slight variations in measured background cation concentration caused by experimental and analytical errors. This applies also to model calculations presented in Figures 1.3 and 1.4, respectively. Although the model captures the general features of the binary adsorption data rather well, significant deviations from the experimental data still remain, particularly at low adsorptive cation concentrations. The deviations are most apparent in the case of Na adsorption isotherms with Ca or Mg as the background cation. The experimental Na adsorption isotherms at low Na concentrations exhibit a slope of approximately 0.9 and 0.7 in Ca and Mg background electrolyte, respectively. In contrast, a slope of unity follows from the Gaines-Thomas convention of cation exchange (Figures 1.1C and 1.1D). For Ca and Mg adsorption isotherms with Na as the background cation, the Gaines-Thomas model provides a rather good description of the experimental data (Figure 1.1A). Only at high Na concentration and low Ca concentration the amounts of sorbed Ca are clearly underestimated by the model. The adsorption data for the binary Ca-Mg system are described well by the Gaines-Thomas model (Figures 1.1E and 1.1F). The model

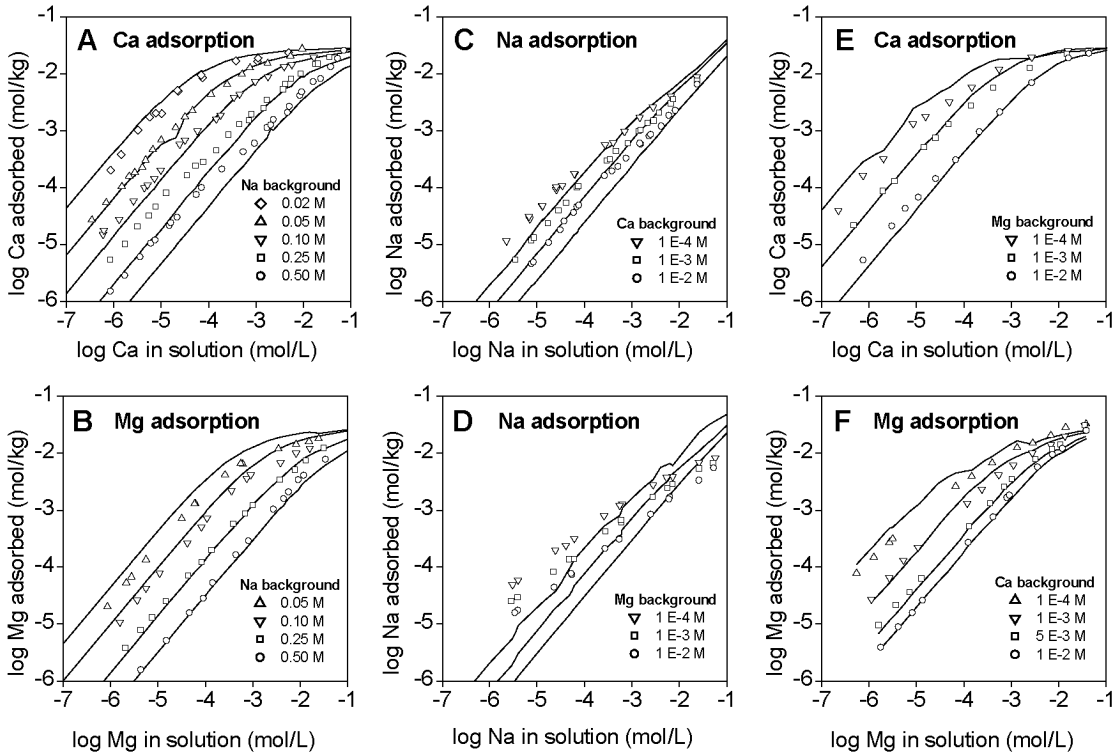

Figure 1.1: Binary sorption data (symbols) and 1-site Gaines-Thomas (lines) model fit. Model calculations based on measured final cation concentrations. Background concentrations indicated before addition of the sorbing cation.

parameters for the 1-site Gaines-Thomas model are provided in Table 1.3. The exchange coefficients indicate that the adsorption affinity to the soil material decreases in the order $Ca^{2+} > Mg^{2+} >> Na^{+}$. Coefficients for the Riedhof soil are in the same range as values reported by other authors for natural soil materials (Valocchi *et al.*, 1981; Dance and Reardon, 1983; Cernik *et al.*, 1994).

Figure 1.2 shows Gaines-Thomas exchange coefficients determined from the individual data points as a function of the respective adsorptive cation concentration in solution and at different background cation concentrations. The constant exchange coefficients used in the 1-site Gaines-Thomas model are shown as horizontal lines for comparison. While the exchange coefficients for Ca and Mg adsorption remain rather constant with increasing Ca or Mg concentration in solution, the exchange coefficients for Na adsorption increase strongly with decreasing Na concentration. In general, the

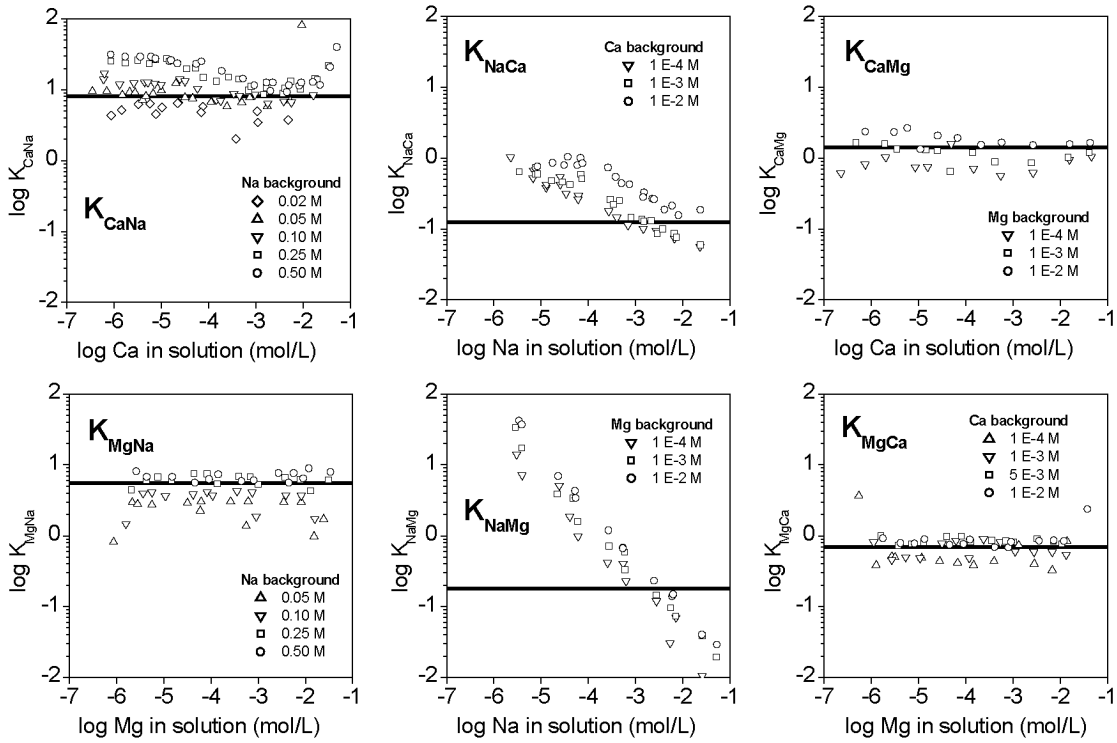

Figure 1.2: Exchange coefficients calculated for individual sorption data points (symbols) and binary exchange coefficients from the 1-site Gaines-Thomas model fit (lines). Individual coefficients higher than the model coefficients indicate sorption data points where sorption is underestimated by the 1-site Gaines-Thomas model.

exchange coefficients seem to increase with increasing concentration of background cations in solution.

Classical exchange isotherms are usually obtained at constant solution normality and, in the case of homovalent exchange, constant ionic strength. In the dataset presented here, ionic strength and solution normality increase with increasing adsorptive cation concentration at a given background electrolyte concentration. However, in the regions of the isotherms where the adsorptive cation concentration is at least 10 times lower than the background cation concentration, solution normality and ionic strength are dominated by the background electrolyte and therefore virtually constant. The presented model calculations implicitly account for complex or ion pair formation in solution and ion activity corrections, which could result in apparent effects of ionic strength on cation exchange. Nevertheless, variations in the calculated selectivity

coefficients are observed over the entire range of the adsorption isotherms, but independently of changes in ionic strength. For example, in the case of K_{MgNa}, K_{CaMg}, K_{MgCa}, and K_{CaNa}, the coefficients vary with the background cation concentration, but remain almost constant over the entire adsorptive cation concentration range even at increasing ionic strength. In the case of K_{NaCa} and K_{NaMg}, the selectivity coefficients steadily decrease with increasing Na concentration in solution, even in the regions of constant ionic strength. These results suggest that the observed changes in cation selectivity coefficients are not due to variations in ionic strength and that other factors must be considered.

One explanation might be the non-ideality of the exchanger phase, resulting in a variation of activity coefficients for adsorbed cations (Sparks, 1995). In the Gaines-Thomas convention, the activity coefficients for adsorbed cations are assumed to equal 1. The Rothmund-Kornfeld formulation accounts for the variability of the activity coefficients in an empirical fashion: Activities of adsorbed cations are assumed to be equal to the charge equivalent fraction raised to the power n^{-1}. This offers the flexibility to fit the slope of an isotherm more accurately by adjusting the exponent parameter n (Equations 1.7 and 1.8). The solid lines in Figure 1.3 represent the best-fit description of the experimental data with the Rothmund-Kornfeld model. An isotherm slope n=0.94 together with slightly adjusted exchange coefficients yielded the best fit over all binary datasets. Model parameters are listed in Table 1.3. Compared to the 1-site Gaines-Thomas model, the fit of the Na exchange isotherms was slightly improved (Figures 1.3C and 1.3D), however, at the cost of slightly lower accuracy for the Ca and Mg exchange isotherms (Figures 1.3E and 1.3F). Furthermore, the slope (=0.9) of the experimental Na adsorption isotherms in Ca background is not the same as the corresponding slope (=0.7) in Mg background electrolyte. The RMSE for the 1-site Rothmund-Kornfeld model is slightly lower than for the 1-site Gaines-Thomas model (Table 1.3). The Rothmund-Kornfeld formulation is often reported to yield an excellent fit of cation exchange data (Bond, 1995; Carlson and Buchanan, 1973). This was also true in our case if each binary dataset was considered separately (not shown). However, the ability of the Rothmund-Kornfeld approach to improve the simultaneous description of all binary datasets within the Ca-Mg-Na-soil system was limited. This was mainly

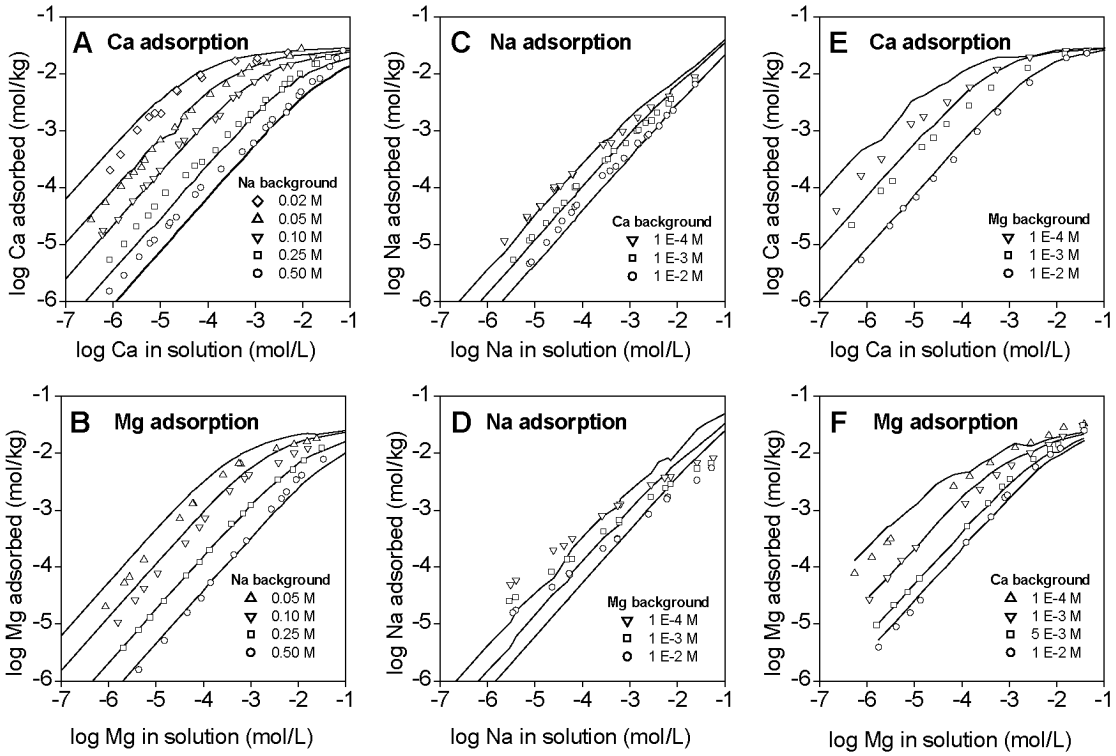

Figure 1.3: Binary sorption data (symbols) and 1-site Rothmund-Kornfeld (lines) model fit. Model calculations based on measured final cation concentrations. Background concentrations indicated before addition of the sorbing cation.

due to the fact that the experimental Na adsorption isotherms exhibited different slopes in Ca and Mg background electrolytes. It should be noted, however, that we used one unique exponent n in our study, while other researchers used either different exponents for different binary systems (Bond and Verburg, 1997), or applied individual exponents to each cation in their system (Carlson and Buchanan, 1973).

Both approaches were also considered in the present study. Using individual exponents for each cation did not further improve the fit, because it offered little additional flexibility to fit different slopes of Na adsorption isotherms in Ca and Mg background electrolytes. The exponent assigned to a cation does not only affect the slope of its model isotherms, but also the vertical displacement of the adsorption isotherms, where the respective cation acts as the background cation. Using a different exponent parameter n for each binary system has the disadvantage that it does not yield a consistent description of the ternary system based on two binary exchange reactions

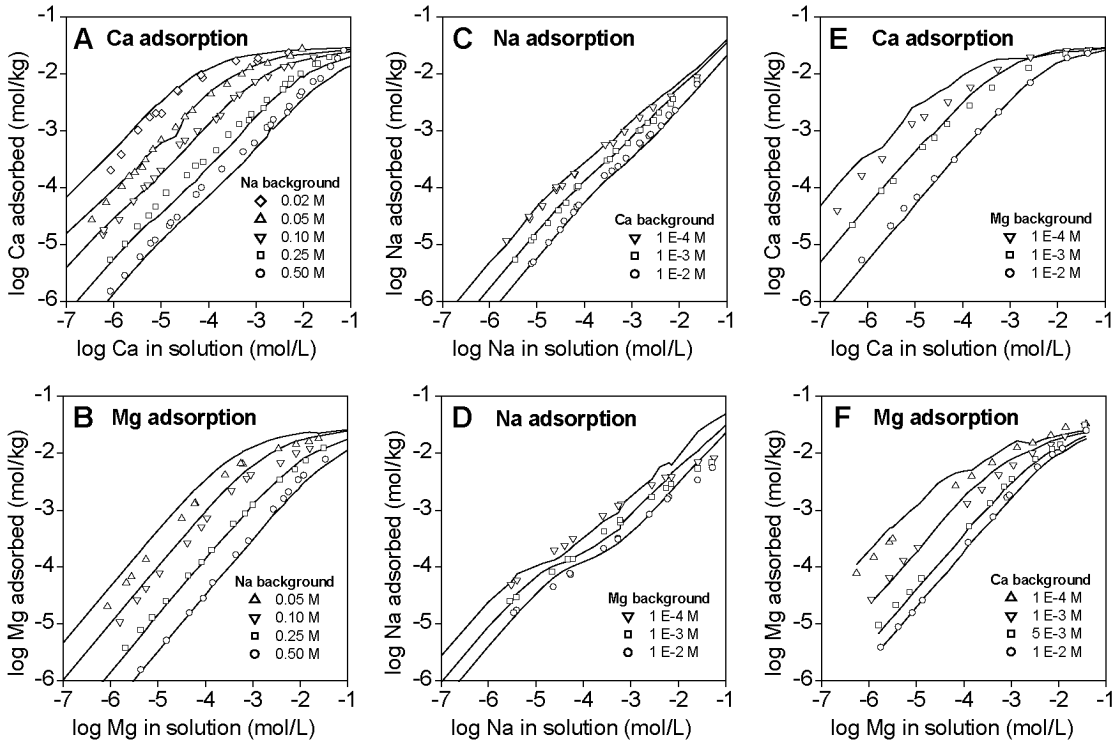

Figure 1.4: Binary sorption data (symbols) and 3-site Gaines-Thomas (lines) model fit. Model calculations based on measured final cation concentrations. Background concentrations indicated before addition of the sorbing cation.

(Equations 1.7 and 1.8) and the charge balance (Equation 1.4), without making assumptions on which binary exchange parameters to be considered in the ternary case (Bond and Verburg, 1997).

Another possible reason for the variation in exchange coefficients may be the chemical heterogeneity of the sorbent. Several chemically different surface sites with different concentrations and selectivities for cations could lead to the observed variation in the overall 'macroscopic' exchange coefficients (Figure 1.2). The soil material used in this study contains a mixture of different exchanger phases including different clay minerals and soil organic matter. Such chemical heterogeneity can be accounted for in an empirical fashion using the multi-site modeling approach (Cernik and Borkovec, 1995; Cernik *et al.*, 1996; Vulava *et al.*, 2000). To improve the model fit, two additional sites were added to the 1-site Gaines-Thomas model to account for sites with high affinity for Na and Ca, respectively. The additional model parameters were optimized by

Table 1.3: Model parameters for the 1-site Gaines-Thomas model, the 1-site Rothmund-Kornfeld model, and the 3-site Gaines-Thomas model.

Model		$\log K_{NaCa,\,i}$	$\log K_{MgCa,\,i}$	n	z_iS_i (mol_c/kg)	RMSE[a] (n=343)
1-site Gaines-Thomas		-0.90	-0.16	1	60.0	0.0752
1-site Rothmund-Kornfeld		-0.84	-0.22	0.94	60.0	0.0660
3-site Gaines-Thomas	site1	-0.90	-0.16	1	60.0	0.0535
	site 2	5.00	-2.00	1	0.1	
	site 3	-4.00	-2.00	1	0.1	

[a]RMSE root mean square error (Equation 1.13)

trial and error. These two additional sites are hypothetical, however, not unrealistic for a natural soil material. Preferential adsorption of Ca on soil organic matter and of Na on montmorillonitic soil clay has been previously reported (Fletcher *et al.*, 1984b; Fletcher *et al.*, 1984a; Sposito and Fletcher, 1985). Model parameters and RMSE for the 3-site Gaines-Thomas model are listed in Table 1.3. Experimental data (symbols) and model fits (solid lines) are depicted in Figure 1.4. The first site was the same as in the 1-site Gaines-Thomas model. Since the concentrations of the additional two sites did not significantly increase the total site concentration, the concentration of site 1 was left unchanged compared to the 1-site Gaines-Thomas model. Site 2 accounts for the higher affinity for Na at low Na concentrations. Ca and Mg isotherms are not significantly affected by this site. Comparing Figures 1.1 and 1.4 illustrates that this site significantly improves the fit of the Na adsorption isotherms at low Na concentrations, especially in Ca background electrolyte. However, overestimation of Na adsorption at high Na concentrations is not corrected. This is also not possible by decreasing the Na-Ca exchange coefficient of site 1, since this would lead to an increase in estimated Ca and Mg adsorption in Na background and therefore deteriorate rather than improve the overall fit. Site 3 with a low Na-Ca exchange coefficient improves the fit of Ca adsorption data at high Na concentrations. The effect of this site becomes apparent when comparing Figures 1.1A and 1.4A. For Mg adsorption in Na background and the Ca-Mg

system, the 3-site Gaines-Thomas model did not change the description as compared to the 1-site Gaines-Thomas model.

1.3.2 Ternary Cation Transport

The results of the first two cation transport experiments (Experiments 1 and 2; Table 1.2) are presented in Figure 1.5A. In both experiments, the feed solution was switched three times after the effluent composition had reached a steady state. Experimental results obtained with the two columns (C1 and C2) at different flow velocities are in excellent agreement, indicating that there was no effect of column dimension or flow velocity on the breakthrough behavior of Ca, Mg, and Na. Because Na was present in similar concentrations as Ca and Mg (Table 1.2), the Na saturation of the cation exchange complex never exceeded 5%. The breakthrough fronts are therefore largely detemined by normality changes and Ca-Mg exchange reactions.

The non-retarded normality fronts appear exactly one pore volume after the influent solution was switched, i.e. at 1, 21, and 66 pore volumes. They reflect the changes in total normality of the feed solution. Due to the preference of the exchanger for Ca over Mg, Ca-Mg exchange results in so-called *self-sharpening* cation exchange fronts observed at around 10 and 71 pore volumes, while the Mg-Ca exchange yields a so-called *self-broadening* cation exchange front ranging from 30 to 55 pore volumes. Na had only minor effects on the breakthrough pattern: a small combined Ca-Na and Mg-Na exchange shoulder after 1 pore volume, a Na-Ca exchange front after 21, and a Ca-Na exchange front after 66 pore volumes. Due to low Na adsorption, Na exchange fronts are almost non-retarded and therefore overlap with the normality fronts.

The predictions of the breakthrough curves for Ca, Mg, and Na resulting from the 1-site Gaines Thomas and the 1-site Rothmund-Kornfeld models are shown as solid and dashed lines, respectively (Figure 1.5A). The predictions obtained from both models are similar, however with minor deviations in different regions of the transport experiment. Generally, the positions of the exchange fronts are correctly predicted, however, small deviations from the experimental data occur in the diffuse Mg-Ca exchange front.

Predictions from the 3-site Gaines-Thomas model for experiments 1, 2, and all subsequent transport experiments are not shown. They are virtually identical to those from the 1-site Gaines-Thomas model. Although the fit of the adsorption data was better with the 3-site Gaines-Thomas model, these improvements were only at low concentration levels that do not play an important role in the transport experiments.

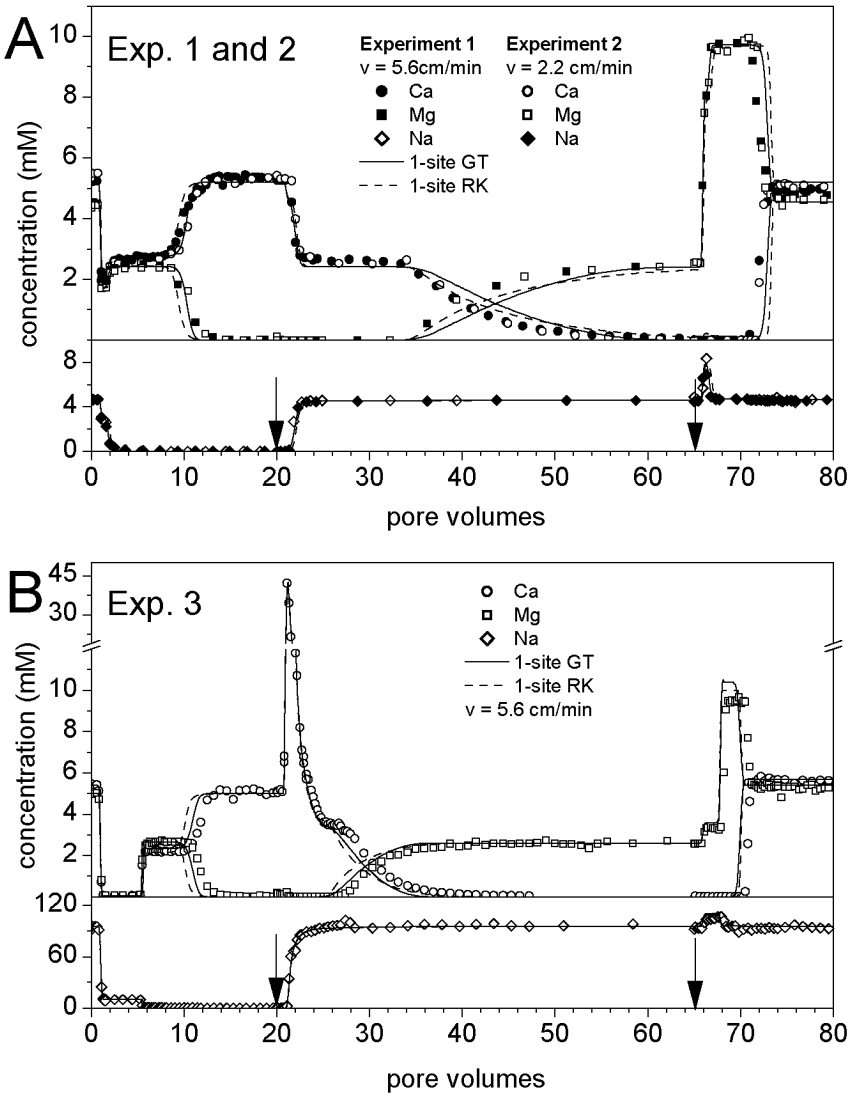

Figure 1.5: Results from transport experiments 1 to 3 (symbols) and model predictions with 1-site Gaines-Thomas (solid lines) and 1-site Rothmund-Kornfeld (dashed lines) model. Experiments 1 and 2 (A) with same solutions. Higher Na concentrations in experiment 3 (B) result in more complex breakthrough curves.

The influence of Na on the cation breakthrough pattern was much greater in Experiment 3, where the Na concentration in the feed solutions was increased by a factor of 20 (Figure 1.5B; Table 1.2). In this experiment, the Na saturation of the exchanger phase was approximately 40% after column preconditioning and reached almost 65% at 50-65 pore volumes. Thus, all three cations had a strong influence on cation sorption, resulting in a more complex breakthrough pattern. Unretarded normality ronts appear as in Experiments 1 and 2, and also the Ca-Mg and Mg-Ca exchange fronts are the same, though at slightly different positions. The main differences in Experiment 3 are the exchange fronts of Ca and Mg with Na, which are now more pronounced.

The 1-site Gaines-Thomas model yields a rather good prediction of the ternary cation transport behavior, although again minor deviations from the experimental data occur in different regions of the experiment. The 1-site Rothmund-Kornfeld model yields a similar prediction, however, slightly less accurate in the region of the Ca-Mg exchange front at 11 pore volumes and the Mg-Ca exchange front around 30 pore volumes.

In Experiments 4 and 5 (Table 1.2), the situation was further complicated by changing the composition of the feed solution before steady state in the outflow was reached, resulting in overlapping breakthrough fronts. The results of these experiments are depicted in Figure 1.6A and 1.6B, respectively. Up to an effluent volume of 4 pore volumes, the breakthrough pattern was similar as described for experiments 1 and 2. Well before the occurrence of the Ca-Mg exchange front, a second change in feed solution composition was applied (Table 1.2), resulting in a non-retarded normality front combined with a slightly retarded Na front at around 5.5 pore volumes. At about 12 pore volumes, the Ca-Mg exchange front originating from the first feed solution change starts to appear in the effluent, but overlaps with the diffuse Mg-Ca exchange front resulting from the second feed solution change. The third change in feed solution composition resulted in additional normality and exchange fronts overlapping with the diffuse Mg-Ca exchange front.

In this case, the model prediction with the Rothmund-Kornfeld model is clearly more accurate than with the Gaines-Thomas model. The complex Ca-Mg exchange front from 12 to 18 pore volumes is accurately predicted with the Rothmund-Kornfeld model.

Therefore, also the height of the Ca peak near 24 and 22 pore volumes in experiments 4 and 5, respectively, is predicted more accurately with the 1-site Rothmund-Kornfeld model. However, as the influent was switched twice before steady state was attained, small errors in transport predictions accumulate. With increasing duration of the experiment, predictions become less accurate for both models.

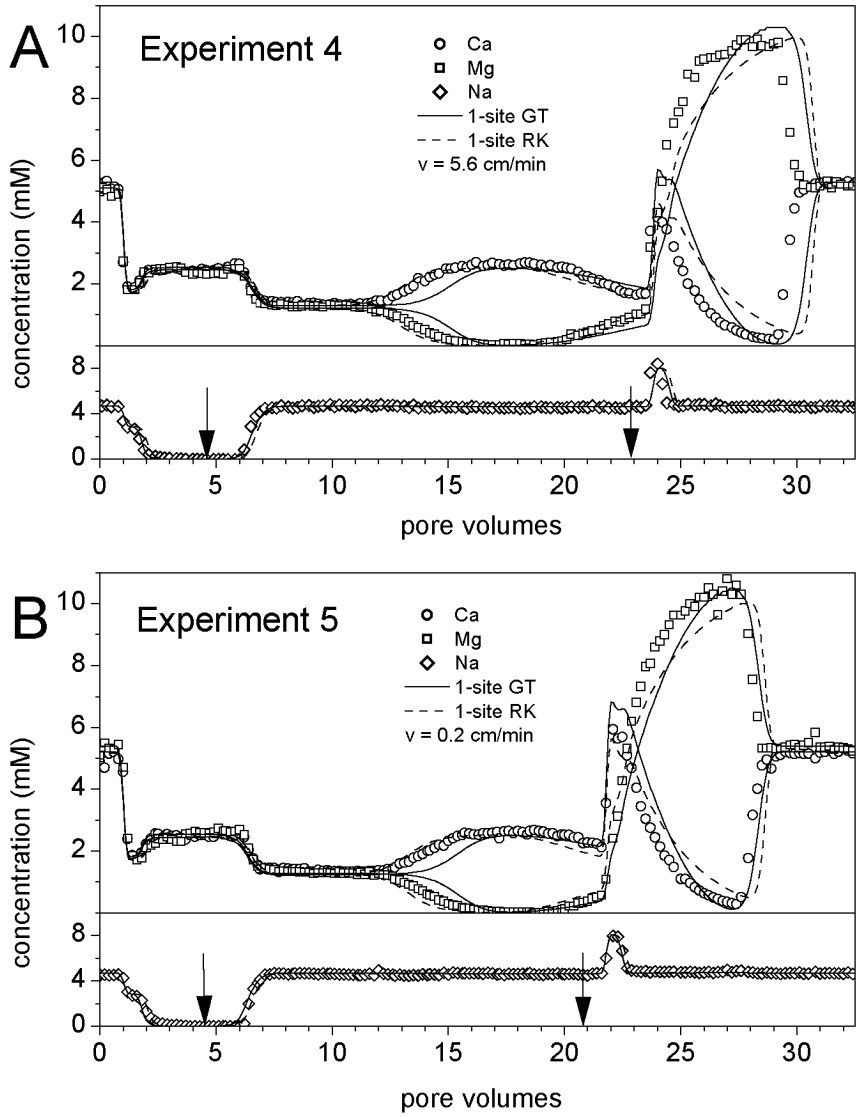

Figure 1.6: Results from transport experiments 4 and 5 (symbols) and model predictions with 1-site Gaines-Thomas (solid lines) and 1-site Rothmund-Kornfeld (dashed lines) model. Similar solutions as in experiments 1 and 2. Switching solutions before steady state results in a complex coupled breakthrough pattern with overlapping fronts.

An additional transport experiment (Experiment 6; Table 1.2) was designed to mimic a seawater-freshwater intrusion system with respect to the concentrations of Ca, Mg, and Na (Gomis-Yagües *et al.*, 1997; Beekman and Appelo, 1990). The experimental results and corresponding model predictions are presented in Figure 1.7. Note, that the concentrations are now plotted on a logarithmic scale to better illustrate the concentration changes over wide ranges. The column was preconditioned with a solution in which the cation concentrations resemble seawater. As a result, around 66% of the exchange sites are saturated with Na, 25% with Mg, and only 9% with Ca. Switching to a solution resembling freshwater (at 0 pore volumes) results in a non-retarded normality front at 1 pore volume. After 9 pore volumes, a Mg-Na exchange front appears, followed by a Ca-Mg exchange front at 15 to 20 pore volumes. After equilibrium with "freshwater" has been achieved, about 87% of the exchange sites are occupied with Ca, 12% with Mg, and only about 1% with Na. Switching back to 'seawater' at 25 pore volumes again results in a sharp Ca-peak due to the normality front combined with a Na-Ca and subsequent Mg-Ca exchange front.

In this experiment, in which the cation concentrations vary over wide ranges, the 1-site Gaines-Thomas model provides a slightly better prediction than the 1-site Rothmund-Kornfeld model. However, both models overestimate the initial amount of adsorbed Na and predict a much sharper Ca-Mg exchange front at around 17 pore volumes than was observed in the experiment. In batch experiments, (Sposito and LeVesque, 1985) observed a decrease in Ca preference of an exchanger with increasing Na-saturation. This effect leads back to the problem of predicting ternary cation systems based on binary adsorption data.

As mentioned earlier, all transport predictions presented in this paper are based on the local equilibrium assumption. To challenge this assumption, the flow velocity was varied from 5.6 cm/h in Experiment 4 to 0.2 cm/h in Experiment 5. Since the model predictions did not improve with decreasing flow velocity, we conclude that kinetic effects are not responsible for the deviations between model calculations and experimental data. Cation exchange reactions are known to be extremely fast (Sparks, 1995). Furthermore, uniformly packed soil material from a sieve fraction between 63 and 400 μm was used, minimizing physical non-equilibrium effects.

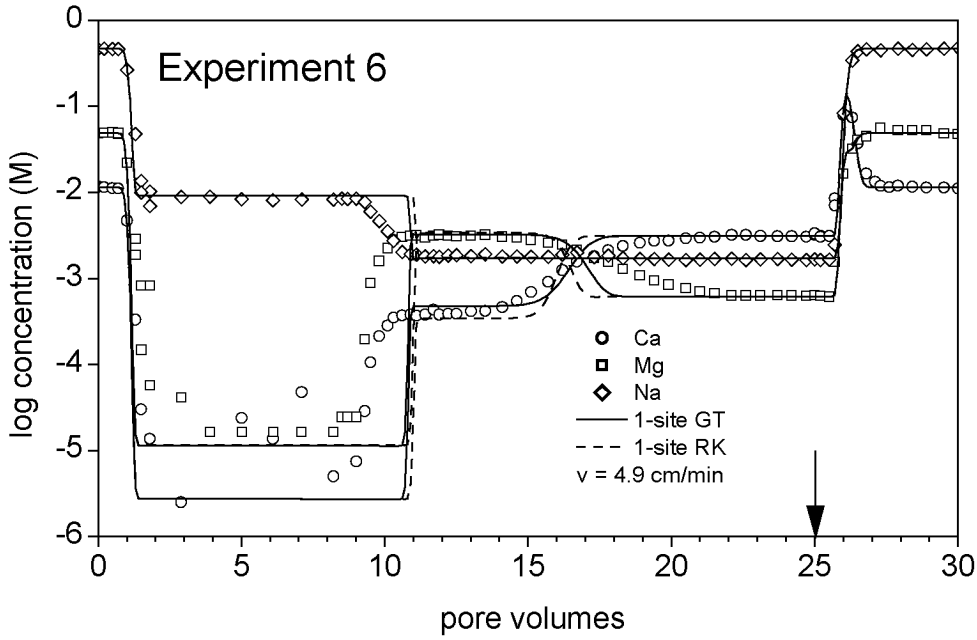

Figure 1.7: Results from transport experiment 6 (symbols) and model predictions with 1-site Gaines-Thomas (solid lines) and 1-site Rothmund-Kornfeld (dashed lines) model. Mimicked sea-freshwater intrusion system with respect to typical concentrations of Ca, Mg, and Na.

Finally, it is important to stress that the correct determination of the cation exchange capacity (CEC) at the condictions of interest is a necessary prerequisite for accurate transport modeling of major cations. For fitting adsorption data shown on a log-scale, an error in the CEC value of up to 20% would not be critical to obtain a good fit. However, transport experiments are usually shown on a linear time scale and the position of exchange fronts depends on the amounts of cations adsorbed. Therefore, special attention should be paid to the determination of the CEC value of the soil material at the pH conditions of interest.

1.4 Conclusions

Our results demonstrate, that all three models calibrated with binary cation adsorption data for Ca, Mg, and Na are able to predict the general transport behavior in a ternary system of major cations with sufficient accuracy. In principle, this should also be true for more complex systems, containing more than three competing cations. The 1-site

Rothmund-Kornfeld model slightly improved the fit of the adsorption dataset. However transport predictions were partly improved and partly deteriorated when compared to the 1-site Gaines-Thomas model. While the 3-site Gaines-Thomas model provided a better description of Na adsorption in Ca or Mg background than both 1-site models, the transport predictions were virtually the same as for the 1-site Gaines-Thomas model. This may be explained by the fact that the improvements of the 3-site Gaines-Thomas model account for adsorption at extremely low adsorptive cation concentrations. In most cases of practical importance, these regions are not decisive for the prediction of the transport patterns of major cations. However, the multisite approach might prove very useful if sorption and transport of trace metal cations at low concentrations are investigated. At the concentration level of major cations that are mainly retained by cation exchange, accurate determination of the CEC at the conditions where transport takes place, is a key prerequisite for accurate transport modeling.

References

Appelo, C.A.J., Willemsen, A., Beekman, H.E., Griffioen, J., *Geochemical calculations and observations on salt water intrusions. II. Validation of a geochemical model with laboratory experiments*. Journal of Hydrology 120, 225-250, **1990**.

Beekman, H.E., Appelo, C.A.J., *Ion chromatography of fresh- and salt-water displacement: laboratory experiments and multicomponent transport modelling*. Journal of Contaminant Hydrology 7, 21-37, **1990**.

Bjerg, P.L., Christensen, T.H., *A field experiment on cation exchange-affected multicomponent solute transport in a sandy aquifer*. Journal of Contaminant Hydrology 12, 269-290, **1993**.

Bond, W.J., *On the Rothmund-Kornfeld description of cation exchange*. Soil Science Society of America Journal 59, 436-443, **1995**.

Bond, W.J., Verburg, K., *Comparison of methods for predicting ternary exchange from binary isotherms*. Soil Science Society of America Journal 61, 444-454, **1997**.

Carlson, R.M., Buchanan, J.R., *Calcium-magnesium-potassium equilibria in some california soils*. Soil Science Society of America Proceedings 37, 851-855, **1973**.

Cernik, M., Barmettler, K., Grolimund, D., Rohr, W., Borkovec, M., Sticher, H., *Cation transport in natural porous media on laboratory scale: multicomponent effects*. Journal of Contaminant Hydrology 16, 319-337, **1994**.

Cernik, M., Borkovec, M., *Regularized least-squares methods for the calculation of discrete and continuous affinity distributions for heterogeneous sorbents*. Environmental Science and Technology 29, 413-425, **1995**.

Cernik, M., Borkovec, M., Westall, J.C., *Affinity distribution description of competitive ion binding to heterogeneous materials*. Langmuir 12, 6127-6137, **1996**.

Dance, J.T., Reardon, E.J., *Migration of contaminants in groundwater at a landfill: a case study, 5. Cation migration in the dispersion test*. Journal of Hydrology 63, 109-130, **1983**.

Fletcher, P., Holtzclaw, K.M., Jouany, C., Sposito, G., LeVesque, C.S., *Sodium-calcium-magnesium exchange reactions on a montmorillonitic soil: II. Ternary exchange reactions*. Soil Science Society of America Journal 48, 1022-1025, **1984a**.

Fletcher, P., Sposito, G., LeVesque, C.S., *Sodium-calcium-magnesium exchange reactions on a montmorillonitic soil: I. Binary exchange reactions*. Soil Science Society of America Journal 48, 1016-1021, **1984b**.

Gaines, G.L.J., Thomas, H.C., *Adsorption studies on clay minerals. II: A formulation of the thermodynamics of exchange adsorption*. The Journal of Chemical Physics 21, 714-718, **1953**.

Gomis-Yagües, V., Boluda-Botella, N., Ruiz-Beviá, F., *Column displacement experiments to validate hydrogeochemical models of seawater intrusions*. Journal of Contaminant Hydrology 29, 81-91, **1997**.

Grolimund, D., Borkovec, M., Federer, P., Sticher, H., *Measurement of sorption isotherms with flow-through reactors*. Environmental Science and Technology 29, 2317-2321, **1995**.

Hendershot, W.H., Duquette, M., *A simple barium chloride method for determining cation exchange capacity and exchangeable cations*. Soil Science Society of America Journal 50, 605-608, **1986**.

Jury, W.A., Flühler, H., *Transport of chemicals through soil: mechanisms, models, and field applications*. Advances in Agronomy 47, 141-201, **1992**.

Keizer, M.G., De Wit, J.C., Meussen, J.C.L., Bosma, W.J.P., Nederlof, M.M., Venema, P., Meussen, V.C.S., van Riemsdijk, W.H., van der Zee, S.E.A.T.M., *ECOSAT, A computer program for the calculation of speciation in soil-water systems.* Wageningen, The Netherlands, **1993**.

Martell, A.E., Smith, R.M., *Critical Stability Constants, Vol. 5*. Plenum Press, New York, **1982**.

McBride, M.B., *Environmental Chemistry of Soils*. Oxford University Press, New York, **1994**.

Rothmund, V., Kornfeld, G., *Der Basenaustausch im Permutit I.* Zeitschrift für anorganische und allgemeine Chemie 103, 129-163, **1918**.

Smith, R.M., Martell, A.E., *Critical Stability Constants, Vol. 6.* Plenum Press, New York, **1989**.

Sparks, D.L., *Environmental Soil Chemistry.* Academic Press, San Diego, **1995**.

Sposito, G., *The Thermodynamics of Soil Solutions.* Oxford University Press, New York, **1981**.

Sposito, G., Fletcher, P., *Sodium-calcium-magnesium exchange reactions on a montmorillonitic soil: III. Calcium-magnesium exchange selectivity.* Soil Science Society of America Journal 49, 1160-1163, **1985**.

Sposito, G., LeVesque, C.S., *Sodium-calcium-magnesium exchange on Silver Hill illite.* Soil Science Society of America Journal 49, 1153-1159, **1985**.

Thomas, G.W., *Exchangeable cations.* In: *Methods in soil analysis, Part 2.* Page, A.L., ed., ASA and SSSA, 159-165, **1982.**

Valocchi, A.J., Roberts, P.V., Parks, G.A., Steel, R.L., *Simulation of the transport of ion-exchanging solutes using laboratory-determined chemical parameter values.* Ground Water 19, 600-607, **1981**.

Vulava, V.M., Kretzschmar, R., Rusch, U., Grolimund, D., Westall, J.C., Borkovec, M., *Cation competition in a natural subsurface material: modeling of sorption equilibria.* Environmental Science and Technology 34, 2149-2155, **2000**.

CHAPTER 2

COMPETITIVE SORPTION AND TRANSPORT OF CD AND NI IN SOIL COLUMNS: APPLICATION OF A CATION EXCHANGE EQUILIBRIUM MODEL

Abstract

Recently published literature data on the competitive sorption and transport of Cd and Ni in a coarse-loamy soil material are reanalyzed using a local equilibrium cation exchange model coupled to a transport code based on a series of mixing cells. In the first publication (Wang *et al.*, 1998), the soil was packed into plexiglass columns and equilibrated with 10 mM KNO_3. The breakthrough of 1 mM Cd, 1 mM Ni, and the coupled breakthrough of 1 mM Cd plus 1 mM Ni in 10 mM KNO_3 and the subsequent desorption of Cd and Ni were then monitored. In the second publication (Wang *et al.*, 1997), soil material equilibrated with 1 mM Cd in 10 mM KNO_3 background electrolyte was leached with 1.25 to 50 mM $CaCl_2$ solutions and Cd desorption was measured. All experiments were carried out with a coarse-loamy soil material (Hayhook soil) at pH~6. Since the concentrations of Cd and Ni were rather high in all experiments and the organic matter content of the soil material was low, cation exchange was assumed to be the major sorption mechanism. In this paper, we show that a local equilibrium cation exchange model is adequate to describe all features of the experimental results presented by Wang and coworkers. The model accurately reproduces the coupled breakthrough of Cd and Ni and the Cd elution curves obtained at various Ca concentrations in the influent. The transport experiments exhibit typical multicomponent cation exchange patterns, which cannot be described correctly with the equilibrium or non-equilibrium Freundlich models used in the original papers.

Voegelin, A., Kretzschmar, R., *Competitive sorption and transport of Cd(II) and Ni(II) in soil columns: Application of a cation exchange equilibrium model.* submitted

2.1 Introduction

Contamination of soils with Cd and Ni can pose a serious threat to environmental quality and represents a long-term risk of groundwater pollution. The mobility and fate of these heavy metals in soils and sediments is governed to a large extent by adsorption and desorption reactions at mineral surfaces and organic matter functional groups (Sparks, 1995; McBride, 1989). The contribution of cation exchange reactions to total metal sorption increases with decreasing soil pH and soil organic carbon content and with increasing clay content and sorptive cation concentration. Under acidic conditions, Cd, Ni, and Zn were found to exhibit very similar sorption and transport behavior (Voegelin *et al.*, 2001).

In two recent papers by Wang and coworkers, Cd and Ni sorption and transport experiments in a coarse-loamy C horizon soil material (Hayhook) at near neutral pH were presented (Wang *et al.*, 1997; Wang *et al.*, 1998). A coupled Cd/Ni column breakthrough experiment evidences the competition between Cd and Ni for sorption sites (Wang *et al.*, 1998). Column and batch experiments show the competitive and mobilizing effect of Ca on Cd and Ni sorbed to the soil material (Wang *et al.*, 1997). In all experiments, Cd and Ni sorb to a similar extend, which is in agreement with other studies (Voegelin *et al.*, 2001). As correctly stated by Wang and coworkers, non-preference cation exchange interactions are likely to dominate heavy metal sorption at the given experimental conditions, i.e., low organic carbon content and high Cd and Ni concentrations. With the Freundlich equation they used to describe Cd and Ni adsorption to the soil material, it was however neither possible to describe the simultaneous transport of Cd and Ni, nor the Ca induced mobilization of Cd from the soil material. While the Freundlich-approach is useful to describe heavy metal sorption over wide experimental conditions (Elzinga *et al.*, 1999; Sauve *et al.*, 2000), its application to multicomponent cation adsorption and transport modeling is limited and may even be misleading. Because the equilibrium Freundlich model failed to correctly describe the Cd and Ni desorption curves, Wang and coworkers postulated a non-equilibrium process to improve the model calculations. However, the observed discrepancies between equilibrium Freundlich model and experimental data do not primarily arise from kinetic processes, but from the inherent inability of the Freundlich

approach to account for exchange processes and resulting concentration patterns in transport experiments, in which several cations compete for adsorption sites.

In this paper, we reanalyze the Cd and Ni transport and sorption data presented by Wang and coworkers using a cation exchange equilibrium model. Such models have previously been applied to describe competitive sorption and transport of major cations, such as Ca^{2+}, Mg^{2+}, K^{+}, and Na^{+} (Appelo, 1994; Cernik *et al.*, 1994; Voegelin *et al.*, 2000), but rarely of heavy metal cations. We show that a local equilibrium cation exchange model with a single type of cation exchange sites is adequate to describe all features of the presented Cd and Ni transport experiments.

2.2 Materials and Methods

2.2.1 Experimental Data

The experimental data analyzed in this paper was taken from Wang *et al.* (1997) and Wang *et al.* (1998), respectively. In both publications, sorption and transport of Cd and Ni in the presence of K and Ca were investigated using a non-calcareous, coarse-loamy soil material (10% clay, 4% silt, 86% sand) which was low in organic matter content (1.1 g/kg). The soil material was sampled from the C-horizon (25-50 cm) of a Hayhook soil in Arizona, USA. Before use, the soil material was air-dried and passed through a 2-mm sieve.

Transport experiments were carried out under saturated flow conditions in plexiglass columns homogeneously packed with soil material. Average column properties are listed in Table 2.1. In order to pre-condition the soil material, the columns were flushed with approximately 200 pore volumes of 10 mM KNO_3. In a first set of experiments, the breakthrough of 1 mM $Cd(NO_3)_2$, 1 mM $Ni(NO_3)_2$, and the coupled breakthrough of 1 mM $Cd(NO_3)_2$ and 1 mM $Ni(NO_3)_2$ were investigated in 10 mM KNO_3 background electrolyte (Wang *et al.*, 1998). In a second set of experiments, the soil material was equilibrated with 1 mM $Cd(NO_3)_2$ in 10 mM KNO_3. The influent was then switched to pure solutions of 1.25, 2.5, 5.0, 10.0, and 50.0 mM $CaCl_2$ and the Cd elution pattern was monitored (Wang *et al.*, 1997).

Batch Cd and Ni sorption experiments were carried out in 10 mM KNO_3 background electrolyte solution at pH 6 using a soil to solution ratio was 0.125 kg/L

(Wang *et al.*, 1997). The soil material was washed with 1 M KNO_3, and subsequently twice with 10 mM KNO_3. Cd and Ni sorption was measured in electrolyte solutions initially containing 10 mM KNO_3, 0, 2.5, or 5 mM $Ca(NO_3)_2$, and 0.15 to 2 mM $Cd(NO_3)_2$ or $Ni(NO_3)_2$. After 2 hours shaking, the suspensions were centrifuged, decanted, and analyzed for Cd or Ni. The sorbed amounts were calculated from the difference between initial and final Cd or Ni concentrations.

Table 2.1: Average column parameters (from Wang *et al.*, 1997 and Wang *et al.*, 1998) and model parameters for the cation exchange sorption model and mixing cell transport model, respectively.

Experimental column parameters (Wang *et al.*)	
Inner diameter (cm)	2.77
Length (cm)	10
Porosity (L/L)	0.34
Packing density (kg/L)[a]	5.27
Pore water velocity (cm/min)	0.5
Péclet number	25
Transport model parameters (this paper)	
Number of mixing cells	4
Time step (in pore volumes)	0.1
Sorption model parameters (this paper)	
ECEC (mmol/kg)	45
K_{CdK}	0.31
K_{NiK}	0.31
K_{CaK}	0.31

[a] packing density in mass of soil material per unit pore volume

2.2.2 Sorption and Transport Modeling

Because of the low organic carbon content of the Hayhook soil material and the high Cd and Ni concentrations applied in all experiments, cation exchange was postulated to be the dominant sorption mechanism. Thus, to model the sorption of K, Ca, Cd, and Ni, three independent exchange equations were defined:

$$2KX + Cd^{2+} \rightleftarrows CdX_2 + 2K^+ \tag{2.1}$$

$$2KX + Ni^{2+} \rightleftarrows NiX_2 + 2K^+ \tag{2.2}$$

$$2KX + Ca^{2+} \rightleftarrows CaX_2 + 2K^+ \tag{2.3}$$

where X denotes exchange sites with charge -1. According to the Gaines-Thomas convention (Gaines and Thomas, 1953), the activities of sorbed species are assumed to correspond to the charge equivalent fractions y_M

$$y_M = \frac{z_M q_M}{ECEC} \tag{2.4}$$

where ECEC is the effective cation exchange capacity of the sorbent (in mol_c/kg), z_M is the charge of cation M, and q_M is the amount of cation M adsorbed (in mol/kg). The ECEC can be expressed as

$$ECEC = q_K + 2q_{Ca} + 2q_{Cd} + 2q_{Ni} \tag{2.5}$$

Having defined the activities of adsorbed species as the equivalent fractions y_M, the mass action laws corresponding to Equations 2.1 to 2.3 can be written as

$$K_{CdK} = \frac{y_{Cd} a_K^2}{y_K^2 a_{Cd}} \tag{2.6}$$

$$K_{NiK} = \frac{y_{Ni} a_K^2}{y_K^2 a_{Ni}} \tag{2.7}$$

$$K_{CaK} = \frac{y_{Ca} a_K^2}{y_K^2 a_{Ca}} \tag{2.8}$$

where K_{XY} are the Gaines-Thomas exchange coefficients for the exchange of cation Y by cation X and a_M are the activities of the free metal ions in solution.

Solution speciation was calculated with thermodynamic complex formation constants derived from conditional constants (Smith and Martell, 1976; Martell and Smith, 1982; Smith and Martell, 1989) using the Davies equation. Complexed species considered (with log K_0 for $M+nL \leftrightarrow ML_n$) were: KNO_3 (-0.19), $CaNO_3^+$ (0.50), $CaCl^+$ (0.58), $CdNO_3^+$ (0.50), $CdCl^+$ (1.98), $CdCl_2^0$ (2.60), and $NiNO_3^+$ (0.40). Transport was calculated with the transport code IMPACT based on a mixing cell approach (Jauzein *et al.*, 1989). Input parameters were the number of mixing cells J, the calculation time step, the bulk density, the sorption model parameters (Table 2.1), the complex formation constants, and the sequence and concentrations of feed solutions. All transport calculations are based on the local equilibrium assumption.

2.3 Results and Discussion

2.3.1 Cd, Ni, and Coupled Cd/Ni Column Breakthrough Experiments

The step breakthrough experiments with 1 mM $Cd(NO_3)_2$, 1mM $Ni(NO_3)_2$, and the coupled breakthrough of 1 mM $Cd(NO_3)_2$ and $Ni(NO_3)_2$ in 10 mM KNO_3 electrolyte are shown in Figure 2.1, along with corresponding model calculations using the cation exchange model. Retardation and shape of the breakthrough fronts was similar for Cd and Ni In the competitive experiment, retention of both metals was reduced by 40-45% due to sorption competition between Cd and Ni. Again, both metal cations exhibited almost identical transport behavior. After metal cation breakthrough was complete, the influent was switched back to pure 10 mM KNO_3 electrolyte solution. Influent normality changed from 12 to 10 meq/L in the two single-metal transport experiments and from 14 to 10 meq/L in the coupled Cd/Ni transport experiment, respectively. As a

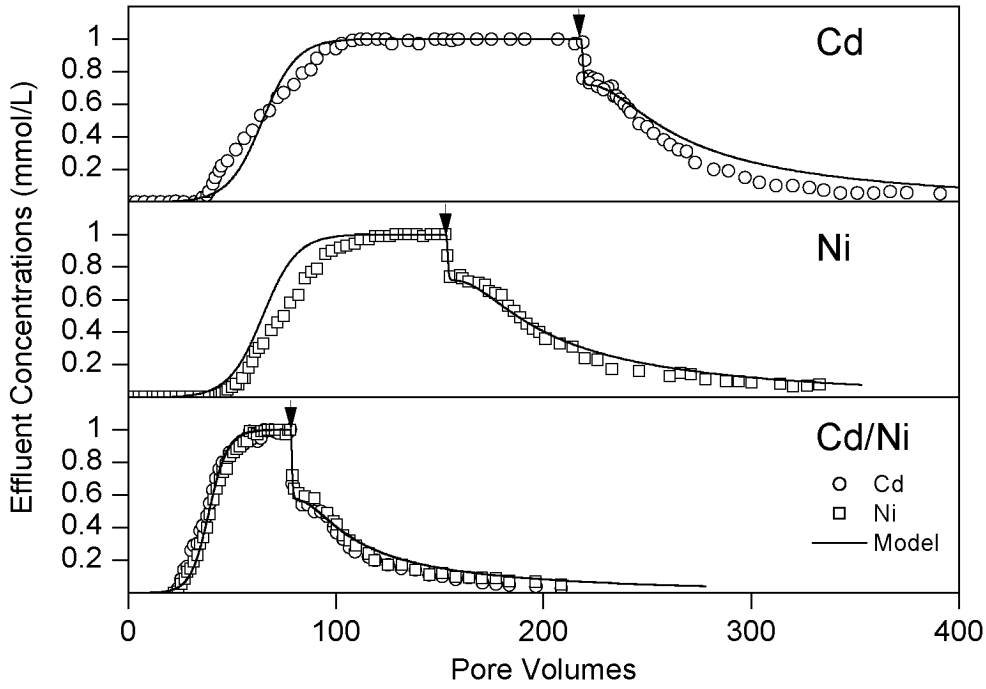

Figure 2.1: Breakthrough of 1 mM $Cd(NO_3)_2$, 1 mM $Ni(NO_3)_2$, and coupled breakthrough of 1 mM $Cd(NO_3)_2$ and 1 mM $Ni(NO_3)_2$ in 10 mM KNO_3. Cd and Ni exhibit similar breakthrough patterns. In the coupled breakthrough experiment, retention of both Cd and Ni is reduced. The exchange model correctly describes the general elution pattern, the coupled Cd/Ni transport, and the normality fronts after the influent change to back to pure electrolyte background (indicated by arrows).

result, unretarded normality fronts are observed one pore volume after the influent was changed, which is documented by a sharp decrease in Cd and Ni concentrations (indicated by arrows in Figure 2.1). The subsequent Cd and Ni release curves exhibited strong tailing. After 350 pore volumes, roughly ~65% of Cd and/or Ni were desorbed from the soil columns and desorption was still not complete.

The lines in Figure 2.1 represent our calculations using the cation exchange model coupled to a mixing cell transport code. The exchange coefficients for Cd and Ni given in Table 2.1 were determined by optimizing the model fit to the experimental breakthrough curves. First, the amount of Cd retained in the Cd breakthrough experiment was obtained from the integrated Cd breakthrough curve. Based on the ECEC of the soil material and speciation calculations for the influent solution, the K_{CdK}

exchange coefficient was then calculated according to Eq. 6. Because the Cd and Ni breakthrough fronts in the coupled Cd/Ni transport experiment overlap (Figure 2.1), the Ni exchange coefficient K_{NiK} was set equal to K_{CdK}. The transport calculations reproduce all features of the breakthrough curves fairly well, not only in single metal breakthrough experiments, but also in coupled Cd/Ni transport experiment in which both metals compete for sorption sites. In contrast to the Freundlich isotherm equations used in the original papers, also the normality fronts following the change to Cd and Ni free influent solution are correctly described. The model slightly underestimates the tailing of the metal desorption fronts. While approximately 65% of the adsorbed metals are desorbed over the duration of the experiments, the model yields around 85% desorption. The experimental tailing might be due to the presence of sorption sites with a high affinity for heavy metal cations, e.g. located on the organic matter. Desorption from such sites by the monovalent K is likely to occur only at low Cd or Ni concentrations and over longer time periods.

2.3.2 Cadmium Mobilization by Calcium

The mobilization and leaching of Cd as influenced by sorption competition with Ca was investigated by Wang *et al.* (1997). Columns equilibrated with 1 mM $Cd(NO_3)_2$ in 10 mM KNO_3 electrolyte background were eluted with solutions of varying $CaCl_2$ concentration and Cd concentration in the effluent was monitored. Figure 2.2 shows the experimental results of Wang *et al.* (1997), along with our model calculations based on the cation exchange model presented above. Generally, a higher $CaCl_2$ concentration in the leaching solution results in higher Cd peak concentrations and faster depletion of the adsorbed Cd in the soil column. In addition, a shoulder or plateau in Cd concentration preceeding the main Cd elution peak is observed. As shown in Figure 2.2, the cation exchange model correctly predicts all features of Cd elution at different Ca concentrations, demonstrating that the breakthrough pattern can be described by cation exchange phenomena (Appelo, 1994; Cernik *et al.*, 1994; Voegelin *et al.*, 2000).

To examine the multicomponent nature of the experiments in greater detail, Figure 2.3 shows the experimental data for Cd elution with 2.5 mM $CaCl_2$ along with the corresponding Ca breakthrough and model calculations (solid lines). The dotted

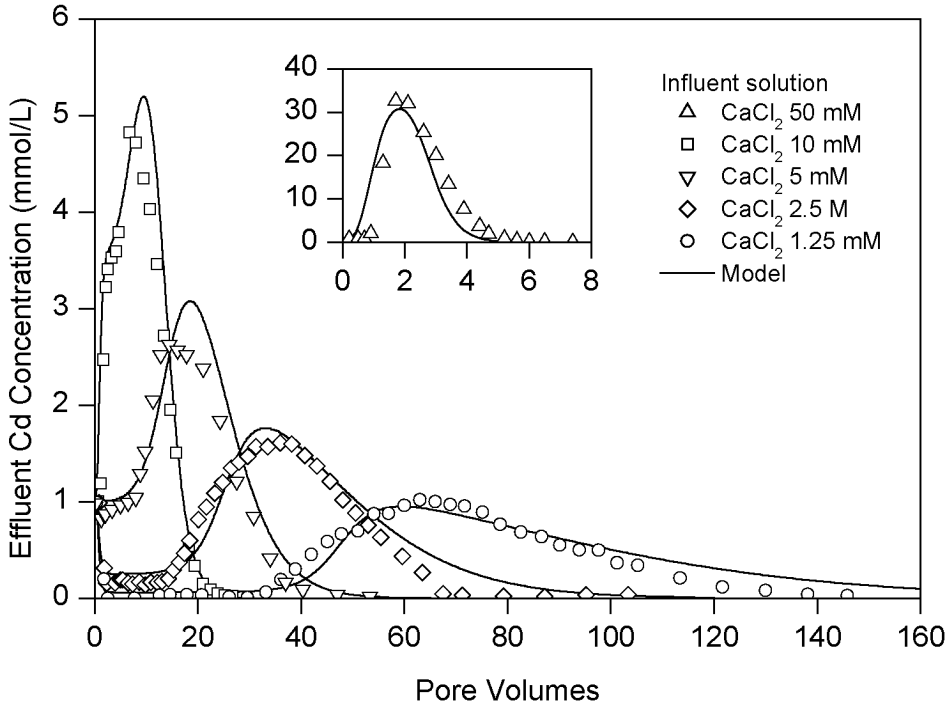

Figure 2.2: Elution of Cd from Hayhook soil with different $CaCl_2$ concentrations after equilibration with 1 mM $Cd(NO_3)_2$ in 10 mM KNO_3. Typical cation exchange patterns are observed and correctly described by the exchange model.

lines are simple transport estimations following the approach of Appelo (1994), which allow to gain a basic understanding of the exchange processes causing the observed chromatographic patterns. In these estimates, complexation of all cations was ignored and free cations and anions were assumed to be the only species in solution. At 0 pore volumes, the column is in equilibrium with a solution containing 10 mM KNO_3 and 1 mM $Cd(NO_3)_2$. The solution normality N is 12 meq/L, and the ionic strength I 13 mM. Using the Davies equation, a conditional K_{CdK} exchange coefficient of 0.25 can be calculated for this ionic strength, which is related to the free cation concentrations rather than activities (with reference concentration c_0 = 1 mol/L)

$$K_{CdK}^{cond} = \frac{y_{Cd}(c_K / c_0)^2}{y_K^2 (c_{Cd} / c_0)} \qquad (2.9)$$

Since only Cd and K are initially present, the exchanger sites are completely occupied by K and Cd, yielding

$$y_K + y_{Cd} = 1 \tag{2.10}$$

From Eqs. 2.9 and 2.10 the equivalent fractions of Cd and K can easily be calculated: y_{Cd} = 0.53, y_K = 0.47. The respective adsorbed amounts are q_{Cd} = 12.0 mmol/kg and q_K = 21.0 mmol/kg. At zero pore volumes, the influent is switched to 2.5 mM $CaCl_2$, which results in an influent normality decrease from 12 to 5 meq/L. During the first pore volume, the effluent concentrations do not change and the residing equilibration solution elutes from the column. After 1 pore volume, the effluent normality has to be equal to the new influent normality, which results in the concentration jump at 1 pore volume referred to as normality front. During the following period, mainly K is eluted

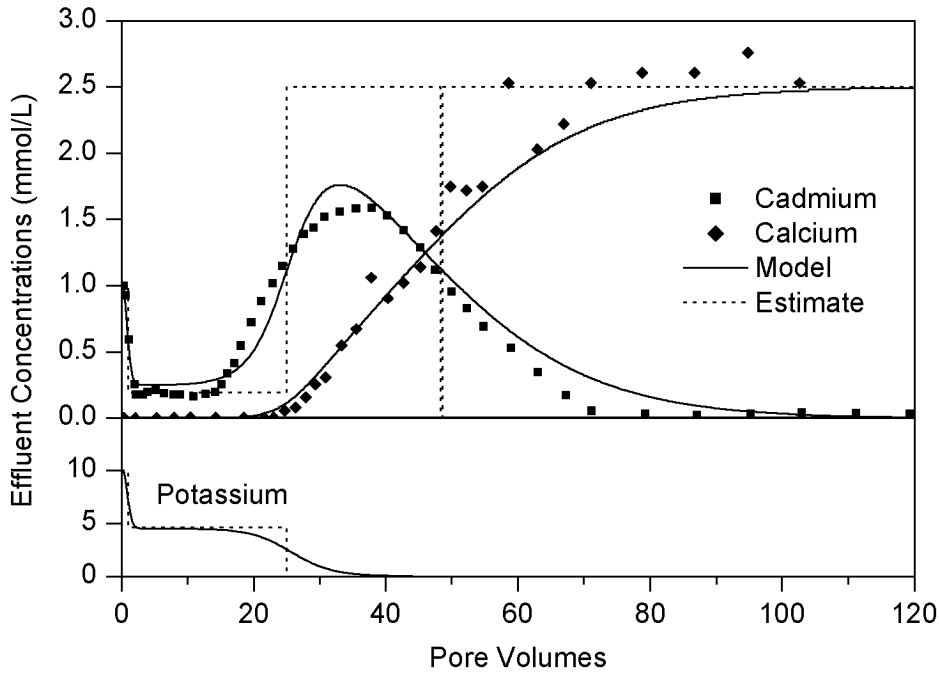

Figure 2.3: Elution of Cd from Hayhook soil with 2.5 mM $CaCl_2$. Integrating the retained Ca yields the ECEC of the Hayhook soil material at experimental conditions. Exchange model calculations (solid lines) correctly describe Cd elution and Ca breakthrough. Simple estimations (dotted lines) allow explaining the rough breakthrough pattern.

from the exchanger, as the monovalent K has a lower affinity to the exchanger than the bivalent Cd. The solution composition is now determined by the initial exchanger phase composition as calculated above, the conditional K_{KCd}, and the solution normality N, which is given by

$$N = c_K + 2c_{Cd} \tag{2.11}$$

The approximate ionic strength is slightly above 5 mM (if only the monovalent K would elute, it would be exactly 5 mM), which yields a conditional K_{CdK} of approximately 0.26. From Eqs. 2.9 and 2.11, the solution composition is calculated: c_{Cd} = 0.194 mM, c_K = 4.61 mM. The K desorption phase continues until all K is eluted from the exchanger. From the initial adsorbed K (q_K), the soil packing density (ρ, Table 2.1), and the K effluent concentration (c_K), the duration of the K elution expressed in number of pore volumes NPV can be calculated

$$NPV = \frac{q_K \rho}{c_K} \tag{2.12}$$

Eq. 2.12 yields 24.0 pore volumes. K desorption hence lasts from 1 to 25.0 pore volumes. During this time, also 0.88 mmol/kg Cd are eluted from the exchanger, resulting in a remaining Cd loading of 11.1 mmol/kg. During the following pore volumes, Cd accounts for the entire solution normality, i.e the Cd effluent concentration is 2.5 mM. In analogy to Eq. 2.12, Cd elution can be calculated to last for another 23.4 pore volumes, i.e. from 25.0 to 48.4 pore volumes. At 48.4 pore volumes, Cd is depleted, and the Ca influent concentration breaks through. Note that the cumulative amount of Ca retained in this experiment was used to derive the ECEC of the Hayhook soil material (Table 2.1). Apparently these transport estimations only yield a rough approximation of the effluent concentration curves, assuming sharp fronts and neglecting diffusion and dispersion. However, they allow discussing the underlying processes, and are able to explain the general effluent pattern. The other Cd elution curves in Figure 2.2 can be interpreted in analogy. The higher the $CaCl_2$ influent

concentration, the shorter the K depletion period and the higher the respective Cd concentration. The following Cd peak should reach the Ca influent concentration. However, due to dispersion and diffusion, this is not the case, except at the lowest Ca concentration, where the Cd elution lasts long enough for the Cd concentration to reach close to the influent Ca concentration. From the initially adsorbed Cd, 95% were removed by $CaCl_2$ over 350 pore volumes irrespective of the Ca concentration applied, while only around 65% were removed with 10 mM KNO_3 over the same time period. Due to its charge, the monovalent K cations are expected to have lower extraction strength than the bivalent Ca cations even on non-preference exchange sites. The difference in extraction strength is likely to be even more pronounced for sites exhibiting a high affinity for bivalent cations in general and heavy metal cations in particular, such as, for example, carboxyl groups on soil organic matter.

2.3.3 Cadmium and Nickel Batch Sorption Data

Cadmium and nickel batch sorption data together with model calculations are shown in Figure 2.4. Again, Cd and Ni exhibit a similar sorption behavior at all Ca concentration levels. The presence of Ca strongly reduces the amounts of Cd or Ni adsorbed. Model calculations are based on the model parameters used to describe the transport experiments (Table 2.1) and are identical for Cd and Ni. The model correctly describes the overall sorption behavior of Cd and Ni, but generally underestimates sorption and overestimates the competitive effect of Ca. The overestimation of Ca competition might be due to the presence of sorption sites with high Cd or Ni affinity. This was discussed before regarding the pronounced tailing of desorption fronts and the incomplete removal of sorbed Cd by Ca. With respect to the model accuracy, it has to be considered that only the initial solution concentrations of K, Ca, and Cd or Ni were given, and that the final Ca and K concentrations were also part of the model calculation.

2.3.4 Comparison of the Exchange and Freundlich Modeling Approaches

Heavy metal adsorption to soils is often described by the Freundlich approach (Buchter *et al.*, 1989; Hooda and Alloway, 1998). Extended formulations of the Freundlich equation were used to account for the effects of H and Ca competition on Cd sorption or

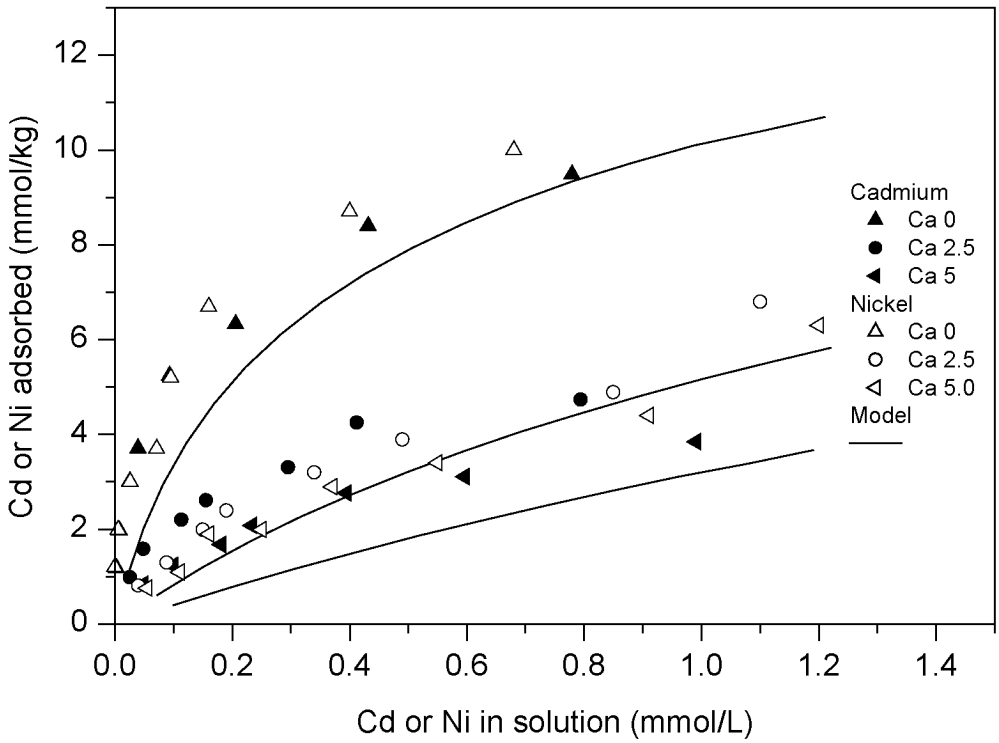

Figure 2.4: Cd and Ni sorption to Hayhook soil in 10 mM KNO_3 and varying $Ca(NO_3)_2$ concentrations (in mM). In batch experiments, similar sorption for Cd (closed symbols) and Ni (open symbols) is observed. Model calculations (lines) correctly describe the general trends in Cd and Ni sorption, however generally underestimate the amounts adsorbed.

for the dependence of Cd sorption on the soil organic carbon content (Temminghoff *et al.*, 1995; Boekhold and van der Zee, 1992). Generalized Freundlich-type equations were also successfully used to describe Cd and Zn sorption over wide experimental conditions in a variety of soil materials (Elzinga *et al.*, 1999), or to estimate the soil solution concentration of a heavy metal from the metal content of contaminated soils (Sauve *et al.*, 2000). Despite this wide applicability to heavy metal sorption, the limitations of the Freundlich approach with respect to multicomponent cation transport modeling have to be considered.

On the first sight, the Freundlich equations presented by Wang *et al.* (1997) yield a slightly more accurate description of the Cd and Ni sorption data at various Ca concentrations than the cation exchange model presented here. However, the Freundlich equation has several severe limitations in modeling the competitive Cd-Ca and Ni-Ca

sorption and transport data. Firstly, a different set of Freundlich parameters is needed for each adsorption isotherm, that is, the description of Cd and Ni adsorption at 3 Ca concentration levels requires 12 model parameters. This compares to only four unique parameters in the cation exchange model including the ECEC, which can be determined independently. Despite the large number of model parameters, the set of Freundlich equations describes the adsorption of Cd or Ni at given experimental conditions, but not the concomitant adsorption/desorption of Ca and K. The Freundlich approach hence does not represent a consistent description of the competitive adsorption of all cations present in the system, and can therefore not correctly reproduce the coupled effluent patterns of Cd, Ca, and K in the Cd mobilization experiments. Furthermore, the Freundlich equations for Cd and Ni sorption in K background can not be combined to predict the coupled breakthrough of Cd and Ni in the presence of background electrolytes with varying composition. Our modeling results demonstrate that a cation exchange model correctly describes all multicomponent sorption and transport patterns in the experiments presented by Wang and coworkers (Fig. 2.1 to 2.3). Finally, Freundlich equations do not yield a charge-balanced description of sorption reactions. In transport experiments, the solution flow leads to a continuous separation of the solution and the sorbent. All sorption processes therefore must be formulated on the basis of charge-balanced reactions accounting for the overall charge neutrality. The unretarded normality fronts observed in the transport experiments (Figs. 2.1 to 2.3) are the apparent result of charge balanced adsorption reactions and are correctly described by the exchange model. These fronts can not be reproduced with the Freundlich equation.

References

Appelo, C.A.J., *Some calculations on multicomponent transport with cation exchange in aquifers*. Ground Water 32, 968-975, **1994**.

Boekhold, A.E., van der Zee, S.E.A.T.M., *A scaled sorption model validated at the column scale to predict cadmium contents in a spatially variable field soil*. Soil Science 154, 105-112, **1992**.

Buchter, B., Davidoff, B., Amacher, M.C., Hinz, C., Iskandar, I.K., Selim, H.M., *Correlation of Freundlich Kd and n retention parameters with soils and elements*. Soil Science 148, 370-379, **1989**.

Cernik, M., Barmettler, K., Grolimund, D., Rohr, W., Borkovec, M., Sticher, H., *Cation transport in natural porous media on laboratory scale: multicomponent effects*. Journal of Contaminant Hydrology 16, 319-337, **1994**.

Elzinga, E.J., van Grinsven, J.J.M., Swartjes, F.A., *General purpose Freundlich isotherms for cadmium, copper and zinc in soils*. European Journal of Soil Science 50, 139-149, **1999**.

Gaines, G.L.J., Thomas, H.C., *Adsorption studies on clay minerals. II: A formulation of the thermodynamics of exchange adsorption*. The Journal of Chemical Physics 21, 714-718, **1953**.

Hooda, P.S., Alloway, B.J., *Cadmium and lead sorption behaviour of selected English and Indian soils*. Geoderma 84, 121-134, **1998**.

Jauzein, M., Andre, C., Margerita, R., Sardin, M., Schweich, D., *A flexible computer code for modeling transport in porous media: IMPACT*. Geoderma 44, 95-113, **1989**.

Martell, A.E., Smith, R.M., *Critical Stability Constants, Vol. 5*. Plenum Press, New York, **1982**.

McBride, M.B., *Reactions Controlling Heavy Metal Solubility in Soils*. Advances in Soil Science 10, 1-56, **1989**.

Sauve, S., Hendershot, W., Allen, H.E., *Solid-solution partitioning of metals in contaminated soils: dependence on pH, total metal burden, and organic matter*. Environmental Science and Technology 34, 1125-1131, **2000**.

Smith, R.M., Martell, A.E., *Critical Stability Constants, Vol. 4.* Plenum Press, New York, **1976**.

Smith, R.M., Martell, A.E., *Critical Stability Constants, Vol. 6.* Plenum Press, New York, **1989**.

Sparks, D.L., *Environmental Soil Chemistry.* Academic Press, San Diego, **1995**.

Temminghoff, E.J.M., van der Zee, S.E.A.T.M., de Haan, F.A.M., *Speciation and Calcium competition effects on Cadmium sorption by sandy soils at various pH levels*. European Journal of Soil Science 46, 649-655, **1995**.

Voegelin, A., Vulava, V.M., Kretzschmar, R., *Reaction-based model describing sorption and transport of Cd, Zn, and Ni in an acidic soil*. Environmental Science and Technology 35, 1651-1657, **2001**.

Voegelin, A., Vulava, V.M., Kuhnen, F., Kretzschmar, R., *Multicomponent transport of major cations predicted from binary adsorption experiments*. Journal of Contaminant Hydrology 46, 319-338, **2000**.

Wang, W.-Z., Brusseau, M.L., Artiola, J.F., *The use of calcium to facilitate desorption and removal of cadmium and nickel in subsurface soils*. Journal of Contaminant Hydrology 25, 325-336, **1997**.

Wang, W.-Z., Brusseau, M.L., Artiola, J.F., *Nonequilibrium and nonlinear sorption during transport of cadmium, nickel, and strontium through subsurface soils*. In: *Adsorption of Metals by Geomedia.* Jenne, E.A., ed., Academic Press, San Diego, 427-443, **1998.**

CHAPTER 3

REACTION-BASED MODEL DESCRIBING COMPETITIVE SORPTION AND TRANSPORT OF CD, ZN, AND NI IN AN ACIDIC SOIL

Abstract

Predicting the mobility of heavy metals in soils requires models, which accurately describe metal adsorption in the presence of competing cations. They should also be easily adjustable to specific soil materials and applicable in reactive transport codes. In this study, Cd adsorption to an acidic soil material was investigated over a wide concentration range (10^{-8} to 10^{-2} M $CdCl_2$) in the presence of different background electrolytes (10^{-4} to 10^{-2} M $CaCl_2$ or $MgCl_2$ or 0.05 to 0.5 M NaCl). The adsorption experiments were conducted at pH values between 4.6 and 6.5. A reaction-based sorption model was developed using a combination of non-specific cation exchange reactions and competitive sorption reactions to sites with high affinity for heavy metals. This combined cation exchange / specific sorption (CESS) model accurately described the entire Cd sorption dataset. Coupled to a solute transport code, the model accurately predicted Cd breakthrough curves obtained in column transport experiments. The model was further extended to describe competitive sorption and transport of Cd, Zn, and Ni. At pH 4.6, both Zn and Ni exhibited similar sorption and transport behavior as observed for Cd. In all transport experiments conducted under acidic conditions, heavy metal adsorption was shown to be reversible and kinetic effects were negligible within time periods ranging from hours up to four weeks.

Voegelin, A., Vulava, V. M., Kretzschmar, R., *Reaction-based model describing competitive sorption and transport of Cd, Zn, and Ni in an acidic soil.* Environmental Science and Technology 35, 1651-1657, **2001**.

3.1 Introduction

Pollution of soils with heavy metals can pose serious threats to soil quality and ecosystem health. Metal contaminants in soils may originate from sewage sludge or fertilizer application, smelter and mining emissions, and other human activities. Initially, the chemical nature of the contaminant material may control metal mobility and bioavailability (Alloway, 1995). In long term however, the chemical speciation of the metal contaminants is altered depending on the metal and soil properties. In acidic soils, metal retention is dominated by adsorption and exchange reactions, and compared to other heavy metals, Cd, Zn, and Ni can be rather mobile (Buchter *et al.*, 1989; Abd-Elfattah and Wada, 1981; Alloway, 1995). Major cations such as Ca effectively compete in the adsorption of these metals to cation exchange sites on clay minerals and soil organic matter (Temminghoff *et al.*, 1995; Christensen, 1984; Wang *et al.*, 1997). In addition, contaminated soils typically contain several metal contaminants, which may also compete with each other for sorption sites (Christensen, 1987a).

Numerous studies have been conducted on Cd, Zn, or Ni sorption to pure soil components such as clay minerals, oxides, or humic substances, and a variety of sorbent-specific models have been developed to describe metal sorption to such materials (Goldberg, 1992; Venema *et al.*, 1996; Benedetti *et al.*, 1995; Kinniburgh *et al.*, 1996). However, predicting metal cation adsorption in soil materials from these results following the component additivity approach is still difficult, because most soils contain a multitude of sorbent phases with different surface properties (Zachara and Westall, 1998; Davis *et al.*, 1998).

Other studies were concerned with heavy metal adsorption to soil materials covering wide ranges in soil properties. The empirical Freundlich equation and various modifications thereof accounting for the effects of soil pH, organic matter content, Ca concentration, and other parameters, are used to model the experimental data (Anderson and Christensen, 1988; Buchter *et al.*, 1989; Boekhold and van der Zee, 1992; Temminghoff *et al.*, 1995; Elzinga *et al.*, 1999; Sauve *et al.*, 2000). Soil pH and soil organic carbon content were often considered to be the key factors in heavy metal binding (Anderson and Christensen, 1988; Lee *et al.*, 1996; Boekhold and van der Zee, 1992; Elzinga *et al.*, 1999; Sauve *et al.*, 2000). However, most studies were carried out

at background electrolyte concentrations, where non-specific heavy metal adsorption to cation exchange sites is suppressed, and may hence underestimate the role of cation exchange in metal adsorption.

In transport experiments, competitive sorption of several interacting cations results in complex breakthrough patterns. Therefore, modeling heavy metal transport in soils requires adsorption models that accurately describe the relevant processes. To be applicable in field situations, such models should be simple enough to be adjustable to specific soil materials. While an approach based on sorbent-specific models may be overparameterized and therefore difficult to adjust (Zachara and Westall, 1998), Freundlich-type equations on the other hand are not applicable, as they cannot correctly describe the coupled adsorption and transport behavior of several cations in multicomponent systems (Voegelin and Kretzschmar, 2001).

In this study, we present an extensive new dataset on Cd adsorption in an acidic soil material as influenced by major cations and solution pH. A model based on a combination of cation exchange and specific sorption reactions was developed to describe the entire dataset. We demonstrate that the model, coupled to a transport code, correctly predicts Cd transport in the presence of varying Ca solution concentrations. The model was also extended to describe coupled Cd/Zn and Cd/Zn/Ni transport experiments.

3.2 Experimental Section

3.2.1 Soil Material

Acidic soil material was collected from the B-horizon (15-25 cm sampling depth) of a forested soil in northern Switzerland (Riedhof soil, aquic dystric Eutrochrept, silt loam texture, pH 4.1). The air-dried soil material was sieved to various fractions smaller than 2 mm. For all experiments, the sieve fraction 63-400 µm was used in order to achieve a homogeneous column packing. This fraction consisted of small soil aggregates containing 37% sand, 47% silt, and 16% clay. The organic carbon content was 9 g/kg organic carbon. From a 0.01 M $Ca(NO_3)_2$-$Mg(NO_3)_2$-$Ca(NO_3)_2$ column exchange experiment at pH 4.6, a pH dependent effective cation cation exchange capacity ($ECEC_{pH}$) at pH 4.6 ($ECEC_{4.6}$) of 0.060 ± 0.002 mol_c/kg was determined.

3.2.2 Cadmium Adsorption Experiments

Cd adsorption experiments were conducted in Ca, Mg, and Na background electrolyte solutions. The solution concentrations of $CdCl_2$ ranged from 10^{-8} to 10^{-2} M, while the concentrations of the respective background cations ranged from 10^{-4} to 10^{-2} M for $CaCl_2$ and $MgCl_2$ and from 0.05 to 0.5 M for NaCl. The adsorption experiments were carried out using a flow-through reactor technique (Grolimund *et al.*, 1995). Weighed soil samples were placed on cellulose-acetate membrane filters (0.45 μm) in flow-through reactor cells. All cells were connected to a peristaltic pump and the soil samples were extensively pre-conditioned by leaching with 500 mL/g soil 0.5 M $CaCl_2$, 0.5 M $MgCl_2$ or 1.0 M NaCl solution at a rate of 3 mL/min. The pH of influent solutions was adjusted by addition of HCl or NaOH. After the pre-washing step, when the soil was completely saturated with the respective background cation, the influent electrolyte concentration was reduced to the desired background cation concentration. After equilibrium was reached, the reactors were drained and weighed to determine the amounts of entrapped electrolyte solution. They were then refilled with a solution containing the same background electrolyte plus a known amount of $CdCl_2$. In this adsorption step, the cell outflow was connected back to the inflow (closed-loop arrangement) and the solution was circulated through the reactor cells for 24 h. After equilibration, cation concentrations were measured in initial and final solutions by atomic absorption (Varian SpectrAA 400 Flame-AAS) and emission (Varian Liberty 200 ICP-AES) spectroscopy. Adsorbed amounts of Cd were calculated from the differences between initial and final solution concentrations and soil weights. The ratio of soil mass to solution volume in each reactor was varied from 50 to 1000 g/L in order to obtain a Cd adsorption between 20% and 80%, allowing reliable estimates of the adsorbed amounts as a function of Cd concentration in solution. A slightly different method was used in the case of Cd adsorption in 10^{-2} M $CaCl_2$ background at pH 5.5: The circulating solution in the closed loop setup was repeatedly spiked with increasing Cd concentrations. Cd, Ca, and pH were monitored online using ion-selective and pH electrodes, respectively. The amount adsorbed was calculated from the difference between the added and the remaining amount of Cd in solution at equilibrium (before next spike). In general, the final pH in the circulating solutions was within initial pH ±

0.3. Only at the highest Cd concentrations and in low background cation concentrations, final pH could decrease to lower values.

3.2.3 Transport Experiments

Solute transport experiments were conducted in Cd/Ca, Cd/Zn/Ca, and Cd/Zn/Ni/Ca cation systems at pH 4.6 using a packed soil column technique. Chromatographic glass columns (Omni) were uniformly packed with dry soil material and flushed with CO_2 gas to displace the air from the pore space. The columns were then connected to a HPLC pump and pre-conditioned by passing several hundred pore volumes of 0.5 M $CaCl_2$ solution adjusted to pH 4.6. Solutions were first passed through a degasser and then through the columns in the upward direction. Due to rapid dissolution of CO_2 gas, complete water saturation was achieved within a few pore volumes. To characterize the hydrodynamic properties of the soil columns, a short (0.1 mL) nitrate pulse was injected and the resulting nitrate breakthrough peak was monitored on-line using an UV-VIS detector set to 220 nm wavelength. Pore volume, dispersivity, and column Péclet number were determined numerically from the flow rate and the first or second

Table 3.1: Transport experiments: column properties, flow conditions, and composition of the feed solution

Exp.	Column parameters							Influent concentrations c_0				
Nr.	L	d	θ	ρ	v_p	Pe	PV	$CdCl_2$	$ZnCl_2$	$NiCl_2$	[a]$CaCl_2$	pH
	cm	cm	%	kg/L	cm/min			μM	μM	μM	mM	
1	9.15	1	58	1.99	1.1	400	35	9.7			10	4.6
2	5.15	1	60	1.99	1.1	200	200	9.8			1	4.6
3	1.85	1	60	2.01	1.1	150	800	9.6			0.101	4.6
4	10.0	1	61	1.95	1.1	400	30	0.98	95		10.1	4.6
5	4.0	1	68	1.87	1.1	100	150	0.99	95		1.01	4.6
6	8.0	2.5	62	1.86	0.41	150	100	28.5	281	29.5	1.03	4.6

[a]background concentration, L=length, d=diameter, θ=porosity, ρ=mass of soil per pore volume, v_p=pore water velocity, Pe=Péclet number, PV=number of pore volumes during which heavy metal containing background electrolyte solution was pumped through the column.

moments of the nitrate breakthrough curves (Villermaux, 1981). Resulting column parameters and further experimental details are given in Table 3.1.

For transport experiments, the columns were first leached with the background electrolyte solution, until the column effluent had the same Ca concentration and pH (4.6) as the influent solution. The influent was then switched to a heavy metal containing solution with the same concentration of $CaCl_2$. After complete heavy metal breakthrough was observed, the influent was switched back to the background electrolyte without heavy metals. Thus, the breakthrough curves corresponding to adsorption and desorption were monitored. The effluents were sampled with a fraction collector and concentrations of Ca, Cd, Zn, and Ni were measured by atomic absorption spectrometry. The duration of heavy metal inputs and the composition of feed solutions are provided in Table 3.1.

3.3 Modeling Section

Metal adsorption in soils can include non-specific (i.e., coulombic, outer-sphere) interactions, such as cation exchange at negatively charged surfaces of clay minerals and organic matter, as well as specific (i.e., covalent, inner-sphere) binding of metal cations at reactive sites of mineral surfaces and organic matter functional groups (Hendrickson and Corey, 1981; Sposito, 1989; McBride, 1994). In our model, non-specific sorption of heavy metals was described by cation exchange equations. For example, Cd-Ca exchange is written as

$$CaX_2 + Cd^{2+} \rightleftarrows CdX_2 + Ca^{2+} \tag{3.1}$$

where X denotes exchanger sites with charge -1. The activities of sorbed species were assumed to correspond to the charge equivalent fractions according to the convention of Gaines and Thomas (Gaines and Thomas, 1953). For the binary Cd-Ca system, the following Cd exchange isotherm is obtained

$$q_{CdX_2} = \frac{1}{2} ECEC_{pH} \frac{K_{CdCa} a_{Cd^{2+}}}{K_{CdCa} a_{Cd^{2+}} + a_{Ca^{2+}}} \tag{3.2}$$

where K_{CdCa} is the Gaines-Thomas exchange coefficient, a_{M2+} is the activity of free metal M, and q_{CdX2} the amount of Cd adsorbed (in mol/kg). The cation exchange coefficients were assumed to be pH-independent. However, the pH dependence of the $ECEC_{pH}$ was derived from a published regression equation, which relates the soil $ECEC_{pH}$ to clay content, organic carbon content, and soil pH (Curtin and Rostad, 1997). By scaling this equation to the measured $ECEC_{4.6}$, the following slightly modified equation for $ECEC_{pH}$ (in mol_c/kg) in the Riedhof soil was obtained (for pH 4 to 7):

$$ECEC_{pH} = -0.0024 + 0.0135pH \tag{3.3}$$

In addition to non-specific cation exchange, heavy metals can specifically adsorb to high-affinity binding sites located on soil organic matter and oxide or clay mineral surfaces. To account for such reactions, we introduced an additional type of sorption sites using non-electrostatic site binding equations. The use of electrostatic correction terms would have been questionable due to the complexity of soil materials (Zachara and Westall, 1998; Davis *et al.*, 1998). The specific sorption sites were assumed to have a much greater affinity for heavy metal cations (Cd, Zn, Ni) than for Ca and Mg, respectively. For the adsorption of Cd^{2+} or Ca^{2+}, this approach yields the following adsorption equation

$$M^{2+} + L^{-} \rightleftarrows ML^{+} \tag{3.4}$$

where L^{-} denotes free sites and ML^{+} sites occupied by metal M^{2+}. The conditional sorption coefficient for Eq. 3.4 at experimental pH is then given by:

$$K_{M,pH} = \frac{q_{CdL^{+}}}{q_L a_{Cd^{2+}}} \tag{3.5}$$

where q_{CdL^+} denotes Cd adsorbed to sites L and q_L is the amount of free sites (both in mol/kg). The pH dependence of metal adsorption to these sites was introduced by assuming that the conditional sorption coefficients vary with pH according to:

$$\log K_{M,pH} = \log K_{M,0} + n_M pH \tag{3.6}$$

where $\log K_{M,pH}$ and $\log K_{M,0}$ are the logarithms of the sorption coefficient at experimental pH and reference pH=0, respectively. The parameter n_M determines the extend of pH dependence of the respective conditional sorption coefficient. For the binary Cd/Ca system, the following Cd competitive adsorption isotherm is then obtained

$$q_{CdL^+} = L_T \frac{K_{Cd,pH} a_{Cd^{2+}}}{1 + K_{Ca,pH} a_{Ca^{2+}} + K_{Cd,pH} a_{Cd^{2+}}} = L_T \frac{K_{Cd,0} a_H^{-n_{Cd}} a_{Cd^{2+}}}{1 + K_{Ca,0} a_H^{-n_{Ca}} a_{Ca^{2+}} + K_{Cd,0} a_H^{-n_{Cd}} a_{Cd^{2+}}} \tag{3.7}$$

where L_T is the total concentration of specific sorption sites (in mol/kg). While the left isotherm in Eq. 3.7 is based on the conditional sorption coefficients for a given pH, the right expression uses the reference sorption coefficients for pH=0. This equation could have also been derived by postulating metal adsorption with fractional proton release ($M^{2+} + L^- \rightleftarrows ML^+ + n_M H^+$ with $K_M = K_{M,0}$). This formulation is often used to account for the observed fractional pH dependence of adsorption reactions on soil organic matter, and the release of protons is either explained by partial hydrolysis of the adsorbing cation or fractional deprotonation of the sorbent (McBride *et al.*, 1997; Temminghoff *et al.*, 1995). The total Cd adsorbed finally is obtained from the sum of Cd adsorbed to the exchange sites (Eq. 3.2) and the specific sorption sites (Eq. 3.7):

$$q_{Cd} = q_{CdX_2} + q_{CdL^+} \tag{3.8}$$

Solution speciation was calculated with thermodynamic complex formation constants K_0 derived from conditional constants (Smith and Martell, 1976; Martell and Smith, 1982; Smith and Martell, 1989) using the Davies equation (Sposito, 1981). Complexed species

considered (with $\log K_0$ for $M + nL \rightleftharpoons ML_n$ in parenthesis) were: $CaCl^+$ (0.58), $MgCl^+$ (0.63), $NaCl^0$ (-0.19), $CdCl^+$ (1.98), $CdCl_2^0$ (2.60), $ZnCl^+$ (0.46), $ZnCl_2^0$ (0.61), $NiCl^+$ (0.40). Transport predictions based on the local equilibrium assumption were calculated with ECOSAT, which numerically solves the convection dispersion equation (Keizer *et al.*, 1993). Input parameters were the column Péclet number (respectively column length, porosity, Darcy velocity, and diffusion coefficient), the bulk density of the soil material, the sorption model parameters, the complex formation constants, and the sequence and composition of feed solutions (Table 3.1).

3.4 Results and Discussion

3.4.1 Cd Adsorption in Ca Background at Constant pH

Experimental adsorption isotherms of Cd in the presence of four different Ca background concentrations at pH 4.6 and corresponding CESS model calculations are presented in Figure 3.1A. Examining the experimental data first, three main features are evident: (i) The maximum amount of Cd adsorbed is limited by the $ECEC_{4.6}$ of the soil material, (ii) at low Cd concentrations, the isotherms exhibit a constant slope near one on a log-log plot, and (iii) the amount of adsorbed Cd generally decreases with increasing Ca concentration. Qualitatively, all of these findings are consistent with Cd adsorption by cation exchange. Hence, as a first approximation, Cd adsorption was modeled with a Gaines-Thomas cation exchange equation only (Eq. 3.1, CE model). While $ECEC_{4.6}$ was determined independently, the value of K_{CdCa} was adjusted to describe Cd adsorption at the lowest Ca concentration, where cation exchange is expected to dominate Cd adsorption. The resulting model calculations show that a pure cation exchange (CE) model can describe Cd adsorption at low Ca concentration, but strongly underestimates Cd adsorption at high Ca concentrations (Figure 3.1A, dashed lines). This suggests that the soil material may contain additional sorption sites with a high Cd affinity (Hendrickson and Corey, 1981). Thus, additional competitive binding sites with higher Cd affinity were introduced (Eq. 3.4). Additional model parameters are the conditional site binding coefficients (Eq. 3.6) and the site concentration. The combined cation exchange / specific sorption (CESS) model returned a greatly improved

description of the experimental data over the entire range in Cd and Ca concentrations (Figure 3.1A, solid lines). Corresponding model parameters are reported in Table 3.2. The conditional sorption coefficients reflect the high Cd affinity of the specific sorption sites. While cation exchange accounts for most Cd adsorbed at low Ca and/or high Cd concentrations, the specific sorption sites account for Cd adsorption in the presence of high Ca concentrations.

The same adsorption data together with a scaled Freundlich fit is presented in Figure 3.1B. The modified Freundlich equation $\log(q_{Cd}) = -0.72 + 0.86\log(a_{Cd2+}) - 0.52\log(a_{Ca2+})$ with only 3 adjustable parameters also yields a good description of the experimental data. However, further use of this model for transport calculation is limited for several reasons. As can be seen from the Cd adsorption data in 10^{-4} M $CaCl_2$ background, the model does not account for the adsorption maximum corresponding to the $ECEC_{4.6}$. It yields a constant isotherm slope of 0.86, which apparently represents a compromise between the experimental slope of 1 at low Cd concentrations and the decreasing slope towards the adsorption maximum. The slight curvature in the plotted Freundlich model calculations at high Cd concentrations result from the measured increase in equilibrium Ca concentration due to Cd-Ca exchange. Finally, the Freundlich model only represents a description of the Cd adsorption data, without assuming any consistent underlying reaction equations with defined stoichiometry. For these reasons, the model can not be extended to systems with additional cations and can not describe coupled multicomponent transport patterns involving several interacting cations (Voegelin and Kretzschmar, 2001).

Figure 3.1C shows the experimental data along with model *predictions* based on a component additivity approach. In these calculations, Cd sorption to the clay fraction was calculated using the Gaines-Thomas cation exchange equation and Cd binding to soil organic matter was predicted with the NICA-Donnan model (Kinniburgh *et al.*, 1996; Kinniburgh *et al.*, 1999). In this prediction, we assumed that 9 g/kg organic carbon correspond to approximately 7.7 g/kg of humic acid, implying that about 50% of the organic matter content consists of reactive humic acids. Cd, Ca, and H adsorption was calculated with ECOSAT (Keizer *et al.*, 1993) using recently published generic NICA-Donnan parameters for humic acid (Milne, 2000). To account for non-

preferential Cd adsorption on the soil clay fraction, a Gaines-Thomas cation exchange site was introduced in analogy to Eq. 3.1 with a K_{CdCa} equal to 1. Based on the measured $ECEC_{4.6}$ and on published regression equations for clay and organic carbon contributions to soil ECEC (Curtin and Rostad, 1997), the ECEC of the soil clay fraction at pH 4.6 was estimated as 0.049 mol_c/kg. The calculated contribution of Cd adsorption to humic substances (dashed lines, Figure 3.1C) indicate that Cd binding to the organic matter fraction plays an important role. The combined model yields a reasonable *prediction* of the Cd adsorption data (solid lines), considering the uncertainty of the assumption made. However, to obtain a more accurate *description* of the Cd adsorption data, further model calibration to the Riedhof soil material would still be necessary. This would again result in an empirical fit to the experimental data, however, with a model approach that has a larger number of adjustable parameters than the CESS model.

Table 3.2: Conditional cation exchange / specific sorption (CESS) model parameters for the Riedhof soil at pH 4.6 and methods of parameter estimation

Cation exchange site[a]		
$ECEC_{4.6}$ (mol_c/kg)	0.060	measured independently
K_{CdCa}	0.5	fitted to Cd adsorption data in 10^{-4} M $CaCl_2$ / pH 4.6
K_{MgCa}	0.7	from Voegelin *et al.* (2000)
K_{NaCa}	0.125	from Voegelin *et al.* (2000)
K_{ZnCa}	0.5	estimated as equal to K_{CdCa}
K_{NiCa}	0.5	estimated as equal to K_{CdCa}
Specific sorption site[b]		
L_T (mol/kg)	0.002	fitted to Cd adsorption data at pH 4.6
$K_{Cd,4.6}$	21000	fitted to Cd adsorption data at pH 4.6
$K_{Ca,4.6}$	450	fitted to Cd adsorption data at pH 4.6
$K_{Mg,4.6}$	315	estimated: $K_{Mg,4.6}= K_{Ca,4.6}K_{MgCa}$
$K_{Zn,4.6}$	10000	fitted to transport experiments 4 and 5 (at pH 4.6)
$K_{Ni,4.6}$	10000	estimated as equal to $K_{Zn,4.6}$

[a] based on Gaines-Thomas cation exchange convention, Eqs. 3.1-3.3;
[b] based on non-electrostatic site binding Eqs. 3.4-3.7

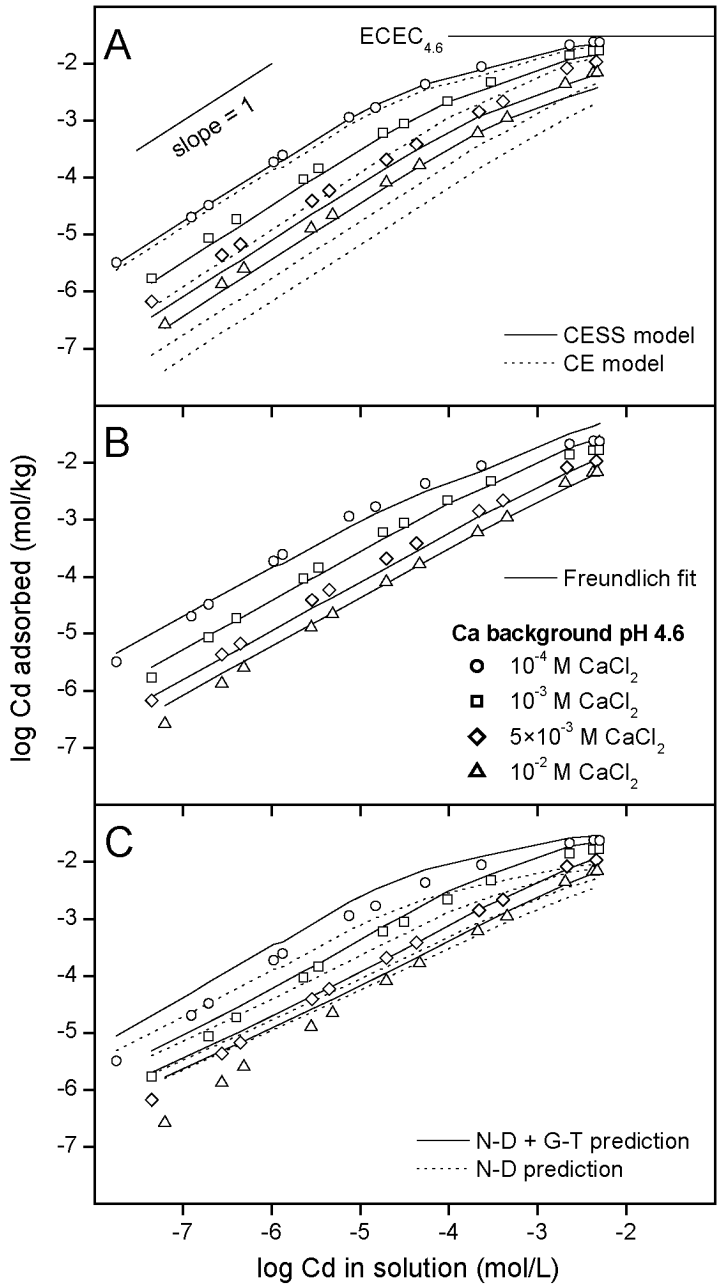

Figure 3.1: Cd adsorption isotherms measured in different $CaCl_2$ background electrolyte concentrations at pH 4.6 (symbols) described by various modeling approaches. Adsorption increases at decreasing Ca cation concentration. Maximum adsorption is limited by the $ECEC_{4.6}$. (A) Cation exchange / specific sorption model *fit* (CESS, solid lines) and cation exchange model *fit* (CE, dotted lines). (B) Freundlich model *fit* (solid lines). (C) NICA-Donnan / Gaines-Thomas model *prediction* (solid lines) and NICA-Donnan part only corresponding to Cd adsorption to soil organic matter (dotted lines). All model calculations are based on measured final cation concentrations

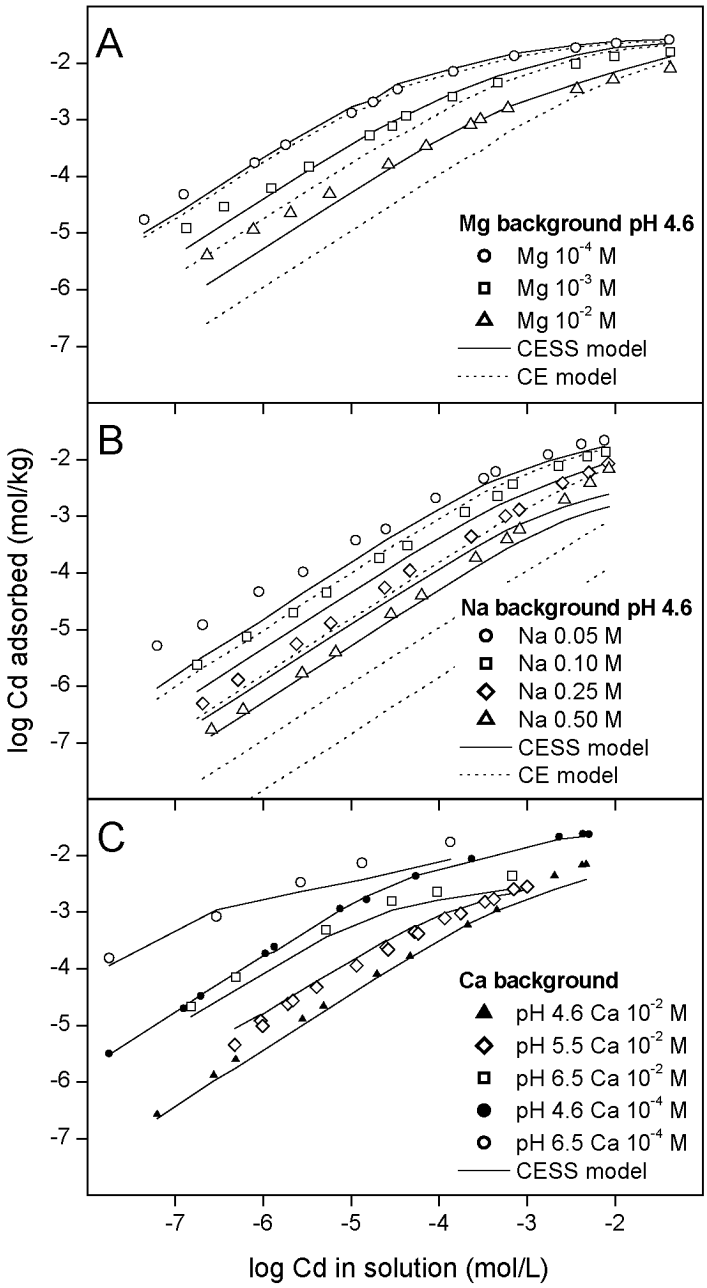

Figure 3.2: Extension of the CESS model to Cd adsorption in (A) Mg and (B) Na background electrolyte solutions at pH 4.6 and (C) to Cd adsorption at variable pH in Ca background electrolyte solutions. CESS model *predictions* (solid lines) for Cd adsorption in Mg and Na background electrolyte (A, B) are clearly improved compared to the CE model (dotted lines). The CESS model could also be *fit* to Cd adsorption at variable pH in Ca background electrolyte (C). All model calculations are based on measured final cation concentrations

3.4.2 Cd Adsorption in Mg and Na Background

In a previous paper, we reported on the competitive sorption of the major cations Ca, Mg, and Na to the same soil material at pH 4.6 (Voegelin *et al.*, 2000). The resulting Gaines-Thomas exchange coefficients were K_{MgCa}=0.70 and K_{NaCa}=0.125, respectively. In the CESS model, these values were adopted for the cation exchange sites, but the conditional sorption coefficients for Mg and Na to the specific sorption sites had to be estimated. For Mg adsorption, we assumed that the specific sorption sites exhibit the same preference for Ca over Mg as indicated by the Gaines-Thomas Ca-Mg exchange coefficient, K_{MgCa} (Table 3.2). This seems reasonable, because the adsorption preference for Ca originates mainly from organic matter in soils (Sposito and Fletcher, 1985). Adsorption of monovalent Na ions to the specific sorption sites was assumed to be negligible. Figures 3.2A and 3.2B show the experimental Cd adsorption isotherms and corresponding model predictions obtained with the pure cation exchange model (dashed lines) and the CESS model (solid lines), respectively. In both types of background electrolyte, the CESS model gave clearly improved predictions of Cd adsorption to the soil material. In $MgCl_2$ background electrolyte, the CESS model predicted Cd adsorption quite accurately. In NaCl background electrolyte, larger deviations are still observed, which may in part be related to the high chloride concentrations in solution, as discussed later.

3.4.3 Cd Adsorption in Ca Background at Variable pH

To account for pH effects on Cd adsorption, the conditional CESS model (Table 3.2) was extended as described earlier (Eqs. 3.3 and 3.6). The pH-dependence of the $ECEC_{pH}$ (Eq. 3.3) was adopted from the literature (Curtin and Rostad, 1997). Hence, only the pH dependence of the specific sorption coefficients, i.e., the parameters n_{Cd} and n_{Ca} (Eq. 3.6), were adjusted to optimize the description of the Cd adsorption data at variable pH. Figure 3.2C shows that the extended model yields a good description (solid lines) of Cd adsorption at pH values above 4.6 (open symbols), notably at Ca background concentration levels differing by two orders of magnitude. It is interesting to note that at low Cd concentrations, the effect of increasing pH by ~2 units is comparable to the effect of decreasing the Ca concentration by two log units. At high Cd concentrations,

Table 3.3: Cation exchange / specific sorption (CESS) model parameters for Cd adsorption to the Riedhof soil at variable pH in Ca background electrolyte and methods of parameter estimation

Cation exchange site[a]		
$ECEC_{pH}$ (mol_c/kg)	-0.0024 + 0.0135pH	adopted from literature, Eq. 3.3
K_{CdCa}	0.5	from Table 3.2
Specific sorption site[b]		
L_T (mol/kg)	0.002	from Table 3.2
n_{Cd}	1.224	fitted to Cd adsorption data with pH>4.6
$\log K_{Cd,0}$	-1.307	calculated from $K_{Cd,4.6}$ and n_{Cd}, Eq. 3.6
n_{Ca}	0.588	fitted to Cd adsorption data with pH>4.6
$\log K_{Ca,0}$	-0.050	calculated from $K_{Ca,4.6}$ and n_{Ca}, Eq. 3.6

[a] based on Gaines-Thomas cation exchange convention, Eqs. 3.1-3.3;
[b] based on non-electrostatic site binding Eqs. 3.4-3.7

however, the decrease in Ca concentration has a larger effect than the increase in pH. This is in agreement with the model assumption that pH mainly affects metal adsorption to the small number of high affinity sites, whereas Ca has a stronger effect on adsorption to the larger number of non-specific exchange sites. The parameters for the pH dependent Cd adsorption model in Ca background electrolyte are given in Table 3.3.

3.4.4 Cd-Ca Transport Experiments

Breakthrough curves of 10^{-5} M Cd in the presence of three different Ca concentrations in the influent (10^{-4} to 10^{-2} M) are presented in Figure 3.3 (Table 3.1, Experiments 1 to 3). Decreasing Ca concentration from 10^{-2} to 10^{-4} M resulted in a strong increase of Cd retention. Note, that the number of pore volumes is shown on a log scale. The arrows indicate the switch to Cd-free influent solutions and subsequent desorption of Cd. The influence of Ca on Cd transport is consistent with the effects on Cd adsorption shown in Figure 3.1. As expected, the pure cation exchange model (CE, dashed lines) provided a reasonable prediction of Cd transport at low Ca concentration (10^{-4} M), but strongly

underestimated Cd retention at higher Ca levels. In contrast, the CESS model (solid lines) accurately predicted Cd transport behavior at all three Ca concentrations.

3.4.5 Cd-Zn-Ca Transport Experiments

Cd contamination most often occurs together with other heavy metals, especially with Zn. The average Zn to Cd ratio in rock materials is typically around 500:1 and a similar ratio is often observed in contaminated soils (Alloway, 1995). More relevant than pure Cd transport experiments may therefore be coupled transport experiments of Cd and Zn. Figures 3.4A and 3.4B show the breakthrough of 10^{-6} M Cd in the presence of 10^{-4} M Zn in 10^{-2} and 10^{-3} M $CaCl_2$ background electrolyte (Table 3.1, Experiments 4 and 5).

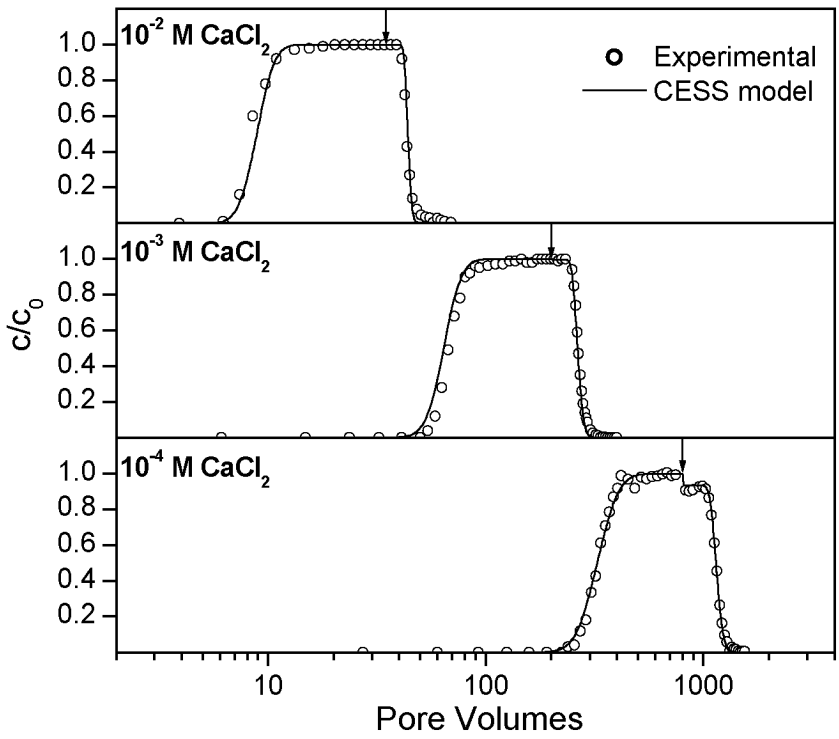

Figure 3.3: Breakthrough curves of Cd in the presence of 10^{-2}, 10^{-3}, and 10^{-4} M $CaCl_2$ background electrolyte at pH 4.6 (Experiments 1-3). The influent solution contained 10^{-5} M $CdCl_2$; arrows indicate the switch back to Cd free influent solutions. Experimental data (symbols) are compared with corresponding model predictions based on a pure cation exchange (CE) model and the cation exchange / specific sorption (CESS) model, respectively.

The addition of Zn resulted in a decrease in Cd retardation by approximately 15-20% when compared to the respective Zn free experiments (data not shown). The mobilizing effect of Zn relative to its concentration is more pronounced than the effect of Ca. Zn is likely to specifically adsorb to the same sites as Cd (Christensen, 1987b) and hence is a stronger competitor for specific sites than Ca. This demonstrates that a model designed to describe a real multicomponent soil system must include the competitive sorption of several heavy metals. Zn adsorption was incorporated into the model by defining the respective exchange and specific sorption reactions in analogy to Cd. The exchange coefficient K_{ZnCa} was set equal to K_{CdCa}, assuming similar adsorption behavior of Zn and Cd to the non-specific cation exchange sites. The specific Zn sorption coefficient $K_{Zn,4.6}$ was adjusted to a lower value than $K_{Cd,4.6}$ to obtain an adequate description of Zn breakthrough in 10^{-3} M $CaCl_2$ electrolyte solution (Figure 3.4B) occurring slightly ahead of Cd breakthrough. In contrast, at the higher $CaCl_2$ concentration (Figure 3.4A), Zn breakthrough occurred slightly after Cd breakthrough. This effect was correctly predicted with the CESS model, and can be explained by the greater stability of the $CdCl^+$ than of the $ZnCl^+$ complex, assuming that metal chloride complexes do not adsorb to the soil material (Doner, 1978).

3.4.6 Cd-Zn-Ni-Ca Transport Experiments

At concentration levels typical for contaminated soils, Ni was reported to exhibit a similar adsorption behavior as Cd or Zn (Buchter *et al.*, 1989; Wang *et al.*, 1997). Experimental results and model predictions for the combined breakthrough of Cd, Zn, and Ni in 10^{-3} M $CaCl_2$ background electrolyte (Table 3.1, Experiment 6) are presented in Figure 3.4C. Breakthrough of Cd and Zn occurs simultaneously, while Ni is slightly more retarded. In the model calculation, Ni sorption parameters were set equal to those of Zn. Though the model is slightly off for all three metals, the experiment clearly shows the similar adsorption behavior, notably at acidic conditions and rather high concentration levels.

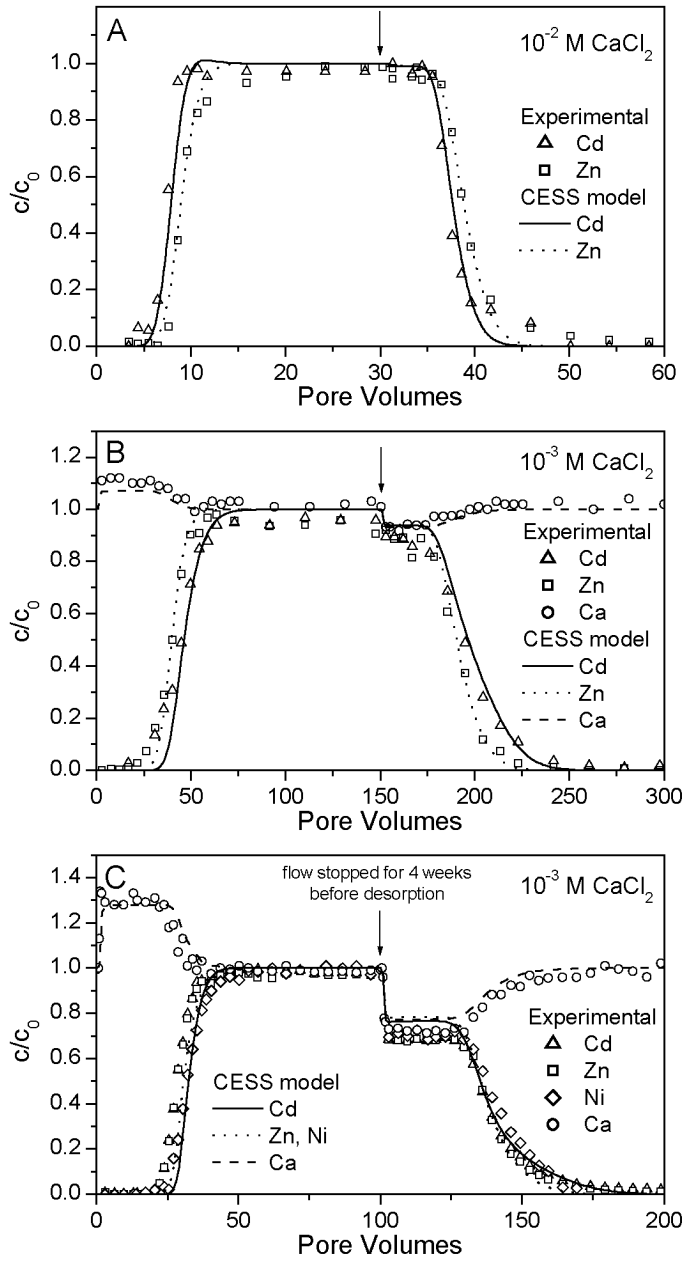

Figure 3.4: Coupled breakthrough curves of Cd, Zn, Ni, and Ca at pH 4.6: (A) 10^{-6} M $CdCl_2$ and 10^{-4} M $ZnCl_2$ in 10^{-2} M $CaCl_2$ background electrolyte solution (Exp. 4) (B) 10^{-6} M $CdCl_2$ and 10^{-4} M $ZnCl_2$ in 10^{-3} M $CaCl_2$ background electrolyte solution (Exp. 5), and (C) 3×10^{-5} M $CdCl_2$, 3×10^{-4} M $ZnCl_2$, and 3×10^{-5} M $NiCl_2$ in 10^{-3} M $CaCl_2$ background electrolyte solution (Exp. 6). Arrows indicate the switch back to heavy metal free influent solutions. In (C), the flow was stopped for 4 weeks prior to leaching with heavy metal free influent solution. Symbols represent experimental data; lines represent CESS model calculations.

The Ca concentration plateaus above influent concentration during heavy metal adsorption, and below influent Ca concentration during heavy metal desorption clearly indicate ongoing exchange and competitive sorption processes between Ca and Zn, Cd, and Ni. The sharp increase of the Ca effluent concentration at 1 pore volume and the sharp decrease of all cation concentrations one pore volume after desorption start result from changes in the influent solution normality. In our experiments, these so-called unretarded normality fronts can be observed, where the metal concentrations significantly contribute to total solution normality, i.e., in Experiments 3, 5, and 6. (Figures 3.1 and 3.4BC). All these phenomena again give reasons for the application of a model based on exchange and competitive sorption reactions, and are correctly described by the CESS model. Considering the two other model approaches discussed earlier, it is apparent that the Freundlich equation is not applicable to such multication systems. The component additivity approach on the other hand is rather complex and overparameterized, making it more difficult to adjust the model parameters.

3.4.7 Influence of Anions

Adsorption of stable $CdCl^+$ complexes was neglected in the CESS model, which correctly predicted the mobilizing effect of Cl on Cd in comparison to Zn (Figure 3.4A). This and the results from a limited number of Cd transport and adsorption experiments in $Ca(NO_3)_2$ background electrolyte solution (not shown) suggest, that adsorption of the monovalent $CdCl^+$ complex was indeed negligibly weak compared to the adsorption of bivalent metal cations, as observed by other researchers (Boekhold *et al.*, 1993; Temminghoff *et al.*, 1995). In the case of Cd adsorption in NaCl background electrolytes, notably at very high Cl concentrations (0.05 to 0.5 M), Cd adsorption was underestimated by the CESS model (Figure 3.2B). This may be due to adsorption of $CdCl^+$ complexes. Compared to the effects of competing cations however, the influence of the background anion is in any case of minor importance, and for most practical purposes, neglecting $CdCl^+$ adsorption seems to be justified.

3.4.8 Kinetic Effects and Reversibility

Transport calculations based on the local equilibrium assumption correctly described adsorption as well as desorption curves (Figures 3.3 and 3.4), suggesting that kinetic effects were not decisive and that adsorption was reversible. These findings were confirmed by further transport experiments where flow rates were varied over two orders of magnitude and by repeated adsorption/desorption cycles in the same soil columns (not shown). In Experiment 6 (Figure 3.4C), the flow was stopped for four weeks after Cd, Zn, and Ni in the effluent had reached the influent concentration levels, leading to an increase in solution residence time by approximately a factor 2000. When desorption was started, solution pH had increased from pH 4.6 to 5.4, probably due to H-Ca exchange. However, it quickly decreased again and reached the influent pH 4.6 within several pore volumes. All cation concentrations in the effluent were slightly lower than predicted, however, the effect was small and may have been caused by physical processes, e.g. slow diffusion of ions into small pores. Overall we found that in the presented experiments, kinetic effects were of minor importance and heavy metal adsorption was reversible. It has to be kept in mind, however, that this applies for experiments carried out at rather high heavy metal concentrations typical for contaminated soils ($>10^{-6}$ M), under acidic conditions, and in a soil material with low organic matter content. More pronounced kinetic effects might occur in soils with higher organic matter contents (Strawn and Sparks, 2000). At higher pH values, greater differences in the sorption behavior of Cd, Ni, and Zn and stronger kinetic effects must be expected. At neutral to basic conditions, slow formation of new solid phases such as hydroxides or layered double hydroxides may cause kinetic effects and immobilization of heavy metals (Roberts *et al.*, 1999; Thompson *et al.*, 2000; Ford and Sparks, 2000; Scheidegger *et al.*, 1998).

3.4.9 Model Performance

The combined cation exchange / specific sorption (CESS) model approach accurately predicted Cd transport in soil columns and was successfully extended to account for competitive sorption and transport of Zn and Ni. The model is based on stoichiometrically balanced sorption reaction equations, and can be extended to

additional components by adding the respective reaction equations. This allows the description of multicomponent systems based on model parameters derived in simpler, e.g., binary systems. The presented model is conditional for one specific acidic soil material. Nevertheless the general approach presented here should be applicable to other soil materials. Due to the inherent heterogeneity of soils, parameter adjustment will be necessary to achieve an accurate description of competitive metal sorption and transport behavior.

References

Abd-Elfattah, A., Wada, K., *Adsorption of lead, copper, zinc, cobalt, and cadmium by soils that differ in cation-exchange materials*. Journal of Soil Science 32, 271-283, **1981**.

Alloway, B.J., ed., *Heavy Metals in Soils*. Chapman & Hall, London, **1995**.

Anderson, P.R., Christensen, T.H., *Distribution coefficients of Cd, Co, Ni, and Zn in soils*. Journal of Soil Science 39, 15-22, **1988**.

Benedetti, M.F., Milne, C.J., Kinniburgh, D.G., van Riemsdijk, W.H., Koopal, L.K., *Metal ion binding to humic substances: Application of the non-ideal competitive adsorption model*. Environmental Science and Technology 29, 446-457, **1995**.

Boekhold, A.E., Temminghoff, E.J.M., van der Zee, S.E.A.T.M., *Influence of electrolyte composition and pH on cadmium sorption by acid sandy soil*. Journal of Soil Science 44, 85-96, **1993**.

Boekhold, A.E., van der Zee, S.E.A.T.M., *A scaled sorption model validated at the column scale to predict cadmium contents in a spatially variable field soil*. Soil Science 154, 105-112, **1992**.

Buchter, B., Davidoff, B., Amacher, M.C., Hinz, C., Iskandar, I.K., Selim, H.M., *Correlation of freundlich Kd and n retention parameters with soils and elements*. Soil Science 148, 370-379, **1989**.

Christensen, T.H., *Cadmium soil sorption at low concentrations: I. Effect of time, cadmium load, pH, and calcium*. Water, Air, and Soil Pollution 21, 105-114, **1984**.

Christensen, T.H., *Cadmium soil sorption at low concentrations: V. Evidence of competition by other heavy metals*. Water, Air, and Soil Pollution 34, 293-303, **1987a**.

Christensen, T.H., *Cadmium soil sorption at low concentrations: VI. A model for zinc competition*. Water, Air, and Soil Pollution 34, 305-314, **1987b**.

Curtin, D., Rostad, H.P.W., *Cation exchange and buffer potential of Saskatchewan soils estimated from texture, organic matter and pH*. Canadian Journal of Soil Science 77, 621-626, **1997**.

Davis, J.A., Coston, D.B., Fuller, C.C., *Application of the surface complexation concept on complex mineral assemblages*. Environmental Science and Technology 32, 2820-2828, **1998**.

Doner, H.E., *Chloride as a factor in mobilities of Ni(II), Cu(II), and Cd(II) in soil*. Soil Science Society of America Journal 42, 882-885, **1978**.

Elzinga, E.J., van Grinsven, J.J.M., Swartjes, F.A., *General purpose Freundlich isotherms for cadmium, copper and zinc in soils*. European Journal of Soil Science 50, 139-149, **1999**.

Ford, R.G., Sparks, D.L., *The nature of Zn precipitates formed in the presence of pyrophyllite*. Environmental Science and Technology 34, 2479-2483, **2000**.

Gaines, G.L.J., Thomas, H.C., *Adsorption studies on clay minerals. II: A formulation of the thermodynamics of exchange adsorption*. The Journal of Chemical Physics 21, 714-718, **1953**.

Goldberg, S., *Use of surface complexation models in soil chemical systems*. Advances in Agronomy 47, 233-329, **1992**.

Grolimund, D., Borkovec, M., Federer, P., Sticher, H., *Measurement of sorption isotherms with flow-through reactors*. Environmental Science and Technology 29, 2317-2321, **1995**.

Hendrickson, L.L., Corey, R.B., *Effect of equilibrium metal concentrations on apparent selectivity coefficients of soil complexes*. Soil Science 131, 163-171, **1981**.

Keizer, M.G., De Wit, J.C., Meussen, J.C.L., Bosma, W.J.P., Nederlof, M.M., Venema, P., Meussen, V.C.S., van Riemsdijk, W.H., van der Zee, S.E.A.T.M., *ECOSAT, A computer program for the calculation of speciation in soil-water systems.* Wageningen, The Netherlands, **1993**.

Kinniburgh, D.G., Milne, C.J., Benedetti, M.F., Pinheiro, J.P., Filius, J., Koopal, L.K., van Riemsdijk, W.H., *Metal ion binding by humic acid: Application of the NICA-Donnan model*. Environmental Science and Technology 30, 1687-1698, **1996**.

Kinniburgh, D.G., van Riemsdijk, W.H., Koopal, L.K., Borkovec, M., Benedetti, M.F., Avena, M.J., *Ion binding to natural organic matter: competition, heterogeneity, stoichiometry and thermodynamic consistency*. Colloids and Surfaces A-physicochemical and engineering aspects 151, 147-166, **1999**.

Lee, S.-Z., Allen, H.E., Huang, C.P., Sparks, D.L., Sanders, P.F., Peijnenburg, W.J.G.M., *Predicting soil-water partition coefficients for cadmium*. Environmental Science and Technology 30, 3418-3424, **1996**.

Martell, A.E., Smith, R.M., *Critical Stability Constants, Vol. 5*. Plenum, New York, **1982**.

McBride, M., Sauvé, S., Hendershot, W., *Solubility control of Cu, Zn, Cd, and Pb in contaminated soils*. European Journal of Soil Science 48, 337-346, **1997**.

McBride, M.B., *Environmental Chemistry of Soils*. Oxford University Press, New York, **1994**.

Milne, C.J. , *Measurement and modelling of ion binding by humic substances*. PhD thesis, University of Reading, Reading, **2000.**

Roberts, D.R., Scheidegger, A.M., Sparks, D.L., *Kinetics of mixed Ni-Al precipitate formation on a soil clay fraction*. Environmental Science and Technology 33, 3749-3754, **1999**.

Sauve, S., Hendershot, W., Allen, H.E., *Solid-solution partitioning of metals in contaminated soils: dependence on pH, total metal burden, and organic matter*. Environmental Science and Technology 34, 1125-1131, **2000**.

Scheidegger, A.M., Strawn, D.G., Lamble, G.M., Sparks, D.L., *The kinetics of mixed Ni-Al hydroxide formation on clay and aluminium oxide minerals: A time-resolved XAFS study*. Geochimica et Cosmochimica Acta 62, 2233-2245, **1998**.

Smith, R.M., Martell, A.E., *Critical Stability Constants, Vol. 4.* Plenum, New York, **1976**.

Smith, R.M., Martell, A.E., *Critical Stability Constants, Vol. 6.* Plenum, New York, **1989**.

Sposito, G., *The Thermodynamics of Soil Solutions.* Oxford University Press, New York, **1981**.

Sposito, G., *The chemistry of soils.* Oxford University Press, New York, **1989**.

Sposito, G., Fletcher, P., *Sodium-calcium-magnesium exchange reactions on a montmorillonitic soil: III. Calcium-magnesium exchange selectivity.* Soil Science Society of America Journal 49, 1160-1163, **1985**.

Strawn, D.G., Sparks, D.L., *Effects of soil organic matter on the kinetics and mechanisms of Pb(II) sorption and desorption in soils.* Soil Science Society of America Journal 64, 144-156, **2000**.

Temminghoff, E.J.M., van der Zee, S.E.A.T.M., de Haan, F.A.M., *Speciation and Calcium competition effects on Cadmium sorption by sandy soils at various pH levels.* European Journal of Soil Science 46, 649-655, **1995**.

Thompson, H.A., Parks, G.A., Brown, G.E.J., *Formation and release of cobalt(II) sorption and precipitation products in aging kaolinite-water slurries.* Journal of Colloid and Interface Science 222, 241-253, **2000**.

Venema, P., Hiemstra, T., van Riemsdijk, W.H., *Comparison of different site binding models for cation sorption: Description of pH dependency, salt dependency, and cation -proton exchange.* Journal of Colloid and Interface Science 181, 45-49, **1996**.

Villermaux, J., *Theory of linear chromatography.* In: *Percolation Processes: Theory and Applications.* Rodrigues, A.E. ,Tondeur, D., eds., Sijthoff and Noordhoff, Alphen aan den Rijn, 83-140, **1981.**

Voegelin, A., Kretzschmar, R., *Competitive sorption and transport of Cd(II) and Ni(II) in soil columns: Application of a cation exchange equilibrium model.* submitted, 2001.

Voegelin, A., Vulava, V.M., Kuhnen, F., Kretzschmar, R., *Multicomponent transport of major cations predicted from binary adsorption experiments.* Journal of Contaminant Hydrology 46, 319-338, **2000**.

Wang, W.-Z., Brusseau, M.L., Artiola, J.F., *The use of calcium to facilitate desorption and removal of cadmium and nickel in subsurface soils.* Journal of Contaminant Hydrology 25, 325-336, **1997**.

Zachara, J.M., Westall, J.C., *Chemical modeling of ion adsorption in soils.* In: *Soil Physical Chemistry.* Sparks, D.L., ed., CRC Press, Boca Raton, 47-95, **1998.**

CHAPTER 4

SORPTION AND REMOBILIZATION OF ZN, NI, CO, AND CD IN AN ACIDIC SOIL: COLUMN TRANSPORT AND XAS RESULTS

Abstract

Rapid adsorption of heavy metals to soil materials can be followed by a slow further decrease in metal solubility over time. Formation of metal bearing precipitates is one possible reason for such aging effects. Spectroscopic studies have shown that upon sorption of Zn^{2+}, Ni^{2+}, and Co^{2+} to clay minerals and aluminum oxides, layered double hydroxides (LDH) and phyllosilicates may form. These studies, however, were mostly conducted with pure minerals, at neutral to alkaline pH, and at high initial metal concentrations (~1 mM). The objective of the present study was to examine if such phases also form in a soil material, at slightly acidic pH, and at lower metal concentrations. Silt loam soil material packed into chromatographic columns was reacted over more than 7000 pore volumes with a slightly acidic solution (pH 6.4) containing Zn, Ni, Co, and Cd (~0.1 mM each). After the initial metal breakthrough (Cd, Ni, and Co at ~ 40 pore volumes, Zn at ~100 pore volumes), a slow process led to further metal sorption during the entire reaction time. Its relevance decreased in the order Zn > Ni > Co > Cd. In the case of Zn, 80% of total sorption were due to slow retention. X-ray Absorption Spectroscopy (XAS) analysis confirmed the incorporation of Zn into a LDH phase. A similar reaction may be postulated for Ni and Co, although concentrations were too low for XAS. By leaching the heavy metal loaded soil material with a dilute acidic solution (pH 3.0), the metal bearing phases were readily dissolved, and almost complete metal removal was attained within 1000 pore volumes. However, 4.6% of the total sorbed Zn and 3.6% of the total sorbed Ni remained in the soil material even after leaching with more than 3000 pore volumes of pH 3.0 solution.

Voegelin, A., Scheinost, A. C., Bühlmann, K., Kretzschmar, R., *Sorption and remobilization of Zn, Ni, Co, and Cd in an acidic soil: Column transport and XAS results.* in preparation

4.1 Introduction

Heavy metal sorption studies with soil model compounds and soil materials show, that following rapid initial metal uptake, sorption may continue over long times, leading to a significant further decrease of metal solubility. Such aging effects are of interest as they might lead to an attenuation of metal bioavailability and mobility in contaminated soils (McBride, 1999; Lothenbach *et al.*, 1999). Sorption of heavy metal cations occurs by non-specific electrostatic cation exchange on negatively charged soil particles, by specific adsorption to oxide minerals, clay minerals, and soil organic matter, and by the formation of new solid phases. At acidic conditions, fast and reversible cation exchange reactions may significantly contribute to total sorption. With increasing pH, however, specific adsorption and precipitation reactions become dominating and kinetic effects and sorption irreversibility increase. Aging effects may be caused by slow metal diffusion into micropores of Fe, Mn, and Al oxides (Trivedi and Axe, 2000; Scheinost *et al.*, 2001) or by the slow formation of heavy metal bearing precipitates (McBride, 1999; Sparks, 1998). The formation of M^{2+}-Al layered double hydroxides (LDH) upon adsorption of Zn^{2+}, Ni^{2+}, and Co^{2+} to clay minerals and aluminum oxides at neutral to alkaline pH levels was observed in numerous studies (Ford and Sparks, 2000; Scheidegger *et al.*, 1997; Roberts *et al.*, 1999; Thompson *et al.*, 2000). Precipitate stability generally increased over time (Scheckel *et al.*, 2000; Ford *et al.*, 1999). These results indicate that LDH phases might represent a sink for heavy metal cations in contaminated neutral to alkaline soils. So far, most studies were carried out with pure minerals in laboratory batch systems. High initial solution concentrations (~1 mM) were applied to attain the surface loading needed to induce precipitation. Initial adsorption lead to a rapid decrease in metal concentration in solution, slowing the formation of heavy metal precipitates down. With respect to the soil environment, the stability and dissolution kinetics of heavy metal bearing precipitates under acidic conditions are of central importance (Lothenbach *et al.*, 1999; Scheckel *et al.*, 2000; Ford *et al.*, 1999). At a decrease in pH, e.g., induced in the rhizosphere or caused by anthropogenic or natural soil acidification, heavy metal bearing precipitates might rapidly be remobilized.

In a recent publication (Voegelin *et al.*, 2001), we reported similar reversible adsorption behavior for Zn, Ni, and Cd in a silt-loam subsoil material at acidic pH (pH

4.6). While Cd sorption at higher pH (6.5) was still reversible, further unpublished data showed, that Zn sorption was not completely reversible anymore. In the present study, sorption and release of Zn, Ni, Co, and Cd in the same soil material at slightly acidic pH (6.4) was further investigated by combining column transport experiments and X-ray absorption spectroscopy (XAS). The objectives were: i) Study fast and slow metal sorption processes over several weeks of continuous metal loading in the column setup. ii) Investigate the subsequent mobilization of metals by leaching with Ca^{2+} and dilute acidic solution (pH 3.0). iii) Determine the binding mechanisms of Zn in metal loaded soil samples using XAS.

4.2 Materials and Methods

4.2.1 Soil Material

The acidic soil material was collected from the B-horizon (15-25 cm sampling depth) of a forested soil in northern Switzerland (Riedhof soil, aquic dystric Eutrochrept, silt loam texture, pH 4.1). The air-dried soil material was sieved to separate soil particles or aggregates between 63-400 µm. This fraction consisted of small aggregates containing 37% sand, 47% silt, and 16% clay. The organic carbon content was 9 g/kg organic carbon. Clay mineralogy was dominated by quartz, vermiculite, illite, kaolinite, and traces of chlorite and goethite. The composition of this sieve fraction corresponded well to the total soil material < 2mm.

4.2.2 Column Breakthrough and Release Experiment

Three chromatographic glass columns (Omni) of 1 cm inner diameter were uniformly packed with 8.0 g of dry soil material each. The resulting columns were 9 cm long. The pore volume was approximately 4.0 mL and the packing density 2.0 g/mL. The columns were flushed with CO_2 gas in order to displace the air from the pore space, then connected to a HPLC pump and preconditioned by passing several hundred pore volumes of 0.5 M $CaCl_2$ solution through the columns. Solutions were first passed through a degasser and then through the columns in the upward direction. Due to rapid dissolution of CO_2 gas, complete water saturation was achieved within a few pore

volumes. The flow rate was set to 0.5 mL/min. In a next step, the column was equilibrated with 200 pore volumes of 10^{-2} M $CaCl_2$ adjusted to pH 6.4 (with NaOH). Then the influent was switched to 10^{-2} M $CaCl_2$ background electrolyte containing 0.944×10^{-4} M $ZnCl_2$, 0.997×10^{-4} M $NiCl_2$, 0.947×10^{-4} M $CoCl_2$, and 0.971×10^{-4} M $CdCl_2$. The pH was adjusted to 6.4. Each column was loaded with 7350 pore volumes, which took about 41 days. After heavy metal loading, the first column was leached with 2 pore volumes of distilled water to elute the remaining metal containing solution. The soil material then was removed from the column and dried at 60°C. The remaining two columns were first leached with 67 pore volumes of 10^{-5} M $CaCl_2$ at pH 6.4 followed by 133 pore volumes of 10^{-2} M $CaCl_2$ at pH 6.4. During the 10^{-2} M $CaCl_2$ leaching, exchangeable cations were desorbed from the soil material due to Ca-metal exchange. After this leaching step, the second column was dissembled and the soil material dried. The third column was leached with 3100 pore volumes of 10^{-2} M $CaCl_2$ adjusted to pH 3.0 (with HCl) to release acid extractable heavy metals. Finally, also the soil material from the third column was dried. Column effluent was sampled using a fraction collector. Effluent concentrations of Zn, Ni, Co, and Cd were measured with flame atomic absorption spectrometry (Varian Spectraa 220).

In the three soil samples collected from the three column experiments (loaded with heavy metals, leached with 10^{-2} M $CaCl_2$, leached with 10^{-3} M HCl) and in the untreated soil material, total metal contents were determined using X-ray fluorescence spectroscopy (Spectro X-Lab 2000). Net retained amounts in the differently treated materials were calculated by subtracting the content of the untreated soil material from the measured. XAS analysis was conducted on the samples collected after heavy metal loading and after desorption of heavy metals with 10^{-2} M $CaCl_2$.

4.2.3 XAS Analysis

Zn K-edge (9659 eV) XAS data were collected on the column soil samples collected after metal loading and after 10^{-2} M $CaCl_2$ leaching and on Zn reference compounds at beamline X-11A at the National Synchrotron Light Source (NSLS), Upton, NY. The electron storage ring was operated at 2.5 GeV and the beam current varied between 300 and 100 mA. The beamline monochromator consisted of two parallel Si(111) crystals

adjusted to an entrance slit of 1 mm. The monochromator was detuned by 25% for reduction of higher harmonics. The samples were run under ambient conditions (24°C) in florescence mode using a Stern-Heald-type detector filled with Ar gas and equipped with an Cu-3 filter (Lytle *et al.*, 1984). Multiple scans were collected on each sample, depending on metal concentration, to improve the signal to noise ratio. All steps of the Extended X-ray Absorption Fine Structure (EXAFS) data reduction were performed with the WinXAS 97 1.3 software package (Ressler, 1998) using standard procedures as described in more detail in e.g., Scheinost and Sparks (2000). Theoretical scattering paths were calculated with FEFF 7.02 (Rehr, 1996) using the structure of lizardite where Zn was substituted for Mg in octahedral positions (Mellini, 1982). Fits were performed in R space. To reduce the number of adjustable parameters, S_0^2 was fixed at 0.95. The deviation between the fitted and the experimental spectra is given by the relative residual in percent, %Res.

4.3 Results and Discussion

4.3.1 Heavy Metal Sorption

The breakthrough curves of Zn, Ni, Co, and Cd are shown in Figure 4.1. Due to the formation of $CdCl^+$ complexes, Cd exhibits a higher mobility than the other cations. Cd therefore adsorbs to sites from which it is subsequently desorbed by the following cations. Desorption after breakthrough results in normalized effluent concentrations above one (Voegelin *et al.*, 2001). For Co, a similar pattern can be observed, likely caused by a compared to Ni slightly lower adsorption affinity. However, the differences between Cd, Co, and Ni are relatively small, and the breakthrough of all three cations takes place at around 40 pore volumes. Zn is significantly stronger adsorbed, resulting in a later breakthrough at around 100 pore volumes. In addition, the Zn effluent concentration increases only to approximately 80% of the influent concentration and from then on shows only a slow further increase. This pattern clearly indicates an ongoing slow retention process. After approximately 2000 pore volumes, Zn effluent concentrations were approaching influent levels. In contrast to Zn, the metals Cd, Co, and Ni rapidly reached effluent concentrations, which analytically could not be discerned from the influent. It was therefore not possible to determine, if a slow

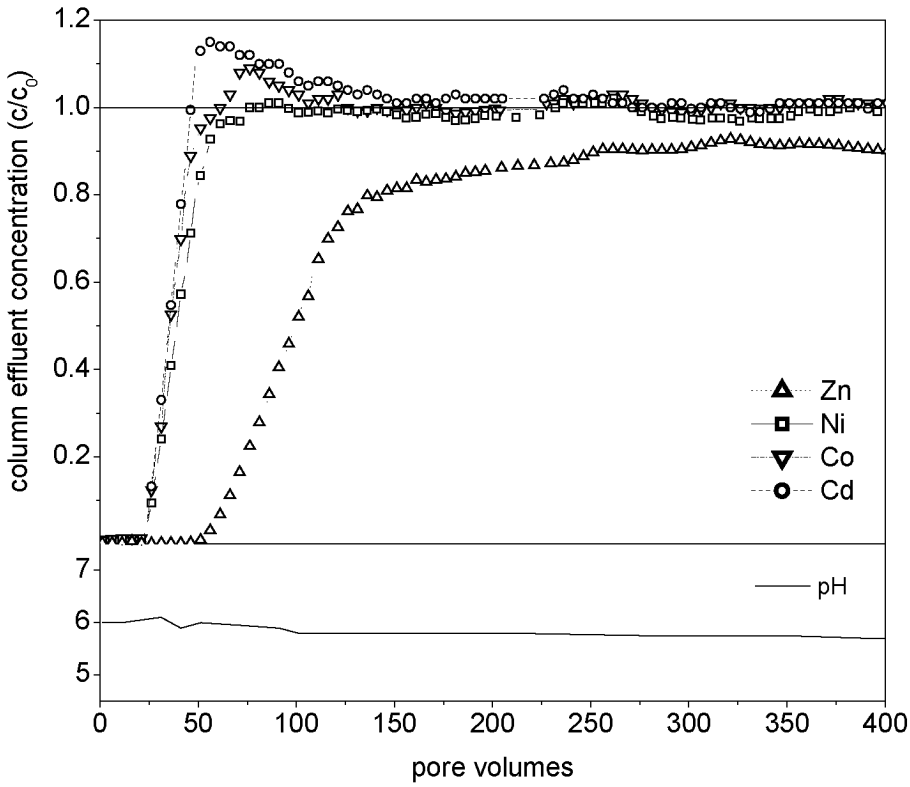

Figure 4.1: Coupled breakthrough of 10^{-4} M Cd, Co, Ni, and Zn in Riedhof soil material in 10^{-2} M $CaCl_2$ background electrolyte adjusted to pH 6.4. Zn is more strongly retarded and the breakthrough front reflects ongoing kinetic retention. Cd is most mobile due to $CdCl^+$ complex formation, resulting in adsorption and subsequent desorption by more retarded metal cations.

retention process occurred in analogy to Zn. To allow such reactions to take place, heavy metal loading was continued up to 7350 pore volumes. From 0 to 400 pore volumes, effluent pH decreased from ~6.1 to ~5.7, where it remained up to 7350 pore volumes.

For Cd, Co, and Ni, the rapidly adsorbed amounts during metal breakthrough were obtained by integration of the breakthrough curves up to 200 pore volumes (Figure 4.1). For Zn, whose breakthrough front was overlapped by the subsequent kinetic process, the rapidly adsorbed amount was estimated from the time of metal breakthrough (where $c/c_0 = 0.5$) and the influent Zn concentration. Slowly sorbed amounts were obtained by subtracting rapidly adsorbed amounts from total metal contents (XRF) after 7350 pore volumes of metal loading. The results presented in

Figure 4.2 unequivocally demonstrate that in addition to the rapidly adsorbed metals, significant amounts were slowly sorbed during the entire metal loading. While the rapidly adsorbed amounts reflect the observed breakthrough patterns (Figure 4.1), the slowly sorbed amounts decrease in the order Zn (-16.7) > Ni (-15.2) > Co (-14.9) > Cd (-14.4) which parallels the sequence of decreasing metal (hydr)oxide solubility products given in brackets (lowest logK for M-(hydr)oxide $\rightleftarrows M^{2+} + 2OH^-$, (Smith and Martell, 1976)). Note, however, that the heavy metal concentration levels in our study were at least two orders of magnitude below the respective solubility limits of metal (hydr)oxides.

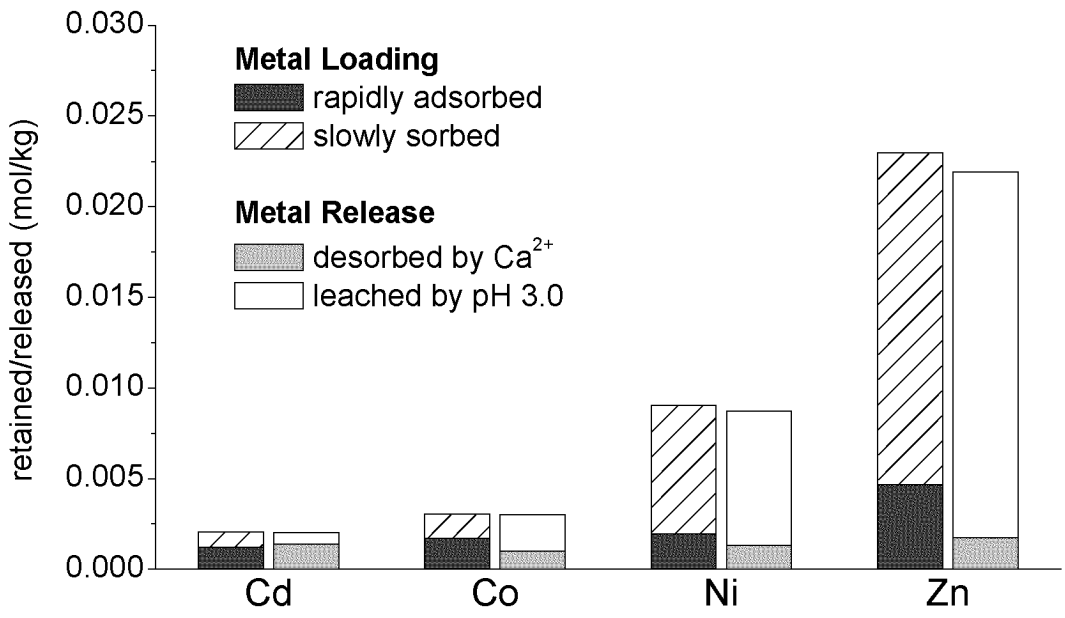

Figure 4.2: Amounts of metals retained and released in the column experiments. Significant amounts of metals were slowly sorbed during metal loading. The extent of slow sorption is paralleling the stability of the respective metal-(hydr)oxides: Zn > Ni > Co > Cd. Desorption with Ca released part of the rapidly adsorbed amounts. By subsequent leaching with pH 3.0 solution, almost the entire retained amounts were released again. Significant fractions of the total sorbed amounts of Zn (4.6%) and Ni (3.6%) were not remobilized by leaching with ~3000 pore volumes of pH 3.0 solution.

4.3.2 Heavy Metal Release

The concentration curves of Zn, Ni, Co, and Cd monitored during metal release are given in Figure 4.3. Concentrations are normalized to the approximate heavy metal influent concentration of 10^{-4} M during metal loading. In the initial conditioning phase up to 67 pore volumes (10^{-5} M $CaCl_2$, pH 6.4), virtually no heavy metals were removed from the soil column. Switching the influent to 10^{-2} M $CaCl_2$ (pH 6.4) lead to an unretarded desorption of Zn, Ni, Co, and Cd. The initial peak concentrations compare to the influent concentrations during metal loading and reflect the equilibrium between influent and soil adsorber attained during metal loading. After the initial elution peak, the metal desorption curves exhibit a tailing, which is most pronounced for Zn and least

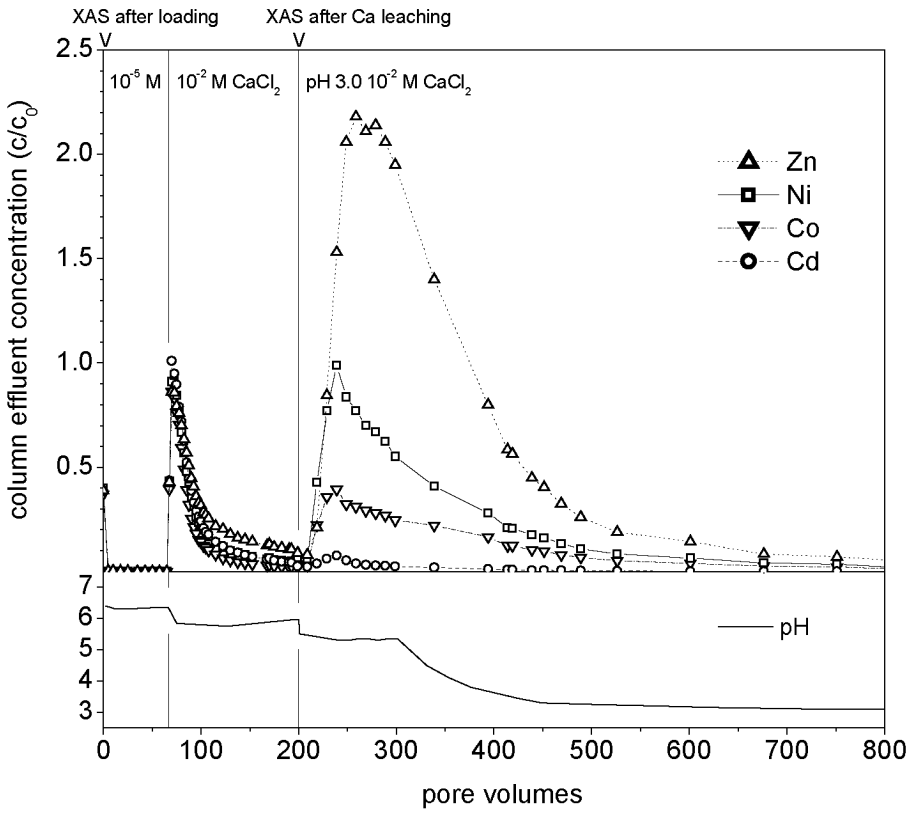

Figure 4.3: Effluent concentration patterns of heavy metals during leaching with 10^{-5} M $CaCl_2$, pH 6.4 (0 to 67 pore volumes), 10^{-2} M $CaCl_2$, pH 6.4 (67-200 pore volumes), and 10^{-2} M $CaCl_2$, pH 3.0 (200-3150 pore volumes). Concentrations are normalized to influent metal concentrations during metal loading ($c_0=10^{-4}$ M). Desorption by Ca^{2+} is comparable for all metals, whereas peak concentrations induced by pH 3.0 leaching reflect the extent of slow metal sorption: Zn > Ni > Co > Cd.

for Co. At 200 pore volumes, the influent is switched to the dilute acidic solution (pH 3.0, 10^{-2} M $CaCl_2$). After a short delay period of ~20 pore volumes, likely due to metal readsorption, metals are released from the soil material. The effluent peak concentrations clearly reflect the extent of the slow sorption process, Zn > Ni > Co > Cd (Fig. 4.2). The breakthrough of the pH 3.0 front takes place only after the major part of all four metals are eluted from the soil material.

The cumulative amounts of Zn, Ni, Co, and Cd desorbed with 10^{-2} M $CaCl_2$ were calculated by integration of the desorption curves from 67 to 200 pore volumes (Fig. 4.3). Metal amounts leached at pH 3.0 were obtained by subtracting the $CaCl_2$ mobilized and the residual amounts after pH 3.0 leaching from the initial total amounts. Less Zn, Ni, and Co were desorbed by Ca^{2+} than had rapidly adsorbed during loading (Fig. 4.2). However, desorption by Ca^{2+} was not completed at 200 pore volumes (Fig. 4.3). Prolonged leaching with Ca^{2+} likely would have removed the remaining amounts of rapidly adsorbed metals. Removal of the slowly sorbed metals by Ca^{2+} exchange, on the other hand, appears unlikely. By leaching with pH 3.0 solution, almost the total remaining metals in the soil material were remobilized. Considering that metal loading lasted over 7350 pore volumes, almost complete metal release was achieved within a comparably short period of 1000 pore volumes. However, small fractions of the initial total amounts of Zn (4.6%) and Ni (3.6%) remained in the soil material even after ~3000 pore volumes of leaching with pH 3.0 solution.

The results from the loading experiment unequivocally demonstrate that in addition to rapid metal adsorption during the initial phase, additional slow metal retention had taken place over the entire time of metal loading. The extent of slow sorption increased from Cd to Co to Ni to Zn, paralleling their increasing metal-(hydr)oxide stability. Slowly sorbed amounts of metals were not mobilized by Ca^{2+}, but only by the subsequent pH 3.0 leaching. However, small fractions of the total amounts retained during loading could not be remobilized even by 3000 pore volumes of pH 3.0 leaching. While these results may indicate that metals had been slowly precipitated, they do not give direct evidence for such a binding mechanism. Therefore, the soil samples collected after metal loading and after desorption with Ca^{2+} were further analyzed using XAS.

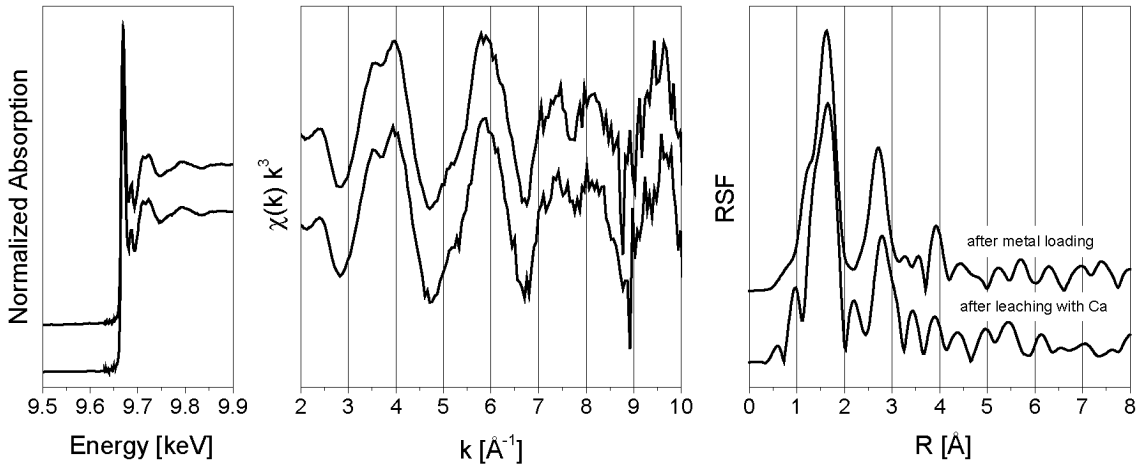

Figure 4.4: Zn-XAS spectra of Zn-reacted soil material after metal loading and after leaching with Ca exchange (see Fig 4.3).

Table 4.1: Zn-K XAFS fit results (S_0^2=0.95)

Sample	Zn-O			Zn-Zn				
	[a]CN	[b]R [Å]	[c]σ^2 [Å^2]	CN	R [Å]	σ^2 [Å^2]	[d]ΔE_0 [Å]	[e]χ^2_{res} %
after metal loading	6.4	2.05	0.011	1.4	3.07	0.003	0.2	11
after Ca leaching	6.0	2.04	0.009	1.5	3.06	0.004	0.0	10
[f]Zn-Al LDH	6.3	2.07	0.009	3.8	3.10	0.009	0.5	-
[f]Zn Pyrophyllite	5.7	2.02	0.010	1.1	3.09	0.006	0.2	-
	-	-	-	-	-	-	-	
	6.2	2.06	0.011	3.1	3.10	0.011	0.7	

[a] Coordination number; [b]Radial distance; [c]Debye Waller factor (fixed); [d]Phase shift; [e]Fit error; [f]from (Ford and Sparks, 2000)

4.3.3 Formation of a Zn Containing Solid Phase

Figure 4.4 shows Zn-edge XAS spectra of the soil materials collected after loading and after desorption with Ca (Fig. 4.3). The near-edge region (XANES), the k^3-weighted chi function of the EXAFS region, and its Fourier transform indicate electron backscattering from at least two different atom shells surrounding the X-ray absorbing Zn atoms. The strongest first shell was fit with 6 oxygen atoms at a radial distance of 2.04 to 2.05 Å,

both coordination number and distance being consistent with a octahedral configuration (Table 4.1). The second shell was fit with 1 to 2 Zn atoms at 3.06 to 3.07 Å (Table 4.1), or with 1 Mn or 1 Fe atom at 3.08 Å (not shown). All three fits performed equally well in terms of visual match and statistics.

The distance and coordination number for Zn are close to the values found by Ford and Sparks (2000) for Zn-Al layered double hydroxide (LDH) surface precipitates (Table 4.1). In this structure, Zn is surrounded by 6 Ni and Al atoms at a distance of 3.06 to 3.11 Å. Due to the anticyclic interference of the Zn and Al scattering waves, however, the fitted coordination number of the second shell is significantly reduced (Scheinost and Sparks, 2000). The formation of a Zn-Al LDH precipitate phase is further supported by the strongly dampened oscillation at about 8 $Å^{-1}$, which is indicative of both a transition metal and Al being distributed over the same crystallographic sites in the highly-symmetrical hexagonal LDH layers (Scheinost and Sparks, 2000).

Alternatively, 1 Mn or 1 Fe atom at 3.08 Å could be explained by the formation of a monodentate inner-sphere sorption complex at the surface of Fe or Mn (hydr)oxides. However, the high structural order indicated by the well-separated second oscillation of the near-edge spectra (Fig. 4.4 left) seems to contradict such a surface configuration. While a highly symmetrical local environment has been observed for bidentate inner-sphere sorption complexes of Ni on gibbsite (Scheinost and Yamaguchi, unpublished data), a high degree of order is less likely for monodentate complexes, which may rotate more freely. Therefore, the XAS results confirm the formation of Zn-Al LDH.

Metal desorption with Ca removed 8% of the totally retained Zn. We would expect that rapidly desorbed Zn occurs predominately in outer-sphere coordination, i.e. without a second shell, and in tetrahedral configuration, i.e. with a oxygen coordination number of 4 and a distance below 2.00 Å. Since the EXAFS spectra should represent the statistical average of Zn in all coordination environments, the oxygen distance and the first-shell coordination number should be smaller and the second-shell coordination should be larger after the Zn loading step than after the Ca desorption step. However, the data in Table 4.1 do not support such differences. Most likely, the local environment

of aqueous Zn is far more disordered than that of Zn in LDH, producing a relatively weak EXAFS signal that is not detectable in the presence of the stronger signal from LDH.

While the spectroscopic data confirm the incorporation of Zn into a solid phase, the total concentrations of Ni, Co and Cd were too small to detect their local environment by XAS. With respect to Ni and Co, it is reasonable to assume that they reacted in analogy to Zn (Scheinost and Sparks, 2000). The observed sequence of metal precipitation could be related to the stability of M-Al LDH phases, which follows the stability of the respective metal-(hydr)oxide phases (Boclair and Braterman, 1999). Cd-Al LDH was synthesized and characterized (Vichi and Alves, 1997), its formation hence is theoretically possible. From a conditional Zn-Al LDH formation coefficient determined by Boclair and Braterman (1999), Ford and Sparks (2000) derived a Zn-Al LDH formation constant. Based on this constant, the heavy metal containing solution was by two orders of magnitude undersaturated with respect to Zn-Al LDH. However, this constant was derived from freshly precipitated Zn-Al LDH. Aged precipitates are expected to be more stable (Scheckel *et al.*, 2000). Heavy metals might also coprecipitate, and the solubility product of amorphous $Al(OH)_3$ ($\log K_{so}=10^{-31.62}$ for $Al(OH)_3 \rightleftarrows Al^{3+} + 3OH^-$), which Ford and Sparks (2000) factored into the Zn-Al LDH formation constant, might be too low. Finally, metal adsorption might promote precipitation.

4.3.4 Environmental Implications

The results of this study give evidence of the formation of a heavy metal bearing precipitate in a soil material at slightly acidic pH. Metal concentrations were realistic for contaminated soils and at least 100 times below the solubility limits imposed by metal-(hydr)oxide phases. Precipitated metals were not accessible by Ca^{2+} exchange, were rapidly remobilized by leaching with a dilute acidic solution (pH 3.0). Precipitated metals hence might still be mobilized in the plant-root zone or due to soil acidification. Further research is required to assess the stability of metal bearing precipitates and their relevance for permanent metal immobilization in soils.

References

Boclair, J.W., Braterman, P.S., *Layered double hydroxide stability. 1. Relative stabilities of layered double hydroxides and their simple counterparts.* Chemistry of Materials 11, 298-302, **1999**.

Ford, R.G., Scheinost, A.C., Scheckel, K.G., Sparks, D.L., *The link between clay mineral weathering and the stabilization of Ni surface precipitates.* Environmental Science and Technology 33, 3140-3144, **1999**.

Ford, R.G., Sparks, D.L., *The nature of Zn precipitates formed in the presence of pyrophyllite*. Environmental Science and Technology 34, 2479-2483, **2000**.

Lothenbach, B., Furrer, G., Scharli, H., Schulin, R., *Immobilization of zinc and cadmium by montmorillonite compounds: Effects of aging and subsequent acidification*. Environmental Science and Technology 33, 2945-2952, **1999**.

Lytle, F.W., Sandstrom, D.R., Marques, E.C., Wong, J., Spiro, C.L., Huffman, G.P., Huggins, F.E., *Measurement of soft x-ray absorption spectra with a fluorescence ion chamber detector*. Nuclear Instruments and Methods in Physics Research 226, 542-548, **1984**.

McBride, M.B., *Chemisorption and precipitation reactions*. In: *Handbook of Soil Science*. Sumner, M.E., ed., CRC Press, Boca Raton, B/265-B/302, **1999.**

Mellini, C., *The crystal structure of lizardite 1T: hydrogen bonds and polytypism*. American Mineralogist 67, 587-598, **1982**.

Rehr, J.J., *FEFF: Ab initio multiple scattering X-ray absorption fine structure and X-ray absorption near edge structure code 7.02*, FEFF Project, Department of Physics, University of Washington, Seattle, Washington, **1996.**

Ressler, T., *WinXAS: a program for X-ray absorption spectroscopy data analysis under MS-Windows*. Journal of Synchrotron Radiation 5, 118-122, **1998**.

Roberts, D.R., Scheidegger, A.M., Sparks, D.L., *Kinetics of mixed Ni-Al precipitate formation on a soil clay fraction.* Environmental Science and Technology 33, 3749-3754, **1999**.

Scheckel, K.G., Scheinost, A.C., Ford, R.G., Sparks, D.L., *Stability of layered Ni hydroxide surface precipitates - A dissolution kinetics study*. Geochimica et Cosmochimica Acta 64, 2727-2735, **2000**.

Scheidegger, A.M., Lamble, G.M., Sparks, D.L., *Spectroscopic evidence for the formation of mixed-cation hydroxide phases upon metal sorption on clays and aluminum oxides*. Journal of Colloid and Interface Science 186, 118-128, **1997**.

Scheinost, A.C., Abend, S., Pandya, K.I., Sparks, D.L., *Kinetic controls on Cu and Pb sorption by ferrihydrite*. Environmental Science and Technology in press, **2001**.

Scheinost, A.C., Sparks, D.L., *Formation of layered single- and double-metal hydroxide precipitates at the mineral/ water interface: A multiple-scattering XAFS analysis*. Journal of Colloid and Interface Science 223, 167-178, **2000**.

Smith, R.M., Martell, A.E., *Critical Stability Constants, Vol. 4.* Plenum Press, New York, **1976**.

Sparks, D.L., *Kinetics and mechanisms of chemical reactions at the soil mineral/water interface*. In: *Soil Physical Chemistry.* Sparks, D.L., ed., CRC Press, Boca Raton, 135-191, **1998.**

Thompson, H.A., Parks, G.A., Brown, G.E.J., *Formation and release of cobalt(II) sorption and precipitation products in aging kaolinite-water slurries*. Journal of Colloid and Interface Science 222, 241-253, **2000**.

Trivedi, P., Axe, L., *Modeling Cd and Zn sorption to hydrous metal oxides.* Environmental Science and Technology 34, 2215-2223, **2000**.

Vichi, F.M., Alves, O.L., *Preparation of Cd/Al layered hydroxides and their intercalation reactions with phosphonic acids*. Journal of materials chemistry 7, 1631-1634, **1997**.

Voegelin, A., Vulava, V.M., Kretzschmar, R., *Reaction-based model describing sorption and transport of Cd, Zn, and Ni in an acidic soil*. Environmental Science and Technology 35, 1651-1657, **2001**.

CHAPTER 5

EVALUATING HEAVY METAL MOBILIZATION POTENTIAL FROM CONTAMINATED SOILS USING COLUMN LEACHING EXPERIMENTS

Abstract

Continuous contamination by atmospheric deposition or sewage sludge and fertilizer application leads to an accumulation of heavy metals in soils. Information on mobile and immobile heavy metal pools and their reactivity is required for risk assessment and remediation design. To study metal release from contaminated soils due to cation exchange and acidification processes, high-resolution column experiments with soil materials of different composition and contamination history were conducted. The reactivity of mobile metal pools was assessed by leaching with 10 mM $CaCl_2$. In acidic soils, column effluent concentration patterns reflected the exchange of Zn^{2+}, Cd^{2+}, Mg^{2+}, and K^+ by Ca^{2+}. Similar adsorption behavior was observed for Cd and Zn, and between 40 and 70% of their total contents were mobilized by Ca^{2+} exchange. The amounts of Zn mobilized by Ca^{2+} were larger than amounts extracted in batch using Na^+, Ca^{2+}, NH_4^+ or Ba^{2+} as index cation, but compared well to the sum of the first two fractions of a sequential batch extraction (NH_4NO_3 + NH_4-acetate, pH 6.0). In neutral soils, much less Cd and Zn were released, and relative to total amounts, Cd was significantly more mobile. Only minor amounts of Pb and Cu were released by Ca^{2+} exchange. In a second leaching step, the soil columns were reacted with dilute acidic solutions (pH 3.0, 10 mM $CaCl_2$) to investigate possible effects of soil acidification on metal mobility. The resulting effluent patterns reflected the coupling of proton induced metal release, proton buffering reactions, $CaCO_3$ dissolution, advective metal transport, and metal specific readsorption. By Ca^{2+} exchange and subsequent pH 3.0 leaching, between 65 and 90% of the total contents of Zn, Cd, Pb, and Cu were extracted from the soil materials.

Voegelin, A., Kretzschmar, R., *Evaluating heavy metal mobilization potential from contaminated soils using column leaching experiments.* in preparation

5.1 Introduction

In contaminated soils, various simultaneous processes determine metal mobility and bioavailability. Over time, heavy metals are released from contaminant source materials (e.g., fertilizers, sewage sludge, atmospheric depositions, ammunition, slag) and readsorb to oxide and clay minerals or soil organic matter. Micropore diffusion and precipitation reactions can lead to a slow decrease of metal mobility and availability with time (Alloway, 1995; McBride, 1999). Changes in soil chemistry, e.g. natural and anthropogenic soil acidification, on the other hand, may lead to a remobilization of accumulated heavy metals.

This complexity of coupled processes makes it difficult to assess or predict metal behavior in contaminated soils from total metal contents and bulk soil properties (McBride *et al.*, 1997). To determine metal bioavailability and mobility in contaminated soils or to evaluate potential remediation strategies, additional site-specific data is required. Dilute salt extracts are used to assess heavy metal phytoavailability and mobility in soils and are part of governmental regulations on the assessment of heavy metal contamination of soils (McLaughlin *et al.*, 2000b; McLaughlin *et al.*, 2000a; Gupta *et al.*, 1996). In parallel or sequential batch extractions, heavy metals extracted with different solutions are assigned to different operationally defined binding forms and are attributed different reactivity (Tessier *et al.*, 1979; Ahnstrom and Parker, 1999). By isotopic exchange techniques, it is possible to determining labile and non-labile pools of metals in soils (Ahnstrom and Parker, 2001; Sinaj *et al.*, 1999). In batch systems, side effects can be caused by agitation of soil materials or by changes in extractant composition during equilibration (Grolimund *et al.*, 1995). Such effects can be eliminated in the column setup, where the soil material is fixed and the influent composition remains constant over time. In addition, column experiments yield not only extracted or adsorbed amounts, but also time-resolved effluent concentration curves, which can be interpreted in terms of possible sorption processes and component reactivity. By using homogeneously packed columns, the heterogeneity of the flow path can be minimized and columns of high chromatographic resolution are obtained. This allows studying heavy metal sorption and transport as a results of different coupled processes.

With uncontaminated soil materials, column experiments are carried out to investigate metal sorption processes and to test sorption models (Christensen, 1985; Voegelin *et al.*, 2001; Boekhold and van der Zee, 1992). Flow-through reactors as a simplified column setup allow an accurate measurement of heavy metal sorption on soil materials (Grolimund *et al.*, 1995; Voegelin *et al.*, 2001). With artificially or field contaminated soil materials, the column approach can be used to mimic remediation strategies, to assess heavy metal binding and desorption kinetics, or to assess processes such as DOC or colloid promoted metal transport (Kedziorek *et al.*, 1998; Vulava and Seaman, 2000; Wang *et al.*, 1997; Temminghoff *et al.*, 1997; Grolimund *et al.*, 1996).

The objective of this study was to investigate the mobilization of Zn^{2+}, Cd^{2+}, Pb^{2+}, and Cu^{2+} from contaminated soil materials as a result of cation exchange and acidification processes. Contaminated soil materials were collected from soils of different composition and contamination history. Leaching experiments were conducted in packed soil columns of high chromatographic resolution. To assess the reactivity of mobile metal pools, the columns were leached with 10 mM $CaCl_2$ solution. Subsequently, the reactivity of non-exchangeable metals was studied by leaching the columns with dilute acidic (pH 3.0) solution. Effluent concentration patterns are interpreted in terms of potential release processes and extracted amounts are compared to results from batch extractions.

5.2 Materials and Methods

5.2.1 Soil Materials

Soil samples taken from four metal-contaminated soil profiles were investigated in this study (Table 5.1). The first soil (Worksop) collected in the East Midlands of England is a well-drained field soil developed on sandstone. Until ~1980, large amounts of sewage sludge were applied resulting in severe Zn pollution. Reduced plant growth due to Zn toxicity can still be observed today. The second and third soil (Evin Wood and Evin Field) located in northern France developed from a quarternary clay deposit. They are poorly drained, and the shallow water table is at 1 meter below ground level. Evin Wood soil is forested with poplar trees, while Evin Field soil is used for growing of crops. Both soils were contaminated by Zn, Pb, and Cd containing atmospheric

emissions from a large zinc-lead smelter, which started operation around 1884. In the late 1970's, filters were installed, reducing further soil contamination. The fourth soil (Dornach) collected in northern Switzerland developed from a layer of weathered limestone gravel overlying a fluvial deposit. For approximately 80 years, the soil was contaminated with Zn, Cd, and Cu containing dusts from a nearby brass smelter, before filters were installed in the 1980's.

From the air-dried soil samples, the aggregate fraction 0.1 to 1 mm was used in all experiments. The smaller aggregates were sieved out to limit problems with clogging of soil columns. By removing the larger aggregates, more homogeneous packing of the columns and higher chromatographic resolution were obtained. Soil properties including heavy metal contents are provided in Table 5.1.

Table 5.1: Soil properties and heavy metal contents of soils Worksop, Evin Wood, Evin Field, and Dornach (aggregate fraction 0.1 to 1 mm)

			Soil properties					[a]Total Metal Contents			
Soil	Land use	Sampling depth (cm)	[b]pH	Org. C	Clay	[c]$CaCO_3$	[d]ECEC	Zn	Cdx100	Pb	Cu
				(g/kg)			($mmol_c$/kg)	(mmol/kg)			
Worksop	field	0-30	5.7	14.4	68	<5	56	9.71	0.580	0.304	0.346
Evin Wood	forest	0-5	5.1	52.3	229	<5	176	34.2	34.9	11.5	1.38
Evin Field	field	0-30	6.9	16.8	212	7	179	10.8	9.00	2.52	0.460
Dornach	meadow	0-5	6.9	82.3	372	66	461	28.8	3.75	0.557	31.9

[a] measured by X-ray fluorescence spectrometry (XRF); [b] in 10 mM $CaCl_2$ at soil-solution ratio 1:2.5; [c] $CaCO_3$ content determined in aggregate fraction <2 mm; [d] measured with an unbuffered 0.1 M $BaCl_2$ extraction at soil-solution ratio 1:30 (Hendershot and Duquette, 1986).

5.2.2 Column Leaching Experiments

Column leaching experiments were conducted in chromatographic glass columns (Omni) of 1 cm inner diameter and varying length (Table 2). Dry soil material was uniformly packed into the columns and flushed with CO_2 gas to displace the air from the pore space. The column inlet was then connected to a HPLC pump. Solutions passed through a degasser were pumped through the columns in upward direction. The flow

rate was set to 0.25 mL/min. The columns were conditioned with 10^{-5} M $CaCl_2$. Due to rapid dissolution of CO_2 gas, complete water saturation was achieved within a few pore volumes. During this conditioning step, the column was stabilized and small amounts of loose colloidal particles and DOC were removed from the column. After 33.3 mL of preconditioning solution per gram of soil material (mL/g), the leaching sequence was started.

Table 5.2: Column dimensions and properties

Soil	Column Nr.	[a]m_{soil} (g)	[b]length (cm)	[c]V_{pore} (mL)	[d]Pe	[f]Leaching sequence
Worksop	1	15	14.5	5.7	248	Ca^{2+} exchange: A, B
	2	1.5	1.35	0.7	87	pH 3.0 leaching: A, B, C
Evin Wood	3	15	19.4	9.0	169	Ca^{2+} exchange: A, B
	4	1.5	1.9	1.0	36	pH 3.0 leaching: A, B, C
Evin Field	5	15	17	7.8	182	Ca^{2+} exchange: A, B
	6	1.5	1.7	0.9	62	pH 3.0 leaching: A, B, C
	7	1.5	1.7	0.8	113	low Ca pH 3.0 leaching: A, B, D
	8	1.5	1.7	0.9	[e]174	low flow pH 3.0 leaching: A, B, E
Dornach	9	15	20.3	9.4	163	Ca^{2+} exchange: A, B
	10	1.5	2.0	1.4	46	pH 3.0 leaching: A, B, C
	11	1.5	1.9	1.0	50	low Ca pH 3.0 leaching: A, B, D
	12	1.5	1.9	1.3	[e]179	low flow pH 3.0 leaching: A, B, E

[a]mass of soil material packed into column; [b]all columns had an inner diameter of 1 cm; [c]column pore volume; [d]column Péclet number, determined at 0.25 mL/min, except columns 8 and 12; [e]determined at 0.05 mL/min; [f]leaching solutions (duration in mL/g, flow rate in mL/min): A 10^{-5} M $CaCl_2$ (33.3, 0.25); B 10^{-2} M $CaCl_2$ (66.7, 0.25); C pH 3.0, 10^{-2} M $CaCl_2$ (1400, 0.25); D pH 3.0, 10^{-5} M $CaCl_2$ (1400, 0.25); E pH 3.0, 10^{-2} M $CaCl_2$ (1400, 0.05).

To investigate the mobilization of heavy metal cations due to Ca^{2+} exchange, columns packed with 15 g of soil material were used (Table 2, columns 1, 3, 5, and 9). After the conditioning, the columns were fed with 10^{-2} M $CaCl_2$ solution (66.7 mL/g). Effluents were sampled using an automated fraction collector. The concentrations of Ca,

Mg, K, Zn, Cd, Pb, and Cu were measured using flame atomic absorption spectrometry (Varian SpectrAA 400).

Further column experiments were conducted to study metal release induced by an acidification front (pH 3.0). Because these experiments lasted much more pore volumes than the previous Ca exchange experiments, columns filled with only 1.5 g of soil material were used (Table 2, Columns 2, 4, 6, and 10). The conditioning and leaching with 10 mM $CaCl_2$ were carried out as described above. Subsequently, the columns were leached with 10 mM $CaCl_2$ adjusted to pH 3.0 with HCl (1400 mL/g). Column effluents were analyzed for Al, Si, Fe, Mn, Ca, Mg, K, Zn, Cd, Pb, and Cu using using ICP-AES (Varian Liberty 200) equipped with an ultrasonic nebulizer (Cetac U-5000 AT).

With soils Evin Field and Dornach, two more sets of acid leaching experiments were carried out. General conditions were the same as described above. To study the readsorption of acid mobilized metal cations on the soil materials, acid leaching in a first set was conducted with 10^{-5} M (instead of 10^{-2} M) $CaCl_2$ adjusted to pH 3.0 (Table 5.2, Columns 7 and 11). In a second set, the flow rate during acid leaching was reduced to 0.05 mL/min to investigate the relevance of kinetic effects for desorption or dissolution processes (Table 2, Columns 8 and 12).

After each column experiment, a short (0.1 mL) nitrate pulse was injected into the column and the resulting nitrate breakthrough peak was monitored on-line using an UV-VIS detector set to 220 nm wavelength. Pore volume and column Péclet number (Table 2) were determined numerically from the flow rate and the first or second moments of the nitrate breakthrough curves (Villermaux, 1981). Note that also the small columns filled with only 1.5 g of soil material had rather high Péclet numbers.

5.2.3 Batch Extractions

Batch extractions with different index cations and at different soil-solution ratio (SSR) were conducted to determine the respective exchangeable heavy metal fractions: 0.1 M $NaNO_3$ (SSR 1:25) (Gupta and Aten, 1993), 0.01 M $CaCl_2$ (SSR 1:10) (Houba *et al.*, 2000), and 0.1 M $BaCl_2$ (SSR 1:30) (Hendershot and Duquette, 1986). A sequential batch extraction was carried out consisting of seven extraction steps (Zeien and Bruemmer, 1989; Schwartz *et al.*, 1999). The hypothetical interpretation of the

operational fractions F1 to F7 according to (Zeien and Bruemmer, 1989) is given in brackets: F1: 1 M NH_4NO_3, soil-solution ratio 1:25 (readily soluble and exchangeable); F2: 1 M NH_4-acetate, pH 6.0 (specifically adsorbed, $CaCO_3$ bound, and other weakly bound species); F3: 0.1 M NH_2OH-HCl+1 M NH_4-acetate, pH 6.0 (bound to Mn-oxides); F4: 0.025 M NH_4EDTA, pH 4.6 (bound to organic substances); F5: 0.2 M NH_4-oxalate, pH 3.25 (bound to amorphous and poorly crystalline Fe oxides); F6: 0.1 M ascorbic acid in 0.2 M NH_4-oxalate, pH 3.25, in boiling water (bound to crystalline Fe oxides); F7: $HF/HNO_3/HCl$ (residual fraction). Zn, Cd, Pb, and Cu in extracts were measured using flame AAS. Shown results are the average of duplicate extractions.

5.3 Results and Discussion

5.3.1 Metal Mobilization by Ca^{2+} Exchange

The column results of metal mobilization by Ca^{2+} exchange from Evin Wood soil are shown in Figure 5.1. As in all further graphs, effluent concentrations are plotted versus the volume of leaching solution per gram of soil material (in mL/g). These units allow direct comparison of data from different soil materials with different packing densities. The small amounts of heavy metals and major cations leached from the soil Evin Wood during conditioning (0 to 33.3 mL/g) are likely due to the removal of loose colloidal material and DOC. One pore volume after influent change to 10^{-2} M $CaCl_2$ solution, the unretarded normality front breaks through and Zn, Cd, Mg, and Ca concentrations sharply increase and reach a plateau level. The pH decreases by ~1.4 log units to pH ~4.8, which compares to the pH measured in batch using 10 mM $CaCl_2$ electrolyte (Table 1). The plateau concentration levels following the normality front are determined by the amounts of cations on the exchanger and their respective binding strength. K release exhibits a strong tailing after the initial release peak, which is likely due to specific K adsorption to clay minerals such as vermiculite (Sparks, 1995). In contrast, Mg release ends in a sharp exchange front (~38 mL/g). Subsequently, additional Ca is available to exchange Zn and Cd, therefore their concentrations increase again. However, before reaching a new plateau concentration, Zn and Cd are depleted on the exchanger and their concentrations start to decrease. The almost identical elution patterns of Zn and Cd suggest a very similar adsorption behavior of both cations, which

is in good agreement with results from a column study on Zn and Cd transport in an acidic soil material (Voegelin *et al.*, 2001). In contrast, the effluent concentrations of Pb are approximately three times lower than those of Cd, although the total Pb content of the soil material is roughly 35 times higher (Table 1). The much higher adsorption affinity of Pb as compared to Cd and Zn is in agreement with results from numerous adsorption studies (Abd-Elfattah and Wada, 1981; Buchter *et al.*, 1989; Hooda and Alloway, 1998). Because of its high adsorption affinity, Pb elutes at very low concentrations but over a longer period, resulting in the observed elution plateau. Pb

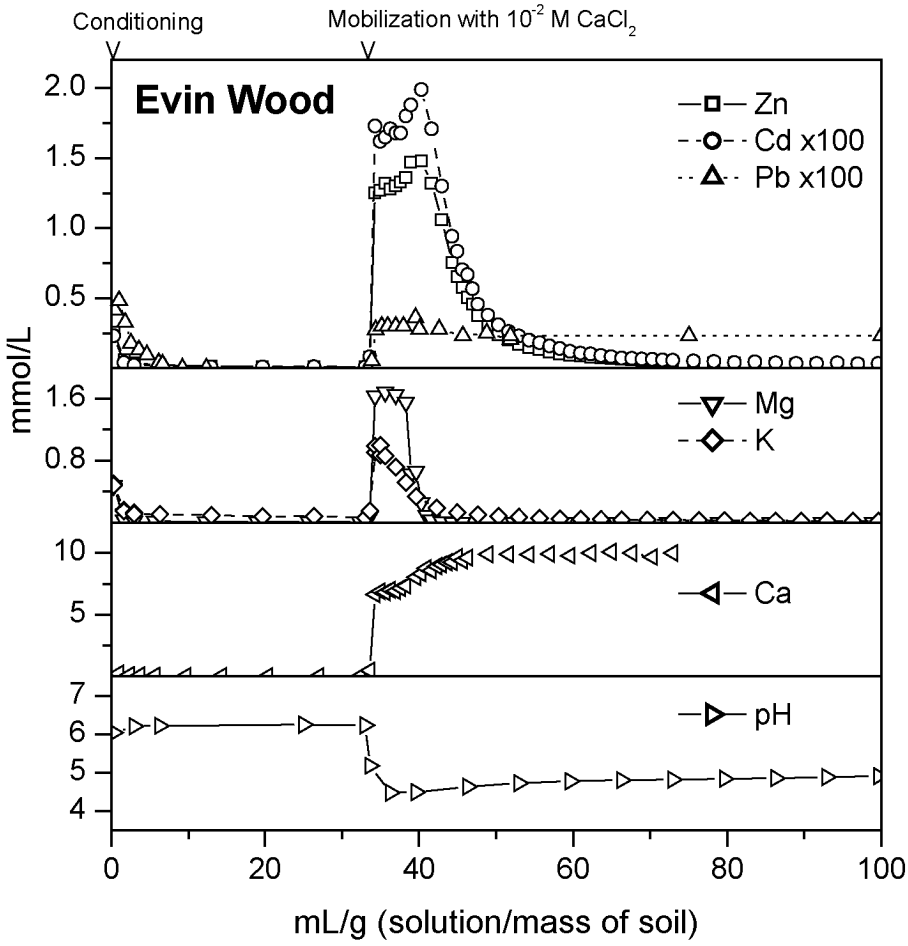

Figure 5.1: Leaching of Evin Wood soil with 10 mM $CaCl_2$ (Table 5.2, Column 3). Zn and Cd exhibit similar effluent concentration patterns, indicating similar adsorption behavior. Their release is coupled to the exchange of Mg and K by Ca. When the influent is switched to 10 mM $CaCl_2$, pH decreases from ~6.2 to ~4.8. Abscissa: 1 mL/g corresponds to ~1.9 pore volumes.

mobilization by Ca^{2+} was not completed at the end of the experiment. In the limed neutral Evin Field soil, Zn and Cd elution curves resembled that of Pb in Evin Wood, with respective plateau concentrations of approximately 7×10^{-7} M and 3×10^{-7} M. Hence, likely as a result of the 2 log units higher pH of the limed Evin Field soil, effluent Cd and Zn concentrations were ~50 and ~3000 times lower, respectively, than in the acidic Evin Wood soil.

The effluent concentrations from the Ca^{2+} exchange experiment with the calcareous Dornach soil are shown in Figure 5.2. As in the neutral Evin Field soil, Zn

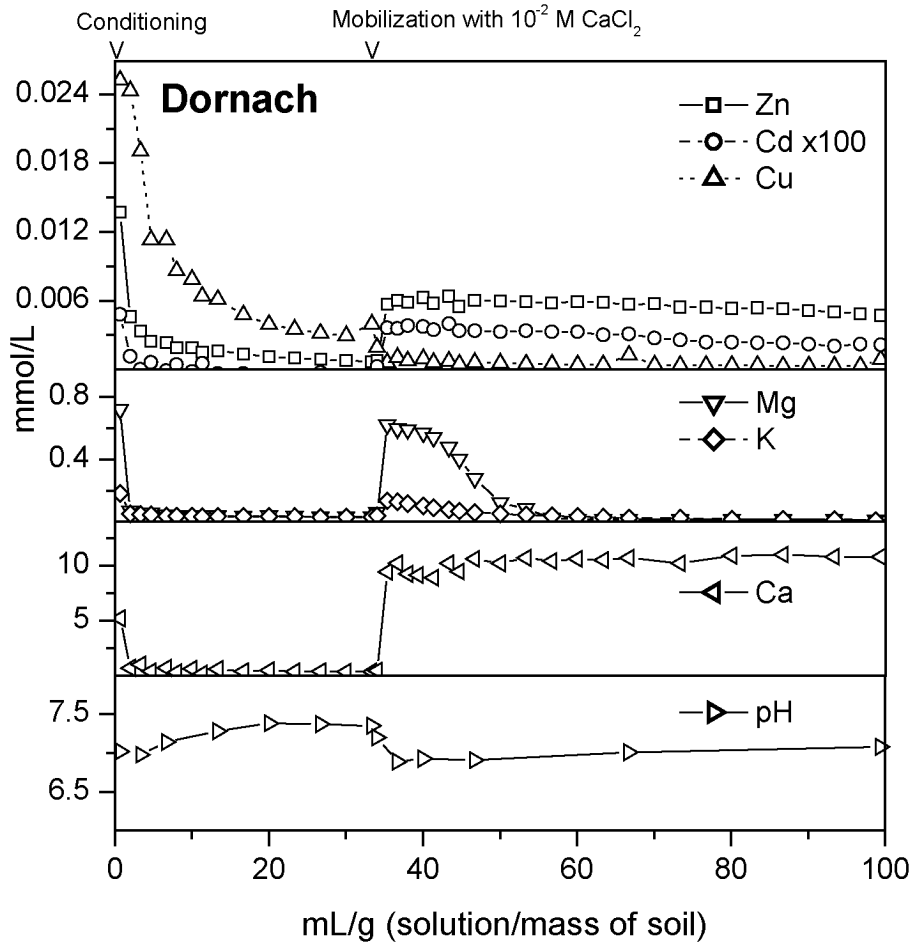

Figure 5.2: Leaching of Dornach soil with 10 mM $CaCl_2$ (Table 5.2, Column 9). Zn and Cd elute at very low concentration levels over the entire mobilization period. Cu in contrast elutes in the conditioning phase, probably due to DOC release at higher pH and lower Ca concentration. Abscissa: 1 mL/g corresponds to ~1.6 pore volumes.

and Cd release patterns resemble that of Pb in soil Evin Wood (Figure 5.1). However, Zn and Cd effluent concentrations from Dornach soil were about 10 times higher than in the Evin Field soil. The release pattern of Cu from the Dornach soil is clearly different to that of Zn and Cd. Cu is mainly released in the conditioning phase, likely due to the mobilization of DOC at alkaline pH and low Ca concentration (Temminghoff *et al.*, 1997; Temminghoff *et al.*, 1994). As soon as the influent Ca concentration is increased, Cu concentrations in the effluent sharply decrease, whereas Zn and Cd start to appear in the effluent.

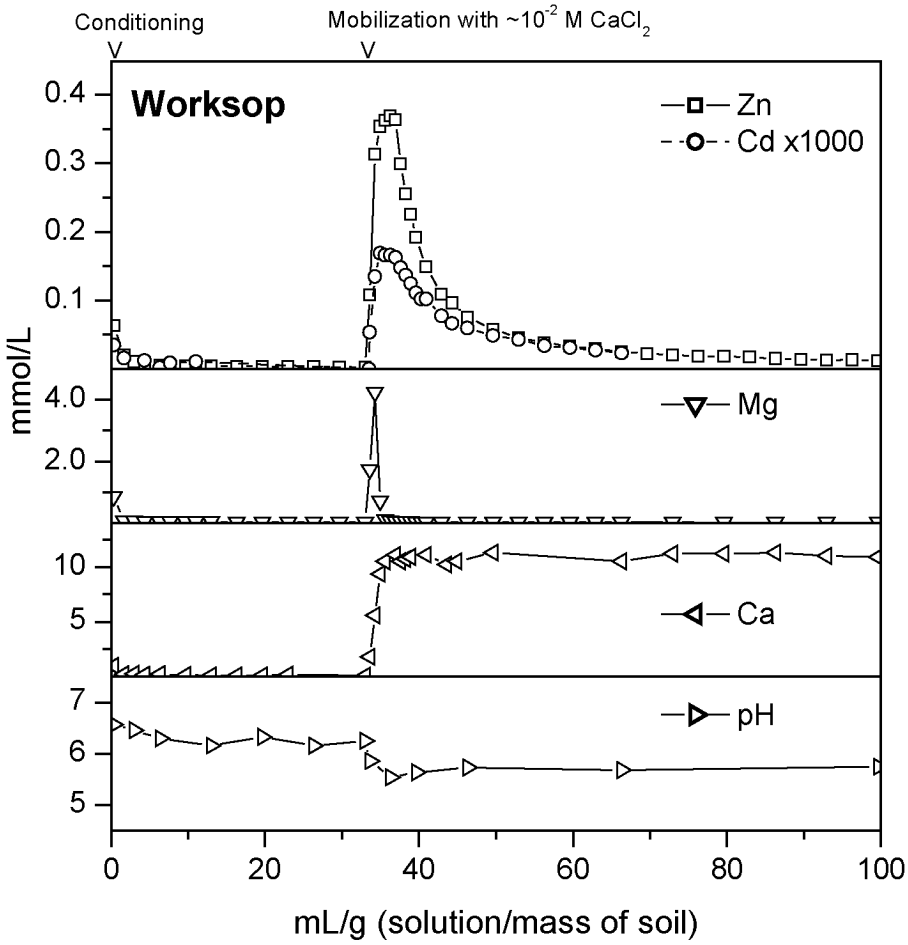

Figure 5.3: Leaching of Worksop soil with 11 mM $CaCl_2$ (Table 5.2, Column 1). Mobilization by Ca^{2+} results in Zn and Cd elution peaks followed by pronounced tailings. The Mg elution front in contrast is very sharp. Abscissa: 1 mL/g corresponds to ~2.6 pore volumes.

The effluent concentration patterns from Worksop soil are presented in Figure 5.3. The Zn and Cd elution peaks compare to the effluent pattern of the Evin Wood soil (Figure 5.1). They likely arise from rapid metal mobilization from sites with low metal affinity. The subsequent tailing, which may be caused by metal release from sites with higher metal affinities, is not completed at the end of the monitored leaching period.

Cumulative amounts of Zn, Cd, Pb, Cu, Mg, and K extracted from Worksop, Evin Wood, Evin Field, and Dornach soil are summarized in Table 5. 3. Comparing these amounts with total metal contents of the soil materials, it can be seen that Zn and Cd in the acidic Worksop and Evin Wood soils were most mobile. The exchangeable amounts of Zn are in the same range as those for the major cations Mg and K. Much less Zn and Cd were released from the neutral Evin Field and Dornach soils.

Table 5.3: Cumulative cation mobilization by Ca^{2+} exchange

	Zn	Cd x100	Pb	Cu	Mg	K
	(mmol/kg)					
Worksop	4.07	0.218	[a]*nd*	*nd*	6.21	0.862
Evin Wood	19.0	24.5	0.159	*nd*	8.93	7.42
Evin Field	0.0190	0.589	*nd*	*nd*	3.42	3.50
Dornach	0.362	0.187	*nd*	0.0354	8.07	1.55

[a] not determined

This can also be seen in Figure 5.4, where the column Ca^{2+} mobilized amounts of Zn are compared to the mobile fractions as determined by different batch extractions. Extracted amounts are normalized to total Zn contents determined by XRF analysis (Table 5.1). Note that amounts extracted in Evin Field and Dornach soils are enlarged by factor 50 and 20, respectively. In the acidic Worksop and Evin Wood soils, the release of exchangeable Zn was almost completed at the end of Ca^{2+} leaching (Figures 5.1 and 5.3). More Zn was extracted in the column than by the batch methods, in which equilibrium between solution and soil, but no complete release of exchangeable cations

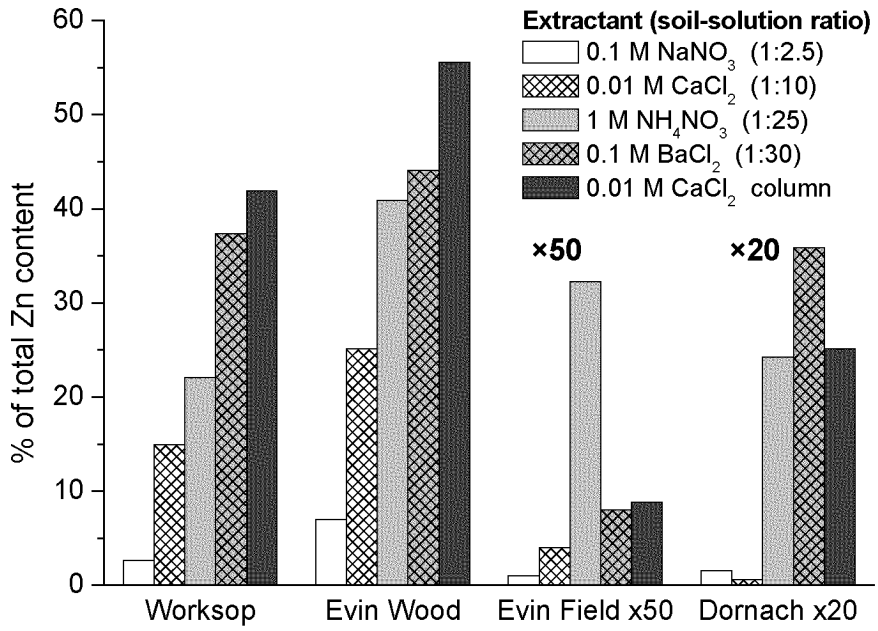

Figure 5.4: Exchangeable Zn in Worksop, Evin Wood, Evin Field, and Dornach soil as determined by different batch extractions and by column Ca^{2+} leaching. Results for Evin Field and Dornach soil are enlarged by factor 50 and 20, respectively.

is attained. Based on the results from 10^{-2} M $CaCl_2$ batch and column extraction, however, it may be assumed that by a number of replenishments, similar amounts of Zn could have been exchanged with all index cations. At the end of the Ca^{2+} mobilization experiments with the neutral Evin Field and Dornach soils, Zn elution was still going (Figure 5.2). Continued leaching with Ca^{2+} would likely have released more Zn than the batch extractions.

In Figure 5.5, the column Ca^{2+} extracted amounts of Zn, Cd, Pb, and Cu are compared to the results from the sequential batch extraction. All data is normalized to total metal contents determined by XRF analysis (Table 5.1). In the acidic Worksop and Evin Wood soils, between 40 and 70% of the total Cd or Zn were mobilized by Ca exchange, which compares well to the sum of the first two batch extraction steps (F1+F2). In contrast, much less Pb was column Ca^{2+} extracted from Evin Wood soil than by F1+F2. Mobilization of Pb, however, was not complete at the end of the column experiment (Figure 5.1). In an additional column experiment, 50% of the total Pb content of Evin Wood soil could be extracted by leaching with 1200 mL of 0.1 M $CaCl_2$

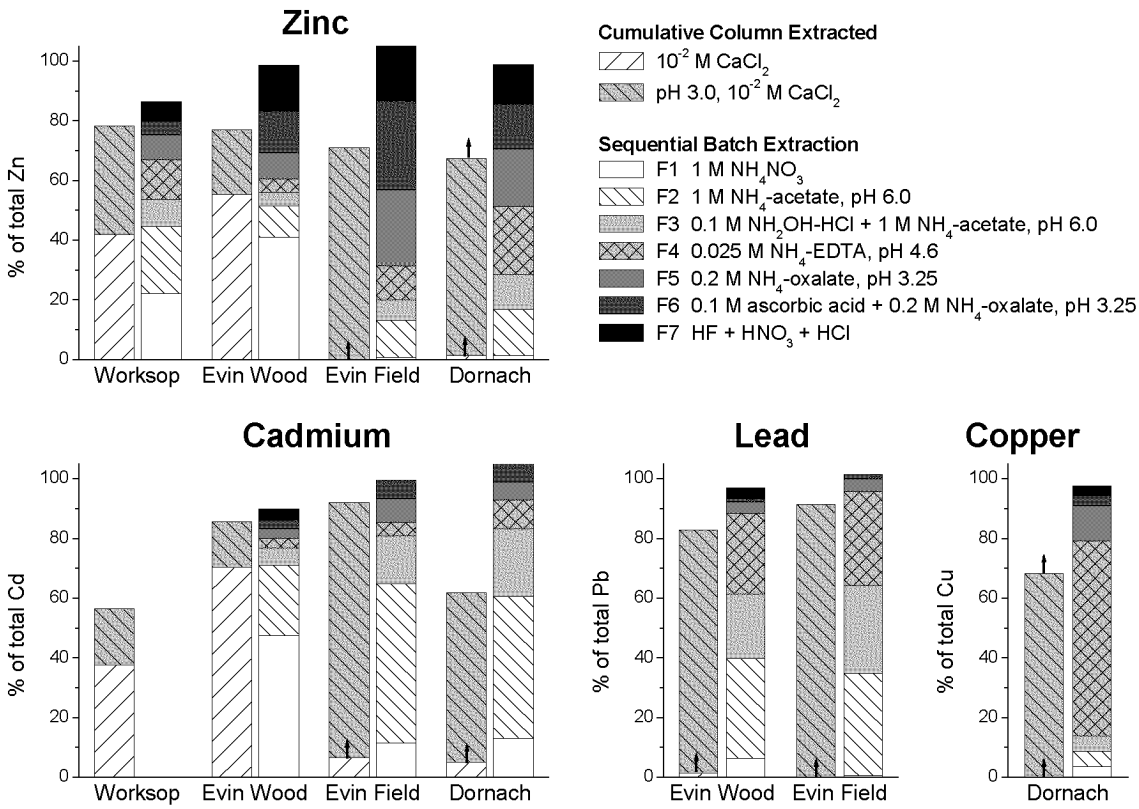

Figure 5.5: Metal fractions extracted by column leaching and in the sequential batch extraction. Extracted amounts as fractions of respective total metal contents (Table 5.1). Amounts leached by 10 mM $CaCl_2$ were obtained by the integration of the column effluent concentrations from 33.3 to 100 mL/g. The pH 3.0 leached amounts were obtained by integration from 100 to 1500 mL/g (columns 2, 4, 6, 10). Small arrows on top of bars indicate that the respective mobilization step was not completed within the experimental time frame.

per gram of soil material (data not shown), and this amount compares again to F1+F2. The sum F1+F2 hence appears to correspond with the amount of a metal that can be mobilized by Ca^{2+} exchange, if the leaching is continued until this pool is depleted. The effluent concentration during mobilization with Ca^{2+}, on the other hand, is determined by the adsorption affinity of the respective metal to the soil material. In the sequential batch extraction, the metal adsorption affinity determines the ratio of F2 over F1. If F1 is larger than F2, like in the case of Zn and Cd in the acidic Evin Wood soil, clear exchange patterns can be observed in the Ca^{2+} mobilization experiment (Figure 5.1), reflecting the low adsorption affinity of the respective cations. For Zn and Cd in the

neutral Evin Field and Dornach soils and for Pb in Evin Wood and Evin Field soils, in contrast, F2 is larger than F1. The resulting elution curves are characterized as a plateau at low concentration levels, which indicates a higher metal affinity to the soil material (Figures 5.1 and 5.2). In the Worksop soil, where the amounts of Zn in the fractions F1 and F2 are comparable, a Zn elution peak followed by a strong tailing is observed (Figure 5.3), which can be rationalized as initial metal release from sites with low metal affinity followed by the release from sites with high metal affinity.

For Cd, the sum F1+F2 is similar in the Evin Wood and Evin Field soil, while in the case of Zn, the sum F1+F2 is much smaller in the neutral Evin Field soil. The effluent concentration of Zn in Evin Field soil was ~3000 times lower than in the Evin Wood soil. For Cd, in contrast, a relatively small decrease of ~50 times was observed. These findings correspond well with spectroscopic data, which suggest, that significant parts of the total Zn in soils Evin Field and Dornach is incorporated into clay minerals and Zn-Al layered double hydroxides (LDH) (Morin, 2000; Kinniburgh *et al.*, 2000), while the fraction of such phases in the acidic Evin Wood soil was much smaller. As recently shown by Ford and Sparks (2000), stable Zn-Al LDH may form upon adsorption of Zn to pyrophyllite at neutral pH. The stability of M-Al LDH phases decreases with the stability of the respective M-(hydr)oxides (Boclair and Braterman, 1999). Therefore, and because of the typically lower Cd concentration levels, immobilization of Cd in an LDH phase is less likely, which may explain the relatively high Cd mobility in the neutral Evin Field soil as compared to Zn. In contrast to Zn, the sum F1+F2 for Pb is not significantly decreased in Evin Field as compared to Evin Wood. This could be attributed to the much higher adsorption affinity of Pb, which may prevent the precipitation of Pb bearing minerals. As can be seen in Figure 5.5, the difference in pH between Evin Wood and Evin Field causes mainly a reduction of the fraction F1, i.e., the pH appears mainly to affect the adsorption affinity of Pb, without strongly affecting the overall mobilizable fraction. However, such interpretations of sequential batch extraction data should be considered hypothetical. Different index cations at different soil-solution ratios extract different amounts of heavy metals, as can be seen for Zn in Figure 5.4. These differences are of minor relevance for the assessment of heavy metal phytoavailability, as mainly the correlation between extracted amounts and plant uptake determines the choice of extractant (Gupta and

Aten, 1993; Gray *et al.*, 1999). For adsorption modeling, however, knowledge of both the total mobilizable pool of a metal as well as its reactivity is required. In the acidic Evin Wood and Worksop soils, the column setup allowed to simultaneously determine the Ca^{2+} mobilizable fractions of Zn^{2+}, Cd^{2+}, Mg^{2+}, and K^{+} and their respective reactivity. The column setup hence represents a useful approach to determine cation binding coefficients in specific contaminated soil materials. In the case of strong adsorption, e.g., Pb in Evin Wood and Cd and Zn in the neutral Evin Field and Dornach soils, prolonged leaching with Ca^{2+} would be required to determine the total mobilizable amounts. In such cases, however, total mobilizable pools can also be estimated from batch extraction data, as was discussed above.

Metals that are strongly adsorbed or incorporated into solid phases are not affected by Ca^{2+} mobilization. However, metals that are considered immobile at present soil pH might become released at lower pH levels. To assess heavy metal mobilization as a result of acidification processes, columns that had been reacted with Ca^{2+} were subsequently leached with dilute acidic solutions (pH 3.0).

5.3.2 Metal Mobilization by Acidification

The mobilization of heavy metals from Worksop soil by leaching with acidic (pH 3.0) 10^{-2} M $CaCl_2$ solution is shown in Figure 5.6. Note that the soil was first leached with 10^{-5} M and 10^{-2} M $CaCl_2$ solution to remove the Ca^{2+} exchangeable fractions. As Worksop soil is slightly acidic and has a low ECEC (Table 5.1), the effluent pH starts decreasing after only ~30 mL/g of acid leaching. The release of Zn, Cd, Mg and K starts immediately after switching to the acidified solution (100 mL/g). The elution of Al in contrast is coupled to the pH breakthrough and is therefore somewhat retarded. While peak effluent concentrations of Zn and Cd are ~10 times lower than in the precedent leaching with non-acidic $CaCl_2$ solution (Figure 5.3), the metal release due to acidification lasts over a longer period of time. Similar elution patterns are also observed in Evin Wood soil as can be seen in Figure 5.7. Again, Zn and Cd elute simultaneously and immediately after switching to pH 3.0 solution. The breakthrough of Pb and Al, on the other hand, is again coupled to the retarded pH breakthrough. Subsequent Pb and Al release continues over the entire duration of the experiment.

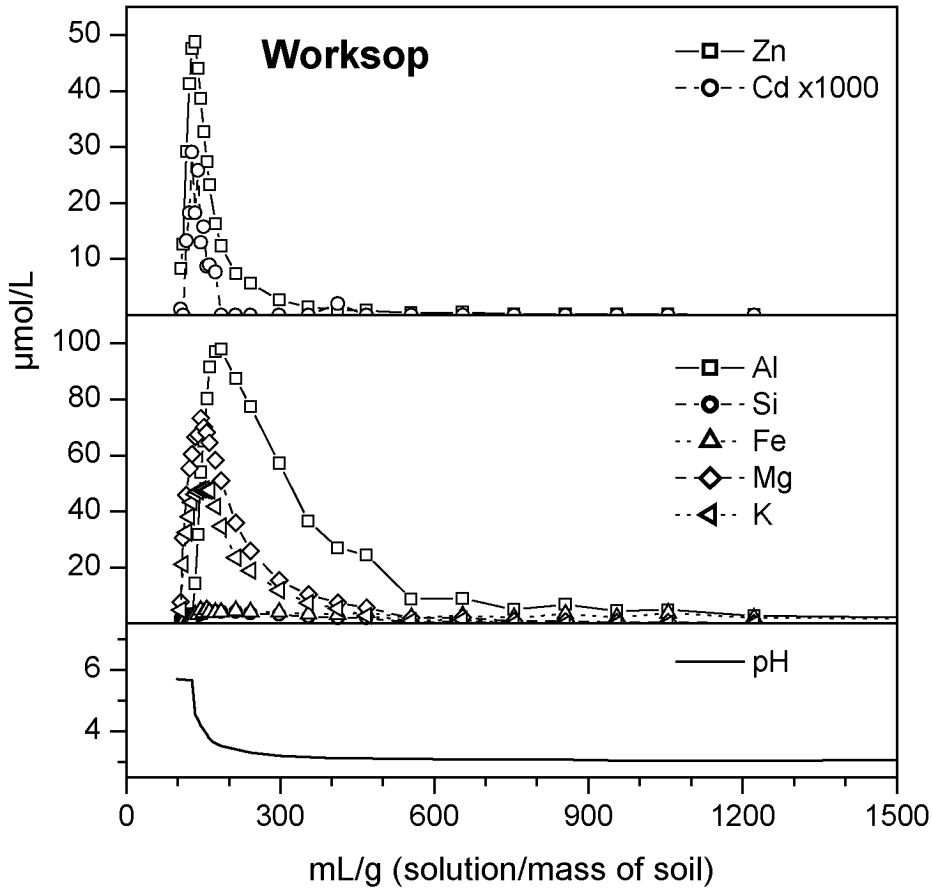

Figure 5.6: Leaching of Worksop soil with pH 3.0 adjusted 10^{-2} M $CaCl_2$ (Table 5.2, Column 2). Zn, Cd, Mg, and K elution starts immediately after the start of pH 3.0 leaching. The release of Al is coupled to the breakthrough of the acidification front. Abscissa: 1 mL/g corresponds to ~2.1 pore volumes.

In Figure 5.8, the effluent concentrations form the pH 3.0 leaching experiment with Evin Field soil are shown. In this case, the pH 3.0 front is much more retarded than in the two acidic soils discussed above. Its position can be explained by the dissolution of $CaCO_3$. Assuming that 2 moles H^+ are required for the dissolution of 1 mol $CaCO_3$, then 140 mL of pH 3.0 (10^{-3} M HCl) solution per gram of soil are required to dissolve 0.07 mol/kg of $CaCO_3$ (7 g/kg, Table 5.1). In the experiment, the pH front arrives slightly later, which is likely due to additional proton buffering by cation exchange. The retarded acidification front results in clearly separated effluent peaks for Cd, Zn, and Pb. The sequence of increasing retardation Cd (-10.1) < Zn (-9.0) < Pb (-7.6) reflects the sequence of increasing metal hydrolysis logK-values (given in brackets), which can be

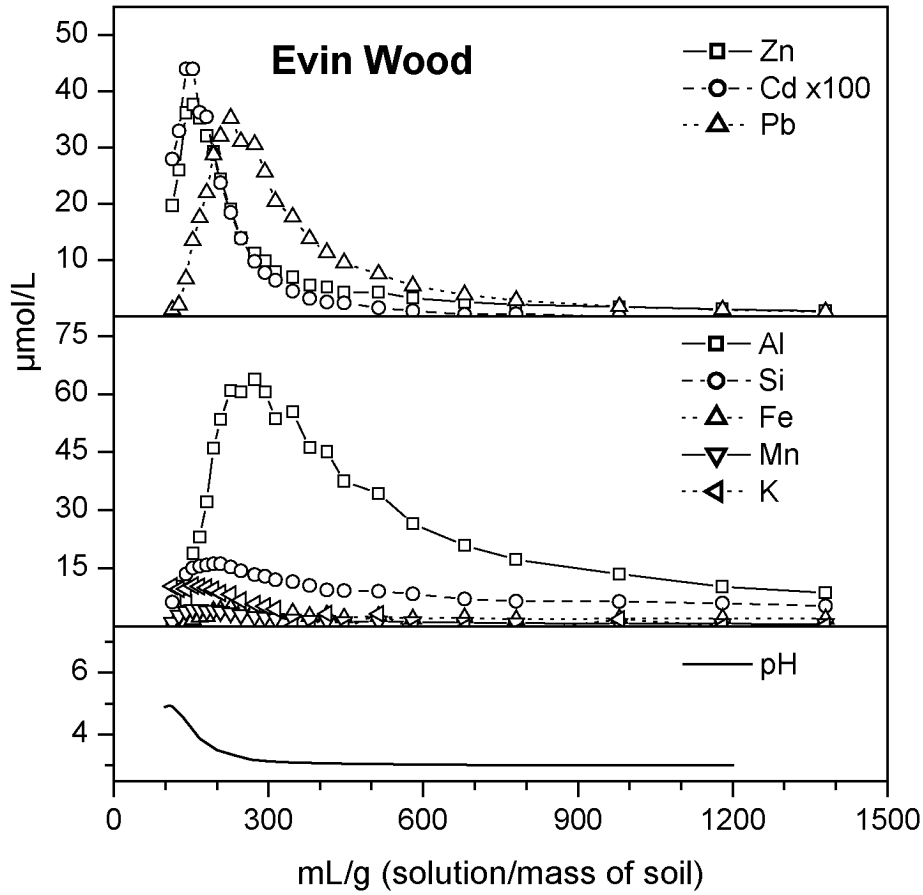

Figure 5.7: Leaching of Evin Wood soil with pH 3.0 adjusted 10^{-2} M $CaCl_2$ (Table 5.2, Column 4). Zn and Cd immediately elute as the pH 3.0 leaching is started. The release of Pb and Al is coupled to the pH breakthrough. Abscissa: 1 mL/g corresponds to ~1.5 pore volumes.

seen as an indicator of cation adsorption affinity (Alloway, 1995). At the pH 3.0 front, Zn, Cd, and Pb are released from the soil material. Mobilized Pb, due to its high adsorption affinity, immediately readsorbs in zones of higher pH, and is therefore coupled to the pH breakthrough (which also applies to Al). Zn and Cd travel faster than the pH front. As they move through the zone of pH ~6.5, Zn is more strongly readsorbed, leading to the separation of the Cd and Zn effluent peaks.

Metal mobilization by pH 3.0. 10 mM $CaCl_2$ leaching of the Dornach soil is shown in Figure 5.9. Here, the effect of $CaCO_3$ dissolution is even more pronounced than in the Evin Field soil. To dissolve the $CaCO_3$ (66 g/kg), 1320 mL/g of pH 3.0 solution would be required. In the experiment, pH breakthrough starts much earlier than

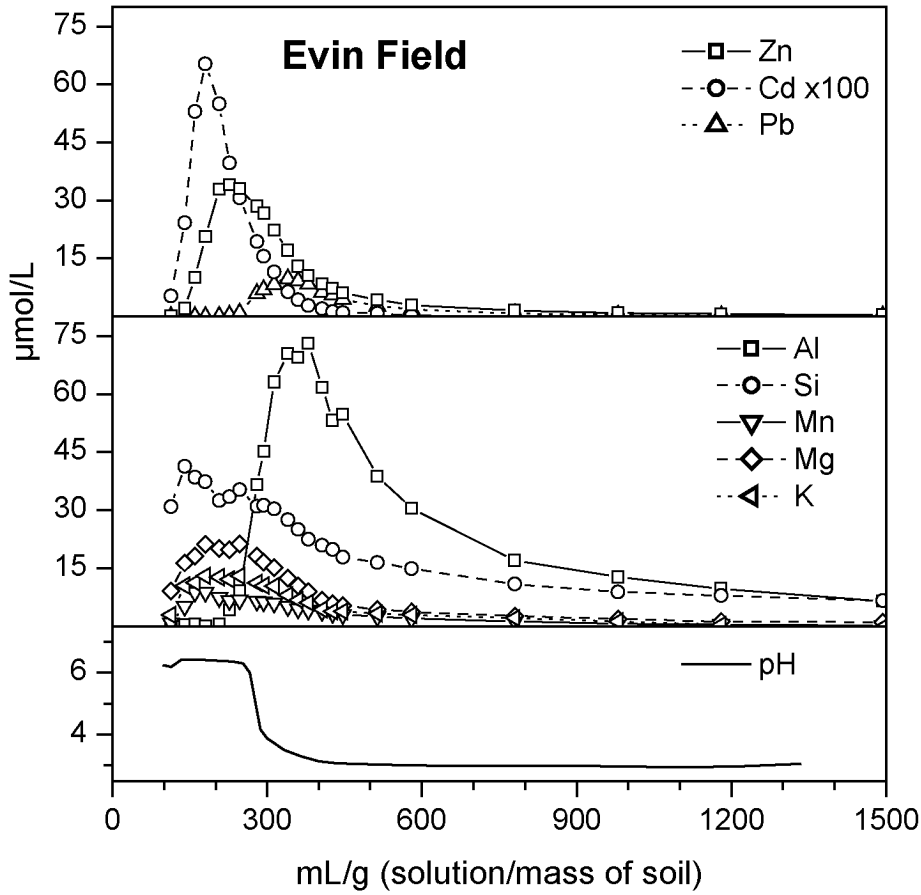

Figure 5.8: Leaching of Evin Field soil with pH 3.0 adjusted 10^{-2} M $CaCl_2$ (Table 5.2, Column 6). Elution peaks of Cd, Zn, and Pb are separated according to adsorption affinity. Zn and Cd move faster than the acidification front, but Zn is more strongly retained in the zone of higher pH. Elution of Pb is coupled to the retarded pH front, which results from the dissolution of $CaCO_3$. Abscissa: 1 mL/g corresponds to ~1.7 pore volumes.

at 1420 mL/g, but effluent pH has not yet reached 3.0 at 1500 mL/g.. Some of the total $CaCO_3$ in the Dornach soil is present as small limestone particles. The dissolution of larger particles takes more time, resulting in a diffuse pH front. However, the early pH decrease does not strongly affect the cumulative proton consumption. The effluent Zn concentration starts to decrease at 500 mL/g, but elution continues even at 1500 mL/g. This pattern might be due to the release of Zn adsorbed to or occluded in $CaCO_3$. On the other hand, the pH buffering also retards simultaneous desorption or dissolution processes. As in the other soil materials, effluent Cd concentrations decrease earlier than Zn concentrations. The effluent peaks of both Cu and Al are coupled to the pH

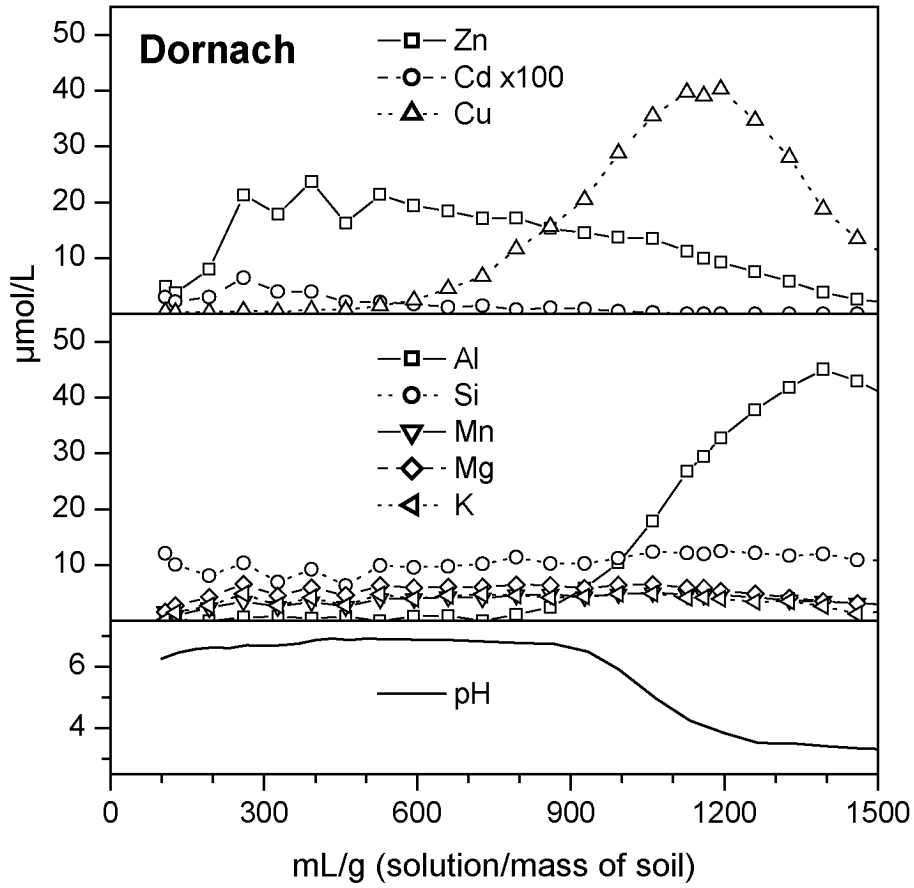

Figure 5.9: Leaching of Dornach soil with pH 3.0 adjusted 10^{-2} M $CaCl_2$ (Table 5.2, Column 8). The release of Zn lasts over the entire time of $CaCO_3$ dissolution. Both Cu and Al elution are coupled to the pH breakthrough, but the Cu peak elutes slightly earlier than Al peak. Abscissa: 1 mL/g corresponds to ~1.1 pore volumes.

breakthrough, but it seems that the slow decrease in effluent pH results in a separation of the two peaks, with Cu (-7.7) eluting earlier than Al (-5.0), which can again be rationalized by interpreting their respective hydrolysis constants as a measure of adsorption affinity (Alloway, 1995).

The effect of metal readsorption upon release is demonstrated in an additional experiment, in which Evin Field soil was leached with pH 3.0 solution containing only 10^{-5} M $CaCl_2$ (Figure 5.10A). The thin dashed lines represent the corresponding experiment with 10^{-2} M $CaCl_2$ (Figure 5.8). The elution peaks of Zn and Cd, which were separated at the higher Ca concentration, now coincide and are coupled to the

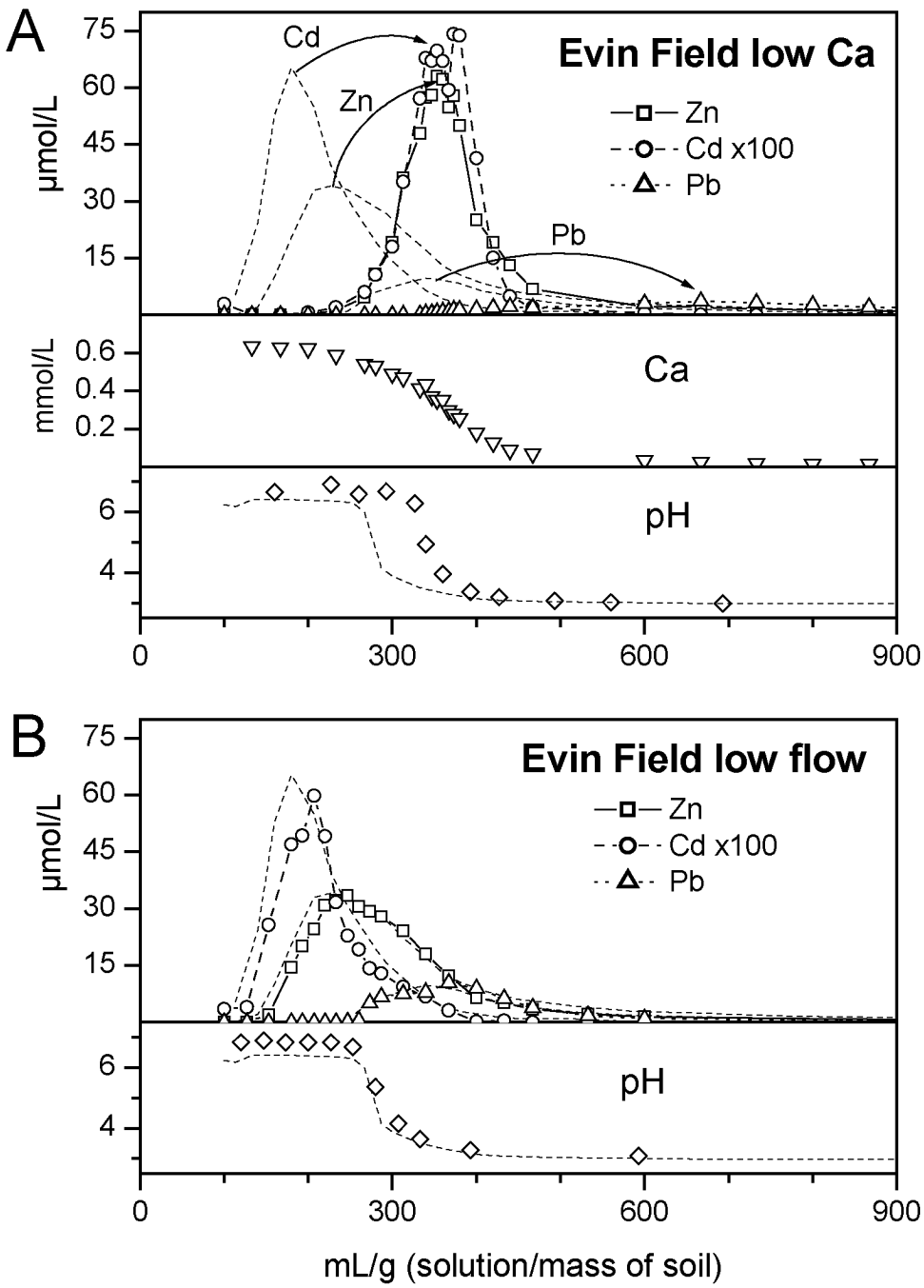

Figure 5.10: The influence of reduced Ca background concentration and reduced flow rate on pH 3.0 leaching of Evin Field soil. Thin dashed lines represent results obtained by leaching with 10^{-2} M $CaCl_2$, pH 3.0 at a flow rate of 0.25 mL/min for comparison (Figure 5.8). (A) At a reduced influent $CaCl_2$ concentration of 10^{-5} M (Column 7, Table 5.2), Zn and Cd released by acidification readsorb and elute coupled to the pH front. Pb is more strongly retarded. Ca release reflects dissolution of $CaCO_3$. (B) At a reduced flow rate of 0.05 mL/min, the release peaks are slightly more retarded. Abscissa: 1 mL/g corresponds to ~1.8 pore volumes

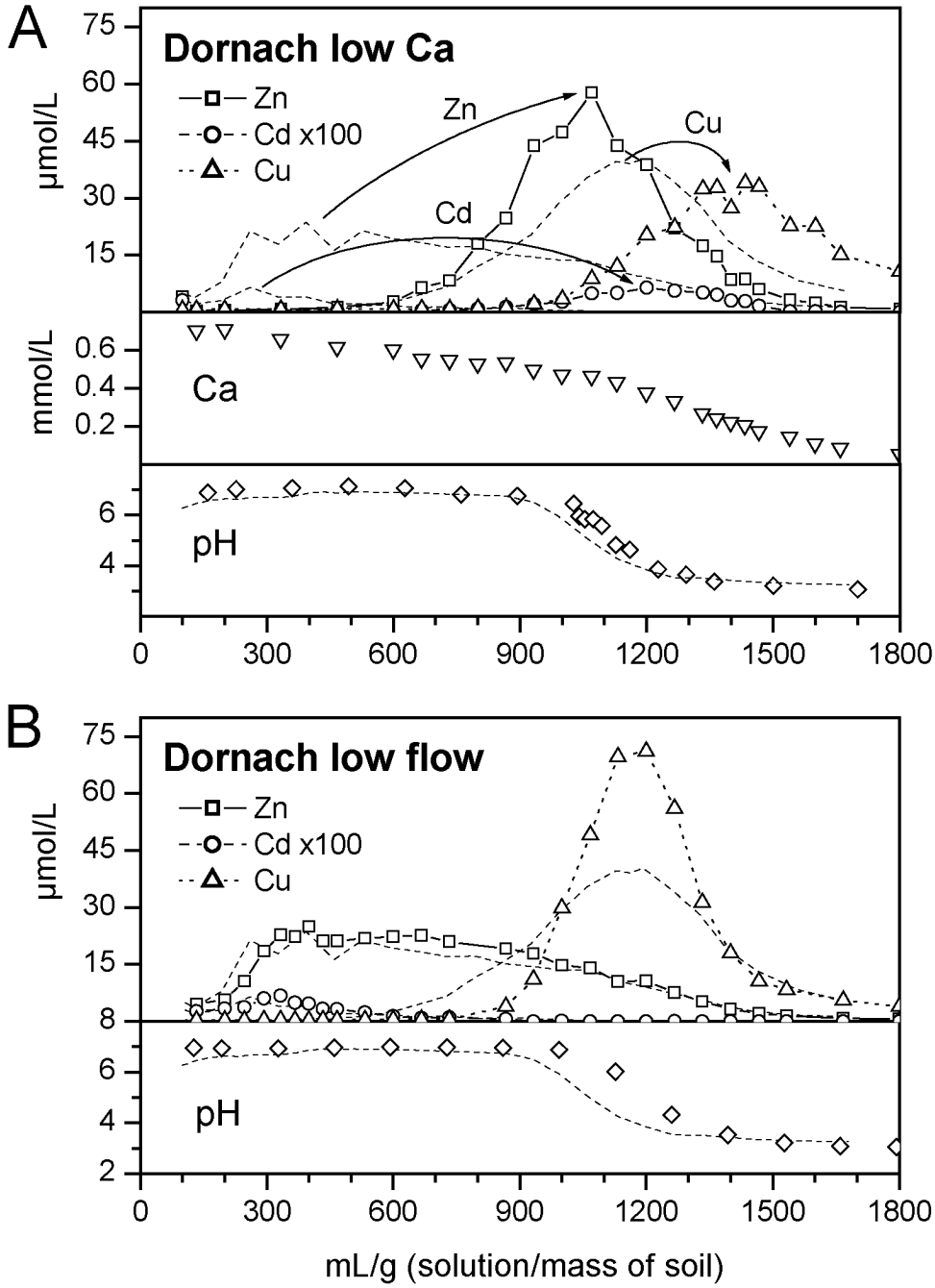

Figure 5.11: The influence of reduced Ca background concentration and reduced flow rate on pH 3.0 leaching of Dornach soil. Thin dashed lines represent results obtained by leaching with 10^{-2} M $CaCl_2$, pH 3.0 at a flow rate of 0.25 mL/min for comparison (Figure 5.9). (A) At a reduced influent $CaCl_2$ concentration of 10^{-5} M (Column 11, Table 5.2), the release of Zn, Cd, and Cu is highly retarded due to metal readsorption. Ca release reflects dissolution of $CaCO_3$. (B) At a reduced flow rate of 0.05 mL/min, the release peaks of Zn and Cd are slightly more retarded. The pH breakthrough front and the coupled Cu release peak are sharper. Abscissa: 1 mL/g corresponds to ~1.3 pore volumes.

acidification front, because both metals readsorb to a similar extent at the low Ca concentration. The shift in the pH breakthrough is likely due to increased proton buffering by cation exchange sites at lower Ca^{2+} concentration. The elution of Ca results from $CaCO_3$ dissolution and Ca exchange by protons. The respective results from Dornach soil are presented in Figure 5.11A. The thin dashed lines represent the corresponding experiment with 10^{-2} M $CaCl_2$ (Figure 5.9). Metal readsorption results in highly retarded metal elution.

The relevance of kinetic effects for metal elution behavior was studied by leaching Evin Field and Dornach soils with acidic (pH 3.0) 10^{-2} M $CaCl_2$ solution at a reduced flow rate of 0.05 mL/min (Figures 5.10B and 5.11B, respectively). The thin dashed lines represent the corresponding experiments at a flow rate of 0.25 mL/min for comparison (Figures 5.8 and 5.9, respectively). In Evin Field soil, the elution curves of Zn and Cd were shifted to somewhat later breakthrough times. The overall elution pattern, however, was similar as in the experiment at higher flow rate. In general, this also applies to the Dornach soil, however, the Cu elution peak was significantly sharper at lower flow rate. In both soils, the observed differences in the elution patterns are most likely related to the higher column Péclet numbers at lower flow rate (Table 5.2), which lead to sharper elution curves.

The amounts of cations released by acidification (integrated from 100 to 1500 mL/g, leaching with 10^{-2} M $CaCl_2$, pH 3.0, flow rate 0.25) are provided in Table 5.4. Mobilized amounts of Zn, Pb, and Cu are in the same range as leached amounts of major elements (Al, Si, Fe, Mn, Mg, K). The released amounts of heavy metals normalized to total heavy metal contents (Table 5.2) are shown in Figure 5.5. During the leaching of soil materials with acidified solution (pH 3.0), metals were released by desorption from sites with high binding affinities and by the dissolution of metal bearing phases. In the neutral Evin Field and Dornach soils, where mobilization by Ca^{2+} exchange was not completed, also the remaining pool of Ca^{2+} exchangeable metals was desorbed. In general, between 70 and 90% of the total metal contents could be mobilized by Ca^{2+} exchange and subsequent pH 3.0 leaching. The low amounts of pH 3.0 leached Cd in Worksop and Dornach soils are an artifact caused by the analytical detection limit (~20 nM).

Spectroscopic data indicate, that between 60 and 80% of Zn in the clay fractions of the Evin Wood, Evin Field, and Dornach soils are incorporated in clay minerals and LDH phases (Kinniburgh *et al.*, 2000; Morin, 2000). This may explain the comparably high residual fractions of Zn as determined in the sequential batch extraction. By leaching with Ca^{2+} and acidic solution, 65 to 80% of the total Zn contents were mobilized. While column results refer to the aggregate fraction 0.1 to 1 mm, spectroscopic data was collected on the clay fraction. A direct quantitative comparison is therefore not possible. Nevertheless do the column data indicate, that Zn bearing precipitates were partly dissolved during leaching with dilute acidic solution.

Table 5.4: Cumulative cation mobilization by [a]pH 3.0 leaching

	Zn	Cdx100	Pb	Cu	Al	Si	Fe	Mn	Mg	K
	(mmol/kg)									
Worksop	3.54	0.110	[b] *nd*	*nd*	24.6	1.44	3.99	0.281	10.5	7.02
Evin Wood	7.47	5.93	9.35	*nd*	30.9	10.5	2.89	1.61	0.858	2.17
Evin Field	7.64	7.69	2.30	*nd*	29.1	21.2	2.06	2.94	7.34	4.57
Dornach	18.9	2.13	*nd*	20.9	20.3	15.1	0.365	5.44	7.61	5.31

[a] leached from 100 to 1500 mL/g with 10^{-2} M $CaCl_2$ at flow rate 0.25 mL/min (Table 5.2, columns 2, 4, 6, and 10); [b] not determined

5.4 Conclusions

From packed column experiments with contaminated soil materials, information on metal reactivity, the coupling of various simultaneous processes, and extractable heavy metal amounts were obtained. In combination with further results, e.g., from spectroscopic studies and batch extractions, such information is valuable for the calibration of sorption models and the assessment of the behavior and fate of heavy metals in contaminated soils.

In the acidic soils, the column Ca^{2+} leaching experiments allowed to simultaneously determine the total exchangeable amounts and their reactivity. Zn and

Cd exhibited similar adsorption behavior and large fractions of the total Cd and Zn contents (40 to 70%) were mobilized by leaching with 10 mM $CaCl_2$. The exchangeable amounts of Zn were equal to or even larger than those of the major cations Mg and K. In the neutral soils, the mobility of both Zn and Cd was much lower. However, the immobilizing effect of pH was much more pronounced for Zn, which may be attributed to the immobilization of Zn in metal bearing solid phases. In comparison to Zn and Cd, Pb and Cu were much less mobile. The effluent patterns obtained from leaching the soil materials with pH 3.0 solutions reflected the coupling of proton buffering reactions, $CaCO_3$ dissolution, proton induced metal release, advective transport, and metal readsorption in zones of higher pH. By leaching with Ca^{2+} and subsequent acidification (pH 3.0) of the soil materials, 65 to 90% of total Zn, Cd, Pb, and Cu contents were released. Though the treatment with pH 3.0 solution is rather harsh, the experiments demonstrate that pools of metals considered immobile at present soil pH, might become mobilized as a result of natural or anthropogenic soil acidification. Metal immobilization in solid phases therefore may not necessarily be permanent.

References

Abd-Elfattah, A., Wada, K., *Adsorption of lead, copper, zinc, cobalt, and cadmium by soils that differ in cation-exchange materials*. Journal of Soil Science 32, 271-283, **1981**.

Ahnstrom, Z.A.S., Parker, D.R., *Cadmium reactivity in metal-contaminated soils using a coupled stable isotope dilution - sequential extraction procedure*. Environmental Science and Technology 35, 121-126, **2001**.

Ahnstrom, Z.S., Parker, D.R., *Development and assessment of a sequential extraction procedure for the fractionation of soil cadmium*. Soil Science Society of America Journal 63, 1650-1658, **1999**.

Alloway, B.J., ed., *Heavy Metals in Soils*. Chapman & Hall, London, **1995**.

Boclair, J.W., Braterman, P.S., *Layered double hydroxide stability. 1. Relative stabilities of layered double hydroxides and their simple counterparts*. Chemistry of Materials 11, 298-302, **1999**.

Boekhold, A.E., van der Zee, S.E.A.T.M., *A scaled sorption model validated at the column scale to predict cadmium contents in a spatially variable field soil*. Soil Science 154, 105-112, **1992**.

Buchter, B., Davidoff, B., Amacher, M.C., Hinz, C., Iskandar, I.K., Selim, H.M., *Correlation of Freundlich Kd and n retention parameters with soils and elements*. Soil Science 148, 370-379, **1989**.

Christensen, T.H., *Cadmium soil sorption at low concentrations: III. Prediction and observation of mobility*. Water, Air, and Soil Pollution 26, 255-264, **1985**.

Ford, R.G., Sparks, D.L., *The nature of Zn precipitates formed in the presence of pyrophyllite*. Environmental Science and Technology 34, 2479-2483, **2000**.

Gray, C.W., McLaren, R.G., Roberts, A.H.C., Condron, L.M., *Cadmium phytoavailability in some New Zealand soils*. Australian Jounal of Soil Research 37, 461-477, **1999**.

Grolimund, D., Borkovec, M., Barmettler, K., Sticher, H., *Colloid-dacilitated transport of strongly sorbing contaminants in natural porous media: a laboratory column study*. Environmental Science and Technology 30, 3118-3123, **1996**.

Grolimund, D., Borkovec, M., Federer, P., Sticher, H., *Measurement of sorption isotherms with flow-through reactors*. Environmental Science and Technology 29, 2317-2321, **1995**.

Gupta, S.K., Aten, C., *Comparison and evaluation of extraction media and their suitability in a simple model to predict the biological relevance of heavy metal concentrations in contaminated soils*. International Journal of Environmental Analytical Chemistry 51, 25-46, **1993**.

Gupta, S.K., Vollmer, M.K., Krebs, R., *The importance of mobile, mobilisable and pseudo total heavy metal fractions in soil for three-level risk assessment and risk management*. The Science of the Total Environment 178, 11-20, **1996**.

Hendershot, W.H., Duquette, M., *A simple barium chloride method for determining cation exchange capacity and exchangeable cations*. Soil Science Society of America Journal 50, 605-608, **1986**.

Hooda, P.S., Alloway, B.J., *Cadmium and lead sorption behaviour of selected English and Indian soils*. Geoderma 84, 121-134, **1998**.

Houba, V.J.G., Temminghoff, E.J.M., Gaikhorst, G.A., van Wark, W., *Soil analysis procedures using 0.01 M calcium chloride as extraction reagent*. Communications in Soil Science and Plant Analysis 31, 1299-1396, **2000**.

Kedziorek, M.A.M., Dupuy, A., Bourg, A.C.M., Compère, F., *Leching of Cd and Pb from a polluted soil during the percolation of EDTA: Laboratory column experiments modeled with a non-equilibrium solubilization step*. Environmental Science and Technology 32, 1609-1614, **1998**.

Kinniburgh, D.G., Benedetti, M.F., van Riemsdijk, W.H., Kretzschmar, R., *Fundamental aspects of metal speciation and transport in metal-contaminated soils and aquifers (FAMEST): Second Annual Report.* Rep. No. WD/00/02, British Geological Survey, Keyworth, Nottinghamshire, **2000.**

McBride, M., Sauvé, S., Hendershot, W., *Solubility control of Cu, Zn, Cd, and Pb in contaminated soils*. European Journal of Soil Science 48, 337-346, **1997**.

McBride, M.B., *Chemisorption and precipitation reactions*. In: *Handbook of Soil Science*. Sumner, M.E., ed., CRC Press, Boca Raton, B/265-B/302, **1999.**

McLaughlin, M.J., Hamon, R.E., McLaren, R.G., Speir, T.W., Rogers, S.L., *Review: A bioavailability -based rationale for controlling metal and metalloid contamination of agricultural land in Australia and New Zealand.* Australian Jounal of Soil Research 38, 1037-1086, **2000a**.

McLaughlin, M.J., Zarcinas, B.A., Stevens, D.P., Cook, N., *Soil testing for heavy metals.* Communications in Soil Science and Plant Analysis 31, 1661-1700, **2000b**.

Morin, G., *personal communication.* **2000**.

Schwartz, A., Wilcke, W., Stýk, J., Zech, W., *Heavy metal release from soil in batch pHstat experiments.* Soil Science Society of America Journal 63, 290-296, **1999**.

Sinaj, S., Mächler, F., Frossard, E., *Assessment of isotopically exchangeable zinc in polluted and nonpolluted soils.* Soil Science Society of America Journal 63, 1618-1625, **1999**.

Sparks, D.L., *Environmental Soil Chemistry.* Academic Press, San Diego, **1995**.

Temminghoff, E.J.M., van der Zee, S.E.A.T.M., de Haan, F.A.M., *Copper mobility in a copper contaminated sandy soil as affected by pH, solid and dissolved organic matter.* Environmental Science and Technology 31, 1109-1115, **1997**.

Temminghoff, E.J.M., van der Zee, S.E.A.T.M., Keizer, M.G., *The influence of pH on the desorption and speciation of copper in a sandy soil.* Soil Science 158, 398-408, **1994**.

Tessier, A., Campbell, P.G.C., Bisson, M., *Sequential extraction procedure for the speciation of particulate trace metals.* Analytical Chemistry 51, 844-851, **1979**.

Villermaux, J., *Theory of linear chromatography.* In: *Percolation Processes: Theory and Applications.* Rodrigues, A.E. ,Tondeur, D., eds., Sijthoff and Noordhoff, Alphen aan den Rijn, 83-140, **1981.**

Voegelin, A., Vulava, V.M., Kretzschmar, R., *Reaction-based model describing sorption and transport of Cd, Zn, and Ni in an acidic soil.* Environmental Science and Technology 35, 1651-1657, **2001**.

Vulava, V.M., Seaman, J.C., *Mobilization of lead from highly weathered porous material by extracting agents.* Environmental Science and Technology 34, 4828-4834, **2000**.

Wang, W.-Z., Brusseau, M.L., Artiola, J.F., *The use of calcium to facilitate desorption and removal of cadmium and nickel in subsurface soils*. Journal of Contaminant Hydrology 25, 325-336, **1997**.

Zeien, H., Bruemmer, G.W., *Chemische Extraktion zur Bestimmung von Schwermetallbindungsformen in Boeden*. Mitteilungen der Deutschen Bodenkundlichen Gesellschaft 59/I, 505-510, **1989**.

CHAPTER 6

MODELING ADSORPTION AND TRANSPORT OF CD AND ZN IN SOILS USING GENERALIZED SCALED EXCHANGE COEFFICIENTS

Abstract

To assess heavy metal adsorption and transport in soils, models are needed, which correctly describe metal adsorption in multicomponent systems, but are still easy to adjust to specific soils. In this study, a model for Cd and Zn adsorption based on cation exchange equations was developed. Scaling factors were introduced to account for the variability of Cd-Ca and Zn-Ca exchange coefficients with soil and solution composition. Generalized scaling parameters were obtained by model calibration to Cd and Zn adsorption data taken from the literature. The compiled adsorption data covered a wide range of adsorptive concentrations (10^{-8} to 10^{-3} M) and were obtained from more than 80 different soils of varying composition (pH 4 -7, organic carbon 2 - 150 g/kg, clay 10 - 550 g/kg). Using generalized parameters, the model could correctly describe experimental Cd and Zn adsorption isotherms at highly variable conditions. Also the coupled transport of Cd and Ca in soil columns was correctly modeled. Column experiments on Ca induced Zn and Cd mobilization from three contaminated soil materials (pH 5.1, 5.9, 6.9) were predicted based on the generalized model parameters and on bulk soil properties. The model correctly predicted the observed effluent concentrations, when adsorbed amounts of Zn and Cd were set equal to the sum of the first two fractions of a sequential batch extraction (NH_4NO_3, NH_4-acetate). In the most acidic soil, an excellent prediction of the coupled effluent patterns of Zn, Cd, Mg, and Ca was obtained.

Voegelin, A., Kretzschmar, R., *Modeling adsorption and transport of Cd and Zn in soils using generalized scaled exchange coefficients.* in preparation

6.1 Introduction

Contamination of soils with Cd and Zn may originate from fertilizer or sewage sludge application, emissions of mining and smelting processes, and further human activities. Cd is highly toxic to plants and animals, and via uptake by crops may pose a threat to human health. Zn is an essential trace element for all organisms, but at elevated concentrations is phytotoxic and may severely affect soil fertility and crop yield (Alloway, 1995). At alkaline conditions, precipitation-dissolution reactions can control Cd and Zn retention in soils. In near-neutral to acidic soils, Cd and Zn retention is dominated by mostly reversible adsorption-desorption reactions (Brümmer *et al.*, 1983; Christensen, 1984b; Voegelin *et al.*, 2001). In acidic soils, Cd and Zn are much more mobile than more strongly adsorbing metals such as Cu and Pb (Abd-Elfattah and Wada, 1981; Buchter *et al.*, 1989; Alloway, 1995). Under such conditions, major cations (e.g. Ca^{2+}, Mg^{2+}) effectively compete with Cd and Zn for sorption sites (Christensen, 1984a; Elzinga *et al.*, 1999; Temminghoff *et al.*, 1995; Voegelin *et al.*, 2001; Harter, 1992). Zn typically occurs at much higher concentration levels than Cd (Alloway, 1995) and was found to competitively adsorb and increase Cd mobility (Christensen, 1987; Wilkens *et al.*, 1998; Voegelin *et al.*, 2001). Accurate modeling of Cd and Zn adsorption processes in the presence of major cations and protons in the soil environment is required in numerous applications such as estimating bioavailability, assessing the risk of contaminated sites, planning clean-up strategies, or predicting and describing metal mobility and transport.

Metal adsorption to model soil compounds, e.g., Fe and Mn oxides, clay minerals, and humic and fulvic acids, is well studied and can be described by sorbent specific models (Goldberg, 1992; Venema *et al.*, 1996; Dzombak and Morel, 1990; Baeyens and Bradbury, 1997; Bradbury and Bayens, 1996; Fletcher and Sposito, 1989; Kinniburgh *et al.*, 1999; Milne, 2000). However, describing metal adsorption in soils on this basis is still difficult if not impossible, because soil materials contain a multitude of intimately associated sorbent phases, which may exhibit sorption properties different to those of pure model compounds (Zachara *et al.*, 1993; Davis *et al.*, 1998). Therefore, there is a clear need for empirical models that can correctly describe metal adsorption in multicomponent systems and can be incorporated into transport codes (Zachara and Westall, 1998; McBride, 1999).

To model heavy metal adsorption in soils, simple adsorption equations have often been used. Non-linear adsorption behavior of metals is typically described by Freundlich equations (Buchter *et al.*, 1989; Jenne, 1998). By scaling the Freundlich coefficient to soil pH, organic matter content, cation exchange capacity (CEC), or solution Ca concentration, generalized Freundlich equations describing Cd and Zn adsorption in soil materials over wide experimental conditions have been derived (Elzinga *et al.*, 1999; Temminghoff *et al.*, 1995; Filius *et al.*, 1998; Boekhold *et al.*, 1993). Other researchers used scaled Freundlich-type approaches to relate extractable Cd or Zn to total amounts in soil and further soil properties (Boekhold and van der Zee, 1992; Streck and Richter, 1997; McBride *et al.*, 1997; Sauve *et al.*, 2000) or to assess heavy metal bioavailability in the soil environment (Plette *et al.*, 1999). Despite its wide applicability, the Freundlich approach is of limited use for describing the competitive adsorption and transport of several interacting cations. Adsorption data of Co, Ni, and Cu presented by Harter (1992) or Cd-Zn-Ni-Ca transport experiments conducted by (Voegelin *et al.* (2001) clearly demonstrate desorption of Ca by adsorbing heavy metal cations. Such apparent cation exchange processes can not be described with the Freundlich approach, as it is not based on a consistent set of reaction equations, and does not account for the adsorption maximum and charge-balance (Jenne, 1998; Voegelin and Kretzschmar, 2001a). An alternative approach is hence needed to describe multication systems with several interacting heavy metal and major cations. To describe the reactive transport of several interacting cations, Borkovec *et al.* (1996) suggested an empirical multisite approach based on competitive Langmuir equations. While this approach accounts for the interaction of several cations and the adsorption maximum, it is, however, not charge-balanced. In addition, the different types of sites result from the fitting procedure and are not conceptually related to specific soil sorbents. Hence, model parameters are highly conditional for the investigated system. Introduction of additional competing cations requires all model parameters are refitted, and parameter application to other soil materials is not possible.

Cation exchange equations present the simplest way to account for the charge balance and maximum of cation adsorption reactions (Voegelin and Kretzschmar, 2001a; Hendrickson and Corey, 1981), and can also be extended from binary to multication systems. They may hence prove a useful approach to describe adsorption

and transport of heavy metal cations such as Cd^{2+}, Zn^{2+}, Ni^{2+} or Co^{2+} in soil materials. The objectives of this study were: i) to develop an adsorption model for Cd and Zn based on apparent exchange coefficients scaled to variations in soil and solution composition, ii) to obtain generalized model parameters from a compilation of literature data on Cd and Zn adsorption in a wide variety of soil materials and over wide ranges in solution composition, iii) to test the model performance with respect to the description of adsorption isotherms and transport experiments, and iv) to assess if and how the model, based on generalized model parameters, can be applied to predict Cd and Zn mobility in contaminated soil materials.

6.2 Materials and Methods

6.2.1 Compilation of Cd and Zn Adsorption Data

Data on Cd and Zn adsorption to non-calcareous (<10 g/kg) soil materials was compiled from the literature. Only Cd and Zn adsorption data measured in $CaCl_2$, $Ca(NO_3)_2$ or $Ca(ClO_4)_2$ background electrolyte was included. The Cd data were taken from Voegelin *et al.* (2001), Temminghoff *et al.* (1995), Boekhold *et al.* (1993), Christensen (1984a), Christensen *et al.* (1996) Buchter *et al.* (1989), Soon (1981), Gray *et al.* (1998), Gray *et al.* (1999), Filius *et al.* (1998), Hooda and Alloway (1998), and Yuan and Lavkulich (1997), and the Zn data from Buchter *et al.* (1989), Elrashidi and O'Connor (1982), Kurdi and Doner (1983), Christensen (1987), and Yuan and Lavkulich (1997). Our own Zn adsorption data for the soil material described in Voegelin *et al.* (2001) was also included (unpublished). Wherever possible, data was directly taken from published figures or tables. In some cases, adsorption data had to be recalculated from isotherm equations based on the reported number of data points and the concentration levels. To calculate the activity of ionic species in solution, activity coefficients based on the Davies equation were used (Sparks, 1995). The only relevant inorganic complex was $CdCl^+$ (with $\log K_0=1.98$ for $Cd^{2+} + Cl^- \rightleftharpoons CdCl^+$ (Smith and Martell, 1976)). The DOC concentration in Ca background electrolytes was assumed to be low and therefore, the complexation of Cd and Zn by DOC was neglected. An overview of the ranges in soil and solution composition covered by the Cd and Zn adsorption datasets is given in Table 6.1.

Table 6.1: Data ranges of the Cd and Zn adsorption data sets

Cadmium	[d]o.c.	[e]clay	pH	[f]logc_{Cd}	[f]logc_{Ca}	[g]logq_{Cd}	[h]log$K_{d,Cd}$
[a]NS=79, [b]NP=618	(g/kg)	(g/kg)		(mol/L)	(mol/L)	(mol/kg)	(L/kg)
average	32	158	5.5	-6.0	-2.2	-4.3	1.7
median	15	160	5.3	-6.3	-2.0	-4.5	1.9
[c]2.5 percentile	2	10	3.9	-8.7	-3.1	-6.5	0
[c]97.5 percentile	170	537	7.7	-3.1	-1.0	-2.1	3.1
Zinc	[d]o.c.	[e]clay	pH	[f]logc_{Zn}	[f]logc_{Ca}	[g]logq_{Zn}	[h]log$K_{d,Zn}$
[a]NS=19, [b]NP=189	(g/kg)	(g/kg)		(mol/L)	(mol/L)	(mol/kg)	(L/kg)
average	23	191	5.5	-4.5	-2.3	-3.2	1.4
median	14	140	5.7	-4.4	-2.3	-3.0	1.3
[c]2.5 percentile	2	9	3.9	-7.9	-3.4	-5.9	0.2
[c]97.5 percentile	116	732	7.0	-2.4	-1.7	-1.8	2.8

[a]NS=Number of soil materials; [b]NP=Number of data points; [c]95% of all values are within the range given by the 2.5 and 97.5 percentile; [d]o.c.=organic carbon content (1 g organic matte was assumed to correspond to 0.59 g organic carbon); [e]clay=clay content; [f]logarithm of total concentrations in solution (in mol/L); [g]logarithm of adsorbed amounts (in mol/kg); [h]logarithm of distribution coefficient K_d (in L/kg); $\log K_{d,M}=\log q_M-\log c_M$.

6.2.2 Cd Breakthrough and Desorption Experiments

Riedhof soil material (acidic, silt loam, 9 g/kg organic matter, 16 g/kg clay) was homogeneously packed into a chromatographic column of 1 cm inner diameter. After Ca saturation of the soil material and equilibration with 1.01×10^{-4} M $CaCl_2$ solution adjusted to pH 4.6, the breakthrough of 9.6×10^{-6} M Cd (added as $CdCl_2$) in the same background electrolyte solution was monitored. The flow rate was set to 0.5 mL/min. After 800 pore volumes, the influent was switched back to the pure $CaCl_2$ electrolyte solution to desorb the retained Cd. The column had a packing density of 2.01 kg/L, a porosity of 60%, a pore volume of 0.92 mL, and a Péclet number of 150. An analogous experiment in the same soil material was carried out at a pH of 5.7. The background electrolyte contained 1.06×10^{-4} M $CaCl_2$ and was adjusted to pH 5.7. The Cd concentration was 9.4×10^{-6} M. The breakthrough of Cd was monitored over 1600 pore volumes before the influent was switched back to the Cd free electrolyte solution. The

column had a packing density of 1.91 kg/L, a porosity of 60%, a pore volume of 1.1 mL, and a Péclet number of 90. Details on the experimental setup were reported elsewhere (Voegelin *et al.*, 2001).

6.2.3 Leaching Experiments with Zn and Cd Contaminated Soil Materials

Column leaching experiments were conducted with three topsoil materials sampled from Zn and Cd contaminated soils (Evin Wood, Worksop, and Dornach). All experiments and analyses were conducted with the aggregate fraction 0.1 to 1.0 mm. A characterization of the soil materials is provided in Table 6.2. In a sequential batch extraction (Zeien and Bruemmer, 1989; Schwartz *et al.*, 1999), Zn and Cd in seven sequential extracts were determined (with hypothetical interpretation according to (Zeien and Bruemmer, 1989) in brackets): F1: 1 M NH_4NO_3, soil-solution ratio 1:25 (mobile fraction, water soluble and exchangeable, non-specifically adsorbed); F2: 1 M NH_4-acetate, pH 6.0 (readily mobilizable fraction, specifically adsorbed, $CaCO_3$ bound, and other weakly bound species); F3: 0.1 M NH_2OH-HCl+1 M NH_4-acetate, pH 6.0 (bound to Mn-oxides); F4: 0.025 M NH_4EDTA, pH 4.6 (bound to organic substances); F5: 0.2 M NH_4-oxalate, pH 3.25 (bound to amorphous and poorly crystalline Fe oxides); F6: 0.1 M ascorbic acid in 0.2 M NH_4-oxalate, pH 3.25, in boiling water (bound to crystalline Fe oxides); F7: $HF/HNO_3/HCl$ (residual fraction). The soil-solution ratio for the extracts F1 to F6 was 1:25.

Glass columns of 1 cm inner diameter were packed with 15 g of soil material and flushed with CO_2 gas to displace the air from the pore space. The column inlet was then connected to a HPLC pump and the outlet to an automated fraction collector. Solutions were first passed through a degasser and then through the columns in upward direction. The flow rate was set to 0.25 mL/min. In a first step, columns were leached with a 10^{-5} M $CaCl_2$ solution (33 mL/g soil material) in order to saturate the column and to remove loose colloidal particles and DOC. Exchangeable cations were then mobilized by increasing the Ca^{2+} concentration in the influent to ~10^{-2} M $CaCl_2$. Evin Wood, Worksop, and Dornach soil columns had lengths of 19.4, 14.5, and 20.3 cm, packing densities of 1.67, 2.62, and 1.59 kg/L, and Péclet numbers of 170, 250, and 160, respectively. Details on the experimental setup were provided elsewhere (Voegelin and Kretzschmar, 2001b).

Table 6.2: Characterization of the contaminated [a]soil materials Evin Wood, Worksop, and Dornach

	Soil properties					[d]Total contents		[e]Batch exchangeable cations					
	o.c.	clay	$CaCO_3$	[b]pH	[c]CEC_{mod}	Zn	Cdx100	Zn	Cdx100	Mg	K	Ca	[f]CEC_{exp}
Soil	—— (g/kg) ——				($mmol_c$/kg)	(mmol/kg)		——— (mmol/kg) ———					($mmol_c$/kg)
[h]Evin Wood	52.3	229	<5	5.1	179	34.2	34.9	14.0	16.5	8.25	11.7	63.9	184
[i]Worksop	14.4	68	<5	5.7	60	9.71	0.580	2.15	[g]0.218	8.36	1.68	18.1	59
[k]Dornach	82.3	372	66	6.9	433	28.8	3.75	0.35	0.308	8.45	3.96	248	518

[a]all data presented refer to the aggregate fraction 0.1 to 1.0 mm used in the release experiments; [b]pH in 10 mM $CaCl_2$, soil-solution ratio 1:2.5; [c]calculated by Eq. 6.6 using o.c., clay, and pH; [d]determined by X-ray fluorescence spectroscopy; [e]batch extracted with 1 M NH_4NO_3, soil-solution ratio 1:25; [f]determined from the sum of exchangeable cations; [g]cumulative extracted amount from leaching experiment (Figure 6.5), batch data not available; [h]clayey and poorly drained, forested, contaminated by smelter emissions, sampling depth 0-5 cm; [i]developed on sandstone, well-drained, arable field, contaminated by sewage sludge application, sampling depth 0-30 cm; [k]developed from limestone gravel, grassland, contaminated by smelter emissions, sampling depth 0-5 cm.

6.2.4 Transport Calculations

Transport was calculated using PHREEQC 2.2 (Parkhurst and Appelo, 1999). Because of the high Péclet numbers of all soil columns, and in order to keep the transport part simple, dispersion was not explicitly accounted for. The experiments on breakthrough and desorption of Cd were modeled using 20 mixing cells. Leaching experiments with contaminated soil materials were calculated with 40 mixing cells. Solution speciation was calculated with thermodynamic complex formation constants K_0 derived from conditional constants (Smith and Martell, 1976; Martell and Smith, 1982; Smith and Martell, 1989) using the Davies equation. Complexed species considered were (with $\log K_0$ for $M + nL = ML_n$ in parenthesis): $CaCl^+$ (0.58), $MgCl^+$ (0.63), KCl^0 (-0.70), $CdCl^+$ (1.98), $CdCl_2^0$ (2.60), $ZnCl^+$ (0.46).

6.3 Model Development

In order to correctly describe the coupled effluent patterns of several interacting cations in transport experiments a charge-balanced adsorption model must be used. In surface complexation models, charge neutrality is maintained by electrostatically adsorbed cations in the diffuse layer (Goldberg, 1992). Simple isotherm equations such as the

Freundlich isotherm however do not provide a charge-balanced description of adsorption. Cation exchange equations represent the simplest way to account for the overall charge-balance of adsorption processes.

In contrast to metal-specific complexation reactions on soil surface sites, adsorption of cations to the negatively charged exchanger is generally considered a non-specific adsorption process determined by electrostatic interactions (McBride, 1989). Exchange of Ca by Cd (all subsequent equations given for Cd also apply to Zn) is written as:

$$CaX_2 + Cd^{2+} \rightleftarrows CdX_2 + Ca^{2+} \tag{6.1}$$

where X^- denotes an exchanger charge of -1. The respective exchange coefficient is given by:

$$K_{CdCa} = \frac{q_{Cd} a_{Ca}}{q_{Ca} a_{Cd}} \tag{6.2}$$

with q_M being the adsorbed amount of metal M (in mol/kg) and a_M representing the activity of metal M in solution. Note that homovalent exchange coefficients do not depend on whether adsorbed amounts, charge fractions, or mole fractions are used to express the activity of adsorbed species (Jenne, 1998). The cation exchange capacity (CEC), i.e. the total negative charge, is assumed to be balanced by exchangeably adsorbed cations. In the binary Cd-Ca system, only Cd^{2+} and Ca^{2+} cations adsorb to the exchanger, the charge balance is hence given by:

$$CEC = \frac{1}{2}\left(q_{Cd} + q_{Ca}\right) \tag{6.3}$$

From Eq. 6.2 and 6.3, the Cd exchange isotherm for the binary Cd-Ca system can be derived:

$$q_{Cd} = \frac{1}{2} CEC \frac{K_{CdCa} a_{Cd}}{a_{Ca} + K_{CdCa} a_{Cd}} \quad (6.4)$$

When Eq. 6.4 is applied to heavy metal adsorption on soil materials, exchange coefficients are found to vary with the composition of the soil matrix and the soil solution (Abd-Elfattah and Wada, 1981; Bruggenwert and Kamphorst, 1979; Hendrickson and Corey, 1981). Apparent exchange coefficients describing the adsorption of heavy metal cations increase with increasing background cation concentration and decreasing heavy metal concentration in solution. This is attributed to the fact that they do not only account for non-specific adsorption to a large number of exchange sites, but also for specific heavy metal adsorption to a limited number of sites with a high affinity for heavy metals (Hendrickson and Corey, 1981). Because the contribution of specific adsorption to total adsorption increases with pH, also apparent exchange coefficients are observed to increase. As heavy metal cations exhibit different affinities to different types of sorbents (McBride, 1989), apparent exchange coefficients vary also with soil material composition. One possible way to account for the observed heterogeneity is to introduce additional types of binding sites with different heavy metal affinities, as was shown by Voegelin *et al.* (2001) for Cd, Zn, and Ni adsorption to an acidic silt-loam soil material. This approach allows conceptualizing the variability of the apparent metal adsorption affinity in a specific soil material at variable solution composition. However, model application in a specific contaminated soil would require the simultaneous determination of both the fractions and the reactivity of heavy metals that can be attributed to different model sites. This in many cases is not possible. Therefore an alternative approach based on a single type of sorption sites was followed in this study. To account for the observed variations in adsorption affinity, scaled apparent exchange coefficients were introduced:

$$\log K_{MCa} = \log K_{MCa,0} + n_{oc,M} \log f_{oc} + n_{cl,M} \log f_{cl} + n_{H,M} \log a_H + n_M \log a_M + n_{Ca,M} \log a_{Ca} \quad (6.5)$$

where K_{MCa} is the apparent exchange coefficient used in Eq. 4, $K_{MCa,0}$ is the reference exchange coefficient, f_{oc} and f_{cl} are the fractional soil organic matter and clay content (e.g., kg/kg), and $n_{M,Y}$ are the scaling parameters for the exchange coefficient of metal

M. With respect to the exchanging cations, Eq.6.5 represents an extended version of the Rothmund-Kornfeld formulation of cation exchange (Rothmund and Kornfeld, 1918; Langmuir, 1981). Following the Rothmund-Kornfeld convention, the same exponent is assigned to the activities of both exchanging cations. In Eq. 6.5, an individual exponent is assigned to each cation. With respect to pH, organic matter content, and clay content, Eq.5 compares to scaled Freundlich coefficients or K_d values (Lee *et al.*, 1996; Boekhold and van der Zee, 1992; Elzinga *et al.*, 1999). To account for variations with soil material composition, organic matter and clay content were included into Eq. 6.5, assuming that these two fractions are most relevant for metal adsorption to soils materials.

According to Eq. 6.4, heavy metal adsorption to soil materials is limited by the CEC. In most cases, this appears reasonable, as high affinity adsorption sites presumably represent only a small fraction compared to the CEC. The soil CEC mainly originates from permanent charge on clay minerals and the variable pH dependent charge of the organic matter. Therefore, it can be estimated from the clay and organic carbon content and pH, assuming that organic matter and clay fraction from different soils exhibit similar properties (Curtin and Rostad, 1997; Helling *et al.*, 1964). According to Curtin and Rostad (1997), who related the measured CEC of approximately 1600 Canadian soils to their soil organic carbon and clay content and pH, the CEC can be estimated as:

$$CEC = [3.97(1-0.183(8.2-pH))f_{oc} + 0.57(1-0.102(8.2-pH))f_{cl}]\,mol_c/kg \qquad (6.6)$$

Eq. 6.6 was used to estimate the CEC in the adsorption datasets, because in most publications, the CEC at the pH of the adsorption experiment was not indicated. For the soil clay fraction, Eq. 6.6 (right term) yields a CEC 0.57 mol_c/kg at pH 8.2, which compares to exchange capacities reported for pure clay minerals and soil clay size isolates (Alloway, 1995; Zachara *et al.*, 1993). The CEC of the soil organic matter at pH 8.2 (left term) of 3.97 mol_c/kg compares to carboxylate group concentrations of 1.5 to 6 mol/kg reported for humic acids (Stevenson, 1994). The pH dependence of the organic carbon contribution to the CEC (left term in brackets) represents a linear approximation to a pH titration curve described with the Henderson-Hasselbach equation using

pK_a=5.5 and n=2, parameters realistic for soil organic matter (McBride, 1994; Stevenson, 1994). The lower pH dependence of the clay contribution to CEC (right term in brackets) is due to permanent charge sites on clay minerals. The pH dependence of the CEC of the clay fraction results from the variable charge of oxides, clay edges, and from humic and oxide coatings on clay minerals (Zachara *et al.*, 1993). Also the blocking of permanent charge exchange sites by aluminum polymers may cause and apparent pH dependence of the CEC (Sparks, 1995). Similar parameters as given in Eq. 6.6 could also be obtained from (Helling *et al.*, 1964).

The scaling parameters of Eq. 6.5 were obtained by applying Eq. 6.4 to the Cd and Zn datasets, minimizing the Mean Square Error MSE:

$$MSE=\frac{1}{n}\sum_{i=1}^{n}(\log q_{i,exp}-\log q_{i,mod})^2 \qquad (6.7)$$

where $q_{i,exp}$ and $q_{i,mod}$ are the experimental and modeled amount adsorbed in mol/kg of the i^{th} data point, n is the total number of data points. Minimizing the MSE with the NLIN procedure of the SAS software package (SAS, 1999), adjusted model parameters and their standard errors were obtained.

6.4 Results and Discussion

6.4.1 Description of Cd and Zn Adsorption Data

Modeled and experimental logarithmic amounts of adsorbed Cd and Zn are compared in Figure 6.1. For both Cd and Zn, the modeled data compare to the experimental data and are arranged around the solid 1:1 relation line. The dotted lines indicate the 95-percentile interval of model deviations. They approximately indicate the 95% confidence limits for model predictions. Data points from different pH ranges do not reveal any systematic pH dependent deviations. Part of the observed scatter around the 1:1 relation line may be caused by uncertainties in the experimental data. In some publications, only the initial solution pH or the soil pH was reported, which may differ from the final equilibrium pH in the adsorption experiments. In addition, only the initial Ca solution concentration was often indicated, and the soil material was not completely saturated with Ca prior to the experiments. The final Ca concentrations in solution

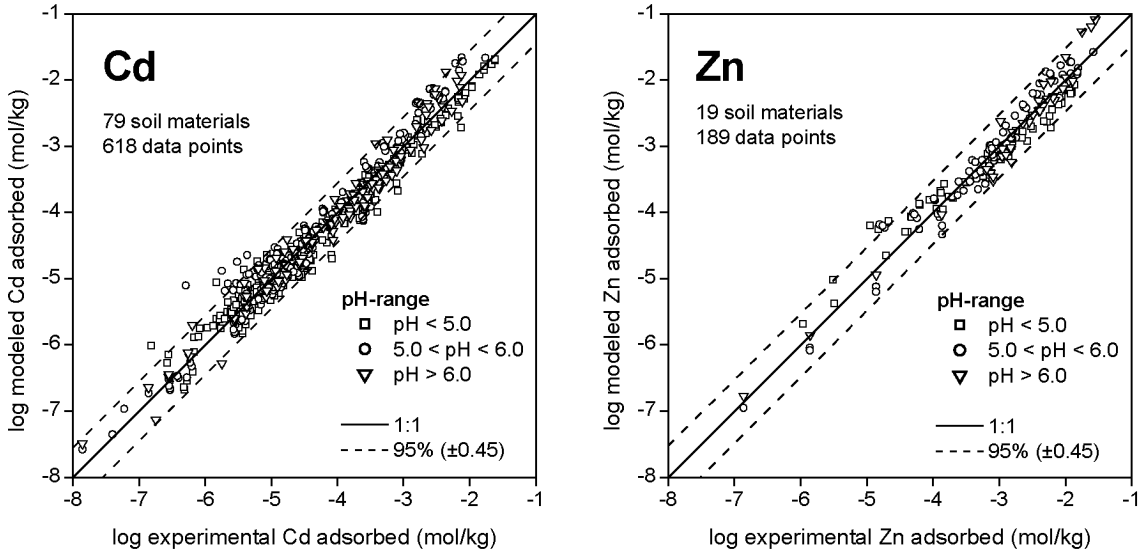

Figure 6.1: Modeled versus experimental logarithmic amounts of Cd and Zn adsorbed to a wide range of soil materials. Modeled data compares well to experimental data and data points are grouped along the 1:1 relation line (solid). No systematic model deviations in different pH-ranges are observed. The 95-percentile interval of model deviations (dotted lines) approximately indicates the 95% confidence limits for model predictions.

hence may be somewhat lower than the reported initial concentrations. Finally, the intrinsic heterogeneity of the soil organic matter and soil clay fraction from different soil materials limits the accuracy that can be obtained by a generalizing adsorption model. Considering the wide variations in soil and solution composition (Table 6.1), the model is in good agreement with experimental data.

Model parameters and statistical information are provided in Table 6.3. The parameters n_M, $n_{Ca,M}$, and $n_{H,M}$ reflect the increase of apparent exchange coefficients with decreasing heavy metal concentration, increasing Ca concentration, and increasing pH (Abd-Elfattah and Wada, 1981; Hendrickson and Corey, 1981). At low Cd or Zn concentration levels, i.e. $a_M << a_{Ca}$, the exchange isotherm (Eq. 6.4) with variable exchange coefficient (Eq. 6.5) reduces to a scaled Freundlich type equation:

$$q_M = \left(\frac{1}{2} CEC \times K_{MCa,0} f_{oc}^{\,n_{oc}} f_{cl}^{\,n_{cl}} a_H^{\,n_{H,M}} a_{Ca}^{\,n_{Ca,M}-1} \right) a_M^{\,n_M+1} \qquad (6.8)$$

The exponent n_M+1 assigned to the adsorptive cation activity in Eq. 6.8 is equal to 0.85 for Cd and 0.77 for Zn. This compares well to respective Freundlich exponents (f_{Cd}=0.85, f_{Zn}=0.73) presented by Elzinga *et al.* (1999), who described a large set of Cd and Zn adsorption data compiled from the literature with scaled Freundlich isotherms. Also the exponents $n_{H,M}$ assigned to the proton activity (-0.48 for Cd and -0.54 for Zn) are found to be similar to exponents reported by Elzinga *et al.* (1999) (-0.44 and -0.46, respectively). In contrast to scaled Freundlich equations from literature, Eq. 6.8 discerns two factors, by which soil organic matter and clay content affect heavy metal adsorption. In a linear form, they contribute to the total available site concentration (Eq. 6.6), and in the exponential term (Eq. 6.5), they determine the overall affinity of the heavy metal cations to the soil material. The respective parameters $n_{oc,M}$ and $n_{cl,M}$ indicate that both Cd and Zn have a higher affinity to the organic carbon fraction than to the clay fraction, which reflects the often stated important role of organic carbon in Cd and Zn adsorption (Boekhold and van der Zee, 1992; Lee *et al.*, 1996; McBride *et al.*, 1997; Sauve *et al.*, 2000).

Table 6.3: Model parameters (with standard errors) and statistical characterization of the model fits

	Cd	Zn
$\log K_{MCa,0}$	-1.441 (0.088)	-2.350 (0.199)
$n_{oc,M}$	0.205 (0.022)	0.326 (0.047)
$n_{cl,M}$	-0.240 (0.026)	-0.078 (0.043)
n_M	-0.149 (0.008)	-0.230 (0.015)
n_{CaM}	0.417 (0.028)	0.268 (0.054)
$n_{H,M}$	-0.475 (0.011)	-0.540 (0.028)
[a]MSE	0.0540	0.0551
[b]Per95	0.454	0.477
[c]r^2	0.958	0.950

[a]Mean Square Error (Eq. 6.7); [b]95 percentile of deviations of modeled $\log q_M$ from experimental $\log q_M$; [c]correlation between modeled and experimental $\log q_M$.

6.4.2 Description of Cd and Zn Adsorption Isotherms

Experimental and modeled adsorption isotherms of Cd and Zn in soil materials from the fitted datasets are shown in Figure 6.2. The examples were chosen to represent a wide range in soil and solution composition and from soils where both Cd and Zn adsorption data was available. In all soil materials, similar adsorption behavior of Cd and Zn is observed. In the Riedhof soil, Cd and Zn adsorption was measured over a wide range of adsorptive concentration and at two Ca background concentrations differing by two orders of magnitude (Figures 6.2A/6.2B, Cd data from Voegelin *et al.* (2001), own unpublished Zn data). Decreasing the $CaCl_2$ concentration from 10^{-2} M to 10^{-4} M results in a strong increase in metal adsorption, which is correctly described with the exchange model. Also the bending of the adsorption isotherms towards the adsorption maximum imposed by the CEC is correctly reproduced. Comparing PRC1 and MCR1 soils (Yuan and Lavkulich, 1997), Cd and Zn exhibit a much higher adsorption affinity to PRC1 than to MCR1 (Figures 6.2C/6.2D). This can be attributed to the lower pH and lower organic carbon content of soil MCR1. The model accurately describes these differences. Also in the Kula and Alligator soil (Buchter *et al.*, 1989), which are highly different in composition, the exchange model yields a reasonable description of Cd and Zn adsorption data (Figures 6.2E and 6.2F, respectively). In the Kula soil, Cd adsorption at high solution concentrations is overestimated. From Eq. 6.8, it can be seen that at low concentration levels, i.e., unaffected by the adsorption maximum, the model yields a constant isotherm slope of n_M+1. This slope represents an average value. Cd and Zn adsorption isotherm slopes observed in different soils may be slightly larger or smaller, depending on the dominant sorbent. Therefore, modeled and experimental isotherms may intersect, and hence adsorbed amounts may be over- and underestimation in different concentration ranges of the same experimental isotherm. In addition, the CEC estimated from organic carbon content, clay content, and pH (Eq. 6.6) may not always correspond to the real CEC, and hence the effect of the CEC on the adsorbed amounts may be over- or underestimated. Despite these complications arising from the wide variability of soil materials, the examples shown in Figure 6.2 demonstrate, that based on a generalized set of parameters, the model is capable to reproduce Cd and Zn adsorption isotherms in soil materials of different composition, at variable pH and Ca solution concentration, and over wide ranges in the adsorptive cation concentration.

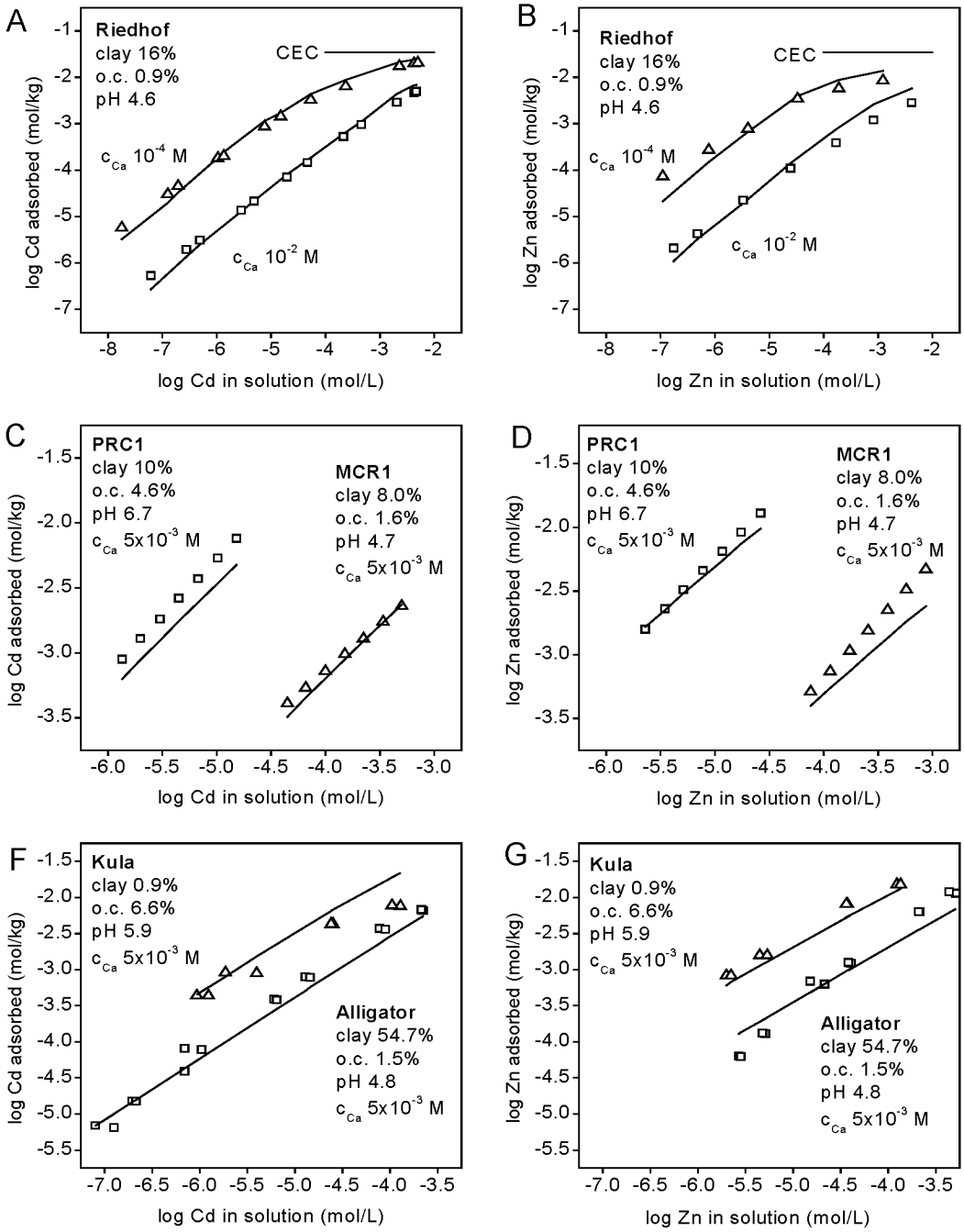

Figure 6.2: Experimental and modeled Cd and Zn adsorption isotherms in different soil materials. Cd and Zn exhibit similar adsorption behavior (symbols), which over wide ranges of conditions is correctly described with the exchange model (lines). (A/B) Riedhof: 15-25 cm, silt loam, dystric Eutrochrept, Cd data: from Voegelin *et al.* (2001), Zn data: own data (unpublished). (C/D) PRC1: 0-15 cm, fine loamy, humic Cryaquept; MCR1: 0-15 cm, fine loamy, typic Cryaquept; Cd and Zn data were recalculated from Freundlich parameters reported by Yuan and Lavkulich (1997). (E/F) Kula: Ap1 horizon, medial, isothermic typic Euthandept; Alligator: Ap horizon, very-fine, montmorillonitic, thermic vertic Haplaquept; Raw data provided by Buchter *et al.* (1989).

6.4.3 Modeling Cd Transport in an Uncontaminated Soil Material

Breakthrough and desorption of Cd (10^{-5} M) in the Riedhof soil material in 10^{-4} M $CaCl_2$ background electrolyte at two pH levels are shown in Figure 6.3. At pH 4.6, Cd elutes at ~320 pore volumes. At the higher pH of 5.7, Cd retardation increases to ~690 pore volumes. Before Cd breakthrough, Ca is released from the exchanger, resulting in normalized effluent concentrations above one. When the influent is switched back to pure Ca background electrolyte (indicated by arrows), the *unretarded normality front*

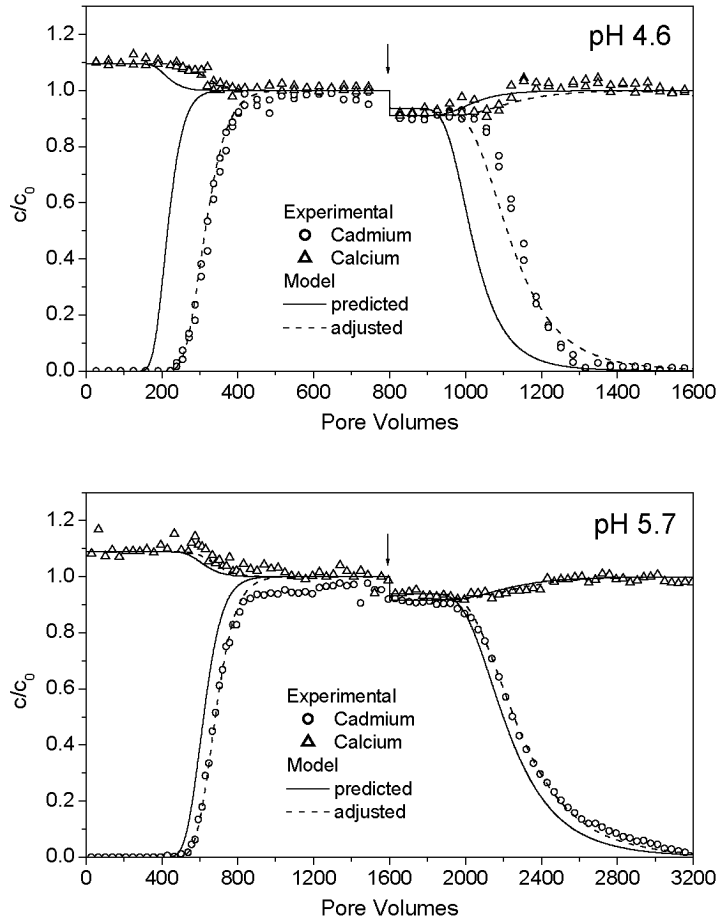

Figure 6.3: Breakthrough and desorption of Cd (~10^{-5} M $CaCl_2$) in the Riedhof soil at pH 4.6 and 5.7 in Ca background electrolyte (~10^{-4} M $CaCl_2$). Experimental data (symbols) reflect the exchange processes between Cd and Ca. One pore volume after desorption start (arrows), an unretarded normality front is observed. The exchange model based on parameters from Table 6.3 correctly reproduces the exchange patters, but slightly underestimates adsorption at pH 4.6 (solid lines). By adjusting the parameters $K_{CdCa,0}$ and $n_{H,M}$, an improved data description can be obtained (dashed lines).

(Appelo, 1994) results in a decrease of both Cd and Ca effluent concentrations. Subsequently, Ca exchanges Cd, and with the Cd desorption front, Ca in the effluent reaches influent concentration again. The exchange model correctly describes these patterns. Using the scaled exchange coefficient obtained from fitting the Cd dataset (Table 6.3), however, the model predicts a slightly lower retardation (~220 pore volumes, solid line) at pH 4.6 than observed in the experiment. On a logarithmic scale, this deviation corresponds to ~0.2 log units, which is well within the 95% confidence limits of the model (Figure 6.1). By adjusting the parameters $\log K_{CdCa,0}$ and $n_{H,M}$ to the specific soil material, an improved transport description can be obtained (dashed lines).

Transport experiments are usually interpreted on a linear time scale, which correlates to linear adsorbed amounts. Slight deviations of adsorption models derived from logarithmic data over wide concentration ranges hence may result in apparent large discrepancies in transport experiments, especially in cases with several competing cations. Modeling heavy metal cation transport in soils therefore requires adsorption models, which can correctly reproduce effluent patterns resulting from adsorption competition, and which can still easily be adjusted to specific soil materials. The exchange model based on scaled exchange coefficients fulfills both of these criteria, which is a prerequisite for its application in more complex systems.

6.4.4 Predicting Zn and Cd Release from Contaminated Soil Materials

Model calculations shown so far applied to laboratory batch and column experiments, where heavy metals in the form of soluble salts were added to soils and reacted over hours to days in order to study metal adsorption and transport behavior. One important motivation for such studies results from the need to understand metal mobility and bioavailability in contaminated soils. There, however, the situation is much more complex. Contaminants of different reactivity and persistence contain heavy metals, which are released over time and subsequently readsorb to the soil matrix. Processes such as metal diffusion into microporous solids or the formation of metal bearing precipitates may cause a gradual decrease in metal solubility with time (McBride, 1999; Axe and Anderson, 1998; Manceau *et al.*, 2000). It is therefore illustrative to see if and how an adsorption model scaled to laboratory adsorption data can be applied in such complex systems.

In general, heavy metal behavior in contaminated soils is assessed based on bulk soil composition parameters and total and extractable metal contents. Respective data for the soils Evin Wood, Worksop, and Dornach are provided in Table 6.2. The drastic decrease of the exchangeable Zn and Cd fractions from the acidic Evin Wood to the calcareous Dornach soil already indicates large differences of Zn and Cd mobility in these soils. To assess the mobilization of Zn and Cd by Ca^{2+} competition, column experiments were conducted in which the soil materials were leached with 10 mM $CaCl_2$ solution. Based on the data from 6.2, the scaled exchange model was used to predict the effluent concentration patterns from these experiments. The affinity of Zn and Cd to the soil material was described with the generalized scaled exchange coefficients (Table 6.3). The difficult point, however, is to determine the fraction of the total metal contents, that reacts as described by these exchange coefficients, i.e., the pool of adsorbed metals that interacts with Ca^{2+}. To predict metal mobilization by Ca^{2+}, it appeared reasonable to assume these pools were given by the amounts of exchangeable cations (Table 6.2). Note that in Evin Wood and Worksop soil, the CEC calculated by Eq. 6.6 is in reasonable agreement with the CEC determined from the extracted cations. Only in the calcareous Dornach soil, large amounts of extracted Ca cause a higher experimental CEC than calculated using Eq. 6.6. Finally, the exchange coefficients for the major cations Mg^{2+} and K^+ had to be defined. Based on a compilation of published exchange coefficients (Bruggenwert and Kamphorst, 1979), the exchange coefficient K_{MgCa} for Mg-Ca exchange was set to 0.7. For the heterovalent K-Ca exchange reaction, the exchange coefficient K_{KCa} was set to 100. This coefficient describes the reaction:

$$CaX_2 + 2K^+ \rightleftarrows 2KX + Ca^{2+} \tag{6.9}$$

using the Gaines-Thomas convention based on equivalent fractions (Sparks, 1995).

The results from the mobilization experiment with the acidic Evin Wood soil are shown in Figure 6.4. Model predictions based on generalized scaled exchange coefficients (Table 6.3) and adsorbed amounts of Zn and Cd determined by a 1 M NH_4NO_3 batch extract (Table 6.2) are shown as solid lines. Effluent patterns of Zn, Cd, Mg, K, and Ca are strongly coupled. With the start of 10 mM $CaCl_2$ leaching, an

unretarded normality front is observed and all effluent cation concentrations simultaneously increase. This also applies for protons. The measured pH during mobilization compares to the pH measured in batch, which was used for model predictions (Table 6.2). The effluent concentration of K rapidly decreases again and exhibits strong tailing. This behavior can be assigned to specific adsorption of K to clay minerals such as vermiculite (Sparks, 1995). When Mg is depleted on the exchanger, its effluent concentration abruptly decreases in a *sharpening front* (Appelo, 1994). This decrease is also reflected in the concentration patterns of Zn, Cd, and Ca. After Mg is exchanged, more Ca is available to desorb Zn and Cd, causing the increase of Zn and Cd effluent concentrations. However, before they reach a new plateau, also the exchangeable adsorbed amounts of Zn and Cd are depleted and concentrations start to decrease. Zn and Cd exhibit almost identical concentration curves, reflecting their similar adsorption behavior (Figure 6.2). The model prediction of Zn mobilization is excellent. Not only the approximate concentration level is correctly described, but also the small bump in the release peak caused by the coupling with Mg desorption. Note that the Zn concentration and exchanger coverage are in the same range as those of the major cations Mg and K. In the case of Cd, the model predicts a 60% lower effluent concentration than observed in the experiment. However, as in the case of Cd transport in the Riedhof soil (Figure 6.3), it is again stressed that this deviation is well within the range of the 95% confidence limits for model predictions (Figure 6.1). Mg desorption is excellently predicted. Note that the effluent patterns of Zn and Cd could not have been correctly explained or predicted if Mg exchange and desorption had been ignored. Desorption of K is not correctly predicted by the exchange model, which does not account for specific adsorption processes of K. Comparing the area below the experimental and predicted elution curves, the amount extracted by 1 M NH_4^+ appears to be larger than the amount released by 10 mM Ca^{2+}. In the case of Zn, Cd, and Mg, these amounts compare well. The effluent patterns of Ca reflect the replacement of Zn^{2+}, Cd^{2+}, Mg^{2+}, and K^+ by Ca^{2+}, and are correctly predicted.

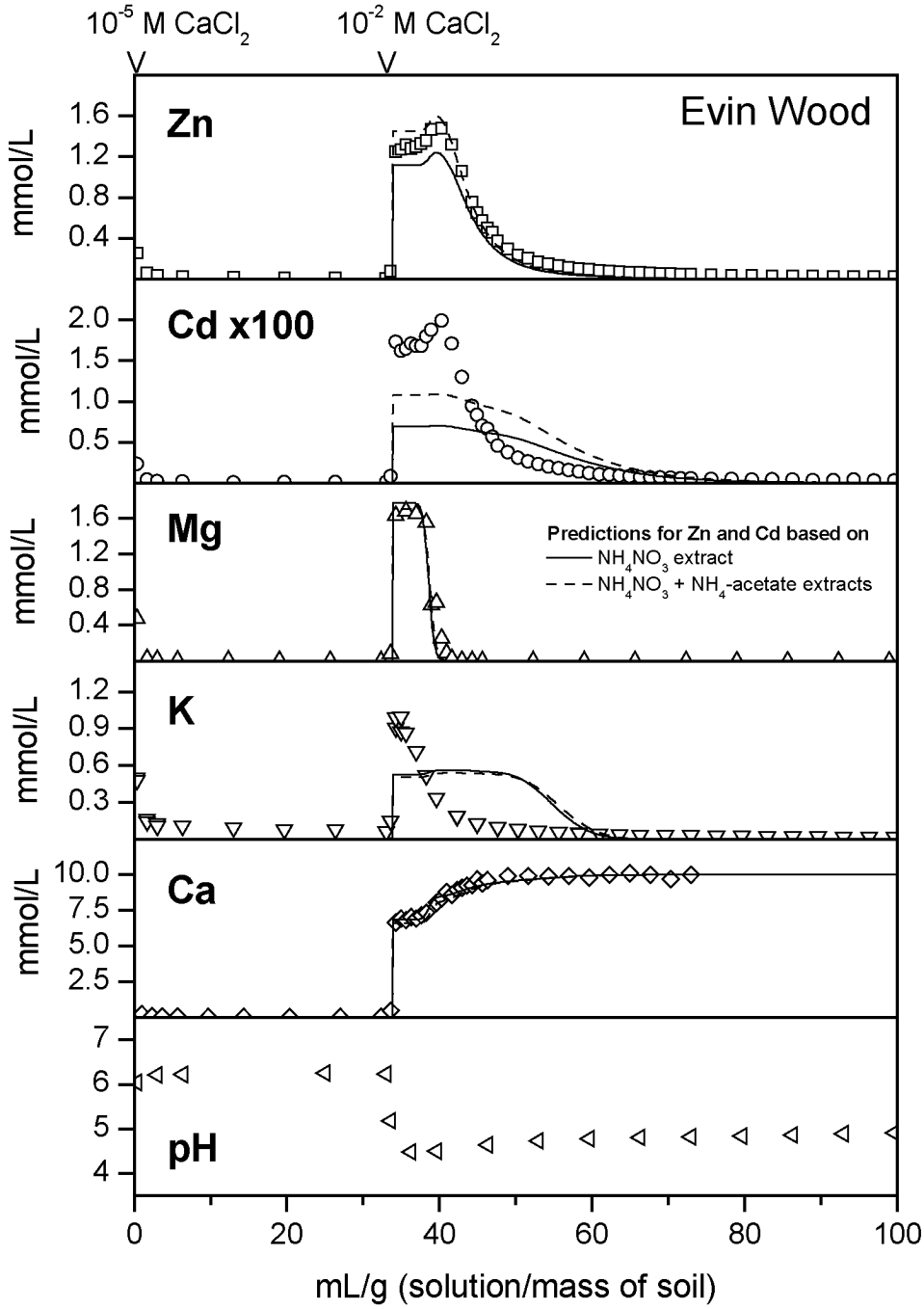

Figure 6.4: Mobilization of heavy metal and major cations from the acidic Evin Wood soil by leaching with 10 mM $CaCl_2$. Coupled exchange fronts of Zn, Cd, Mg, and Ca are observed, while K desorption exhibits a pronounced tailing. Solid lines: predictions based on generalized model (Eq. 6.5, Table 6.3) and adsorbed amounts set equal to the batch determined amounts of exchangeable cations (Table 6.2, Figure 6.7). Dashed lines: predictions with adsorbed amounts of Cd and Zn set equal to the sum of metals extracted in the first two fractions of the sequential batch extraction (Figure 6.7).

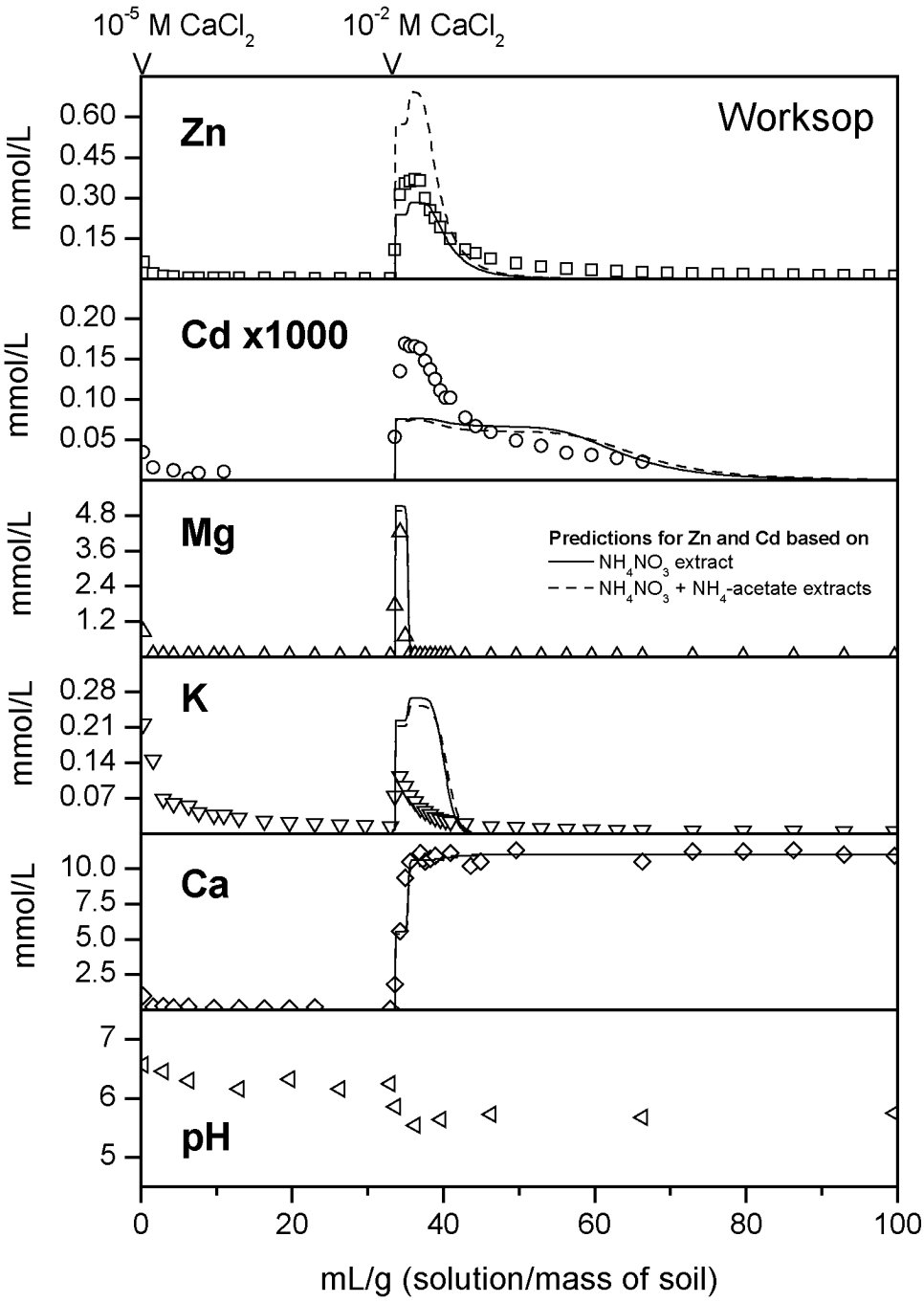

Figure 6.5: Mobilization of heavy metal and major cations from the slightly acidic Worksop soil by leaching with 11 mM $CaCl_2$. The initial desorption peaks of Zn and Cd are followed by a pronounced tailing. Solid lines: predictions based on generalized model (Eq. 6.5, Table 6.3) and adsorbed amounts set equal to the batch determined amounts of exchangeable cations (Table 6.2, Figure 6.7). Dashed lines: predictions with adsorbed amounts of Cd and Zn set equal to the sum of metals extracted in the first two fractions of the sequential batch extraction (Figure 6.7).

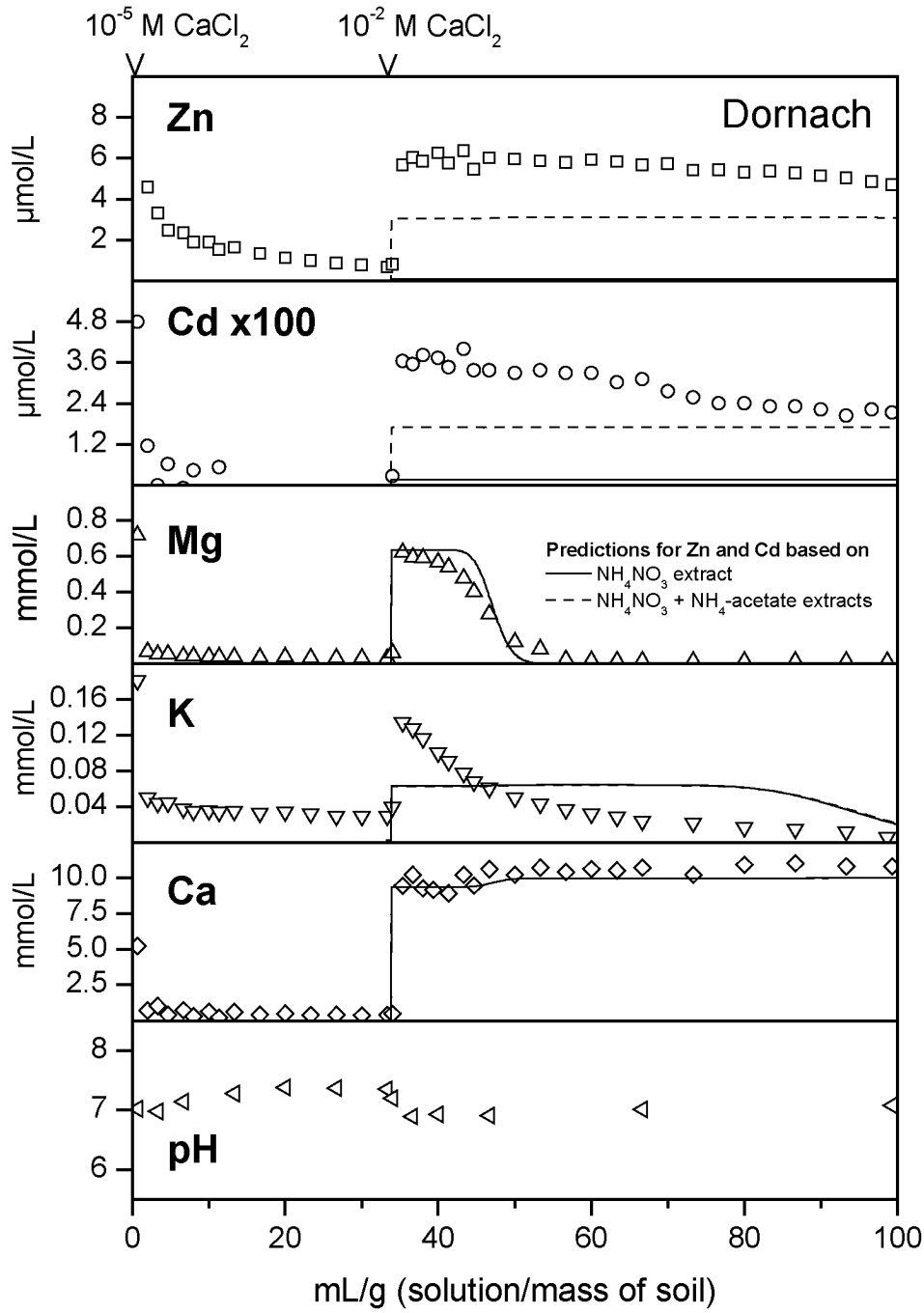

Figure 6.6: Mobilization of heavy metal and major cations from the neutral Dornach soil by leaching with 10 mM $CaCl_2$. Zn and Cd elute at very low concentration levels and their desorption curves exhibit a slow but steady decline. Solid lines: predictions based on generalized model (Eq. 6.5, Table 6.3) and adsorbed amounts set equal to the batch determined amounts of exchangeable cations (Table 6.2, Figure 6.7). Dashed lines: predictions with adsorbed amounts of Cd and Zn set equal to the sum of metals extracted in the first two fractions of the sequential batch extraction (Figure 6.7).

The results for the Worksop soil are shown in Figure 6.5. Model predictions based on scaled exchange coefficients and adsorbed amounts of Zn and Cd determined by a 1 M NH_4NO_3 batch extract are shown as solid lines. Effluent patterns can be interpreted in analogy to the Evin Wood soil. However, the Worksop soil has a rather low CEC with a high Mg coverage, and the resulting Mg elution peak is very narrow. The coupling of Zn, Cd, Mg, and Ca breakthrough is therefore less evident than in Evin Wood soil (Figure 6.4). Zn and Cd exhibit a more pronounced tailing. The model yields a correct prediction of the Mg and Ca patterns (solid lines). The peak Zn concentration is correctly predicted but not the subsequent tailing. It appears that more Zn is released than was predicted based on the exchangeable amount (Table 6.2). As in the Evin Wood soil, the effluent Cd concentration is underestimated. Note that for Cd, the initial adsorbed amount in the model had to be determined from the release experiment itself, as no batch extraction data was available. The pH measured in batch (Table 6.2), which

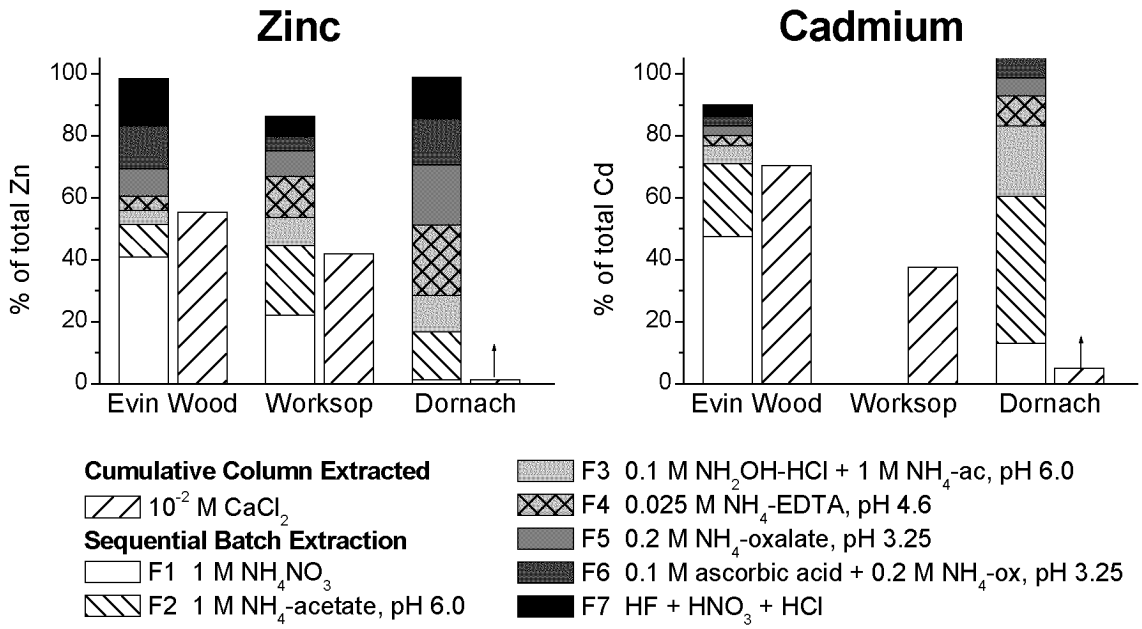

Figure 6.7: Sequential batch extraction of Zn and Cd and cumulative amounts mobilized by leaching with 10 mM $CaCl_2$. All amounts are normalized to total metal contents (Table 6.2). The fractions of Zn and Cd mobilized by Ca^{2+} decrease with increasing pH of the soil material. In the sequential batch extraction, the ratio of F2 over F1 increases with increasing pH. These differences with pH are more pronounced for Zn than for Cd.

was an input parameter to the model, compares to the column effluent pH during metal mobilization. Overall, model predictions for Zn and Cd effluent patterns in Worksop soil were not as good as in Evin Wood soil. However, the model could correctly predict the observed effluent concentration levels.

In Figure 6.6, the mobilization experiment with the calcareous Dornach soil is presented. Model predictions based on scaled exchange coefficients and adsorbed amounts of Zn and Cd determined by a 1 M NH_4NO_3 batch extract are shown as solid lines. The observed effluent patterns for Zn and Cd are clearly different to those observed in the two acidic soils. Compared to the acidic Evin Wood soil, effluent concentrations of Zn and Cd are approximately 500 to 1000 times lower. During leaching with 10 mM $CaCl_2$, the effluent concentrations of Zn and Cd slowly decrease. The Zn concentrations during column conditioning, which are caused by the removal of loose colloidal material and DOC are similar to those during the mobilization step. K release during conditioning likely results from K in colloidal particles. Because Ca dominates the exchanger, only a weak coupling with Mg can be observed. The model predictions of Zn and Cd effluent concentrations are 30 and 6 times too low, respectively (solid lines at bottom of graphs). These deviations either indicate that the scaled exchange coefficients fail to correctly describe the affinities of Zn and Cd to the Dornach soil, or that the amounts of adsorbed Zn and Cd that interact with Ca^{2+} were underestimated by the 1 M NH_4NO_3 batch extract that was used for the model prediction (Table 6.2).

In Figure 6.7, the cumulative amounts of Zn and Cd mobilized by Ca^{2+} in the leaching experiments are compared to the results from the sequential batch extraction. All data was normalized to total Zn and Cd contents (Table 6.2). The fraction of total Zn and Cd mobilized with Ca^{2+} decreases with increasing soil pH. This effect is most pronounced for Zn between the slightly acidic Worksop and the neutral Dornach soil. The fraction F1 of the sequential batch extraction represents the exchangeable cations given in Table 6.2. To predict the leaching experiments, these amounts were assumed to correspond to the fraction, which can be mobilized with Ca^{2+}. As can be seen from Figure 6.7, the validity of this assumption decreases with increasing soil pH. In the acidic soils Evin Wood and Worksop, on the other hand, it is the sum of the first two fractions of the sequential batch extraction that compare well to the Ca^{2+} leached

amounts of Zn and Cd. In the neutral Dornach soil, the sum of these two fractions is significantly larger than the amounts of Zn and Cd mobilized by Ca^{2+}. However, mobilization was not complete at the end of the experiment, and the elution patterns of Cd and Zn indicate a tailing that continues over longer times (Figure 6.6). According to Zeien and Bruemmer (1989), the fraction F1 can be interpreted as "mobile, water soluble and exchangeable", whereas F2 is considered to represent the pool of heavy metal cations that are "readily mobilizable, specifically adsorbed, $CaCO_3$ bound, or bound in weak metal organic-complexes". Such interpretations have to be considered purely hypothetical; however, they may help to rationalize the effluent patterns observed in the mobilization experiments (Figures 6.4 to 6.6). Putting it into simple terms, it may be said that the "mobile" fraction F1 causes the initial metal release peaks, whereas the "mobilizable" fraction F2 yields the subsequent tailing. In the Evin Wood soil, where the "mobile pool" F1 is much larger than the "mobilizable pool" F2, Zn and Cd release is dominated by the initial elution peak and only a relatively weak tailing is observed. In the Dornach soil, in contrast, F2 is much larger than F1, and the effluent patterns may be interpreted as a tailing without precedent pronounced release peak. In the Worksop soil, finally, where the fractions F1 and F2 are of comparable size, both an initial release peak and a subsequent tailing are observed. Based on these findings, it appears reasonable to assume, that the pool of metals which can potentially be mobilized with Ca^{2+} compares to the sum of the first two fractions of the sequential batch extraction, rather than only to the first fraction.

A second model prediction therefore was calculated where the adsorbed amounts of Zn and Cd were set equal to the sum F1+F2. All other model input parameters remained unchanged. Because the low concentration levels of K did not significantly affect the elution patterns of the other cations, no attempt was made to improve the predictions of K desorption. Resulting model predictions are plotted as dashed lines in Figures 6.4 to 6.6. In the acidic soils Evin Wood and Worksop, the recalculated model predictions were not significantly improved or deteriorated, considering the confidence limits of the exchange model (Figure 6.1). This result could be expected as F2 was not significantly larger than F1. In the Dornach soil, in contrast, where F2 is much larger than F1, a clearly improved prediction of the experimentally observed effluent concentration levels of Zn and Cd was achieved. However, while the equilibrium model

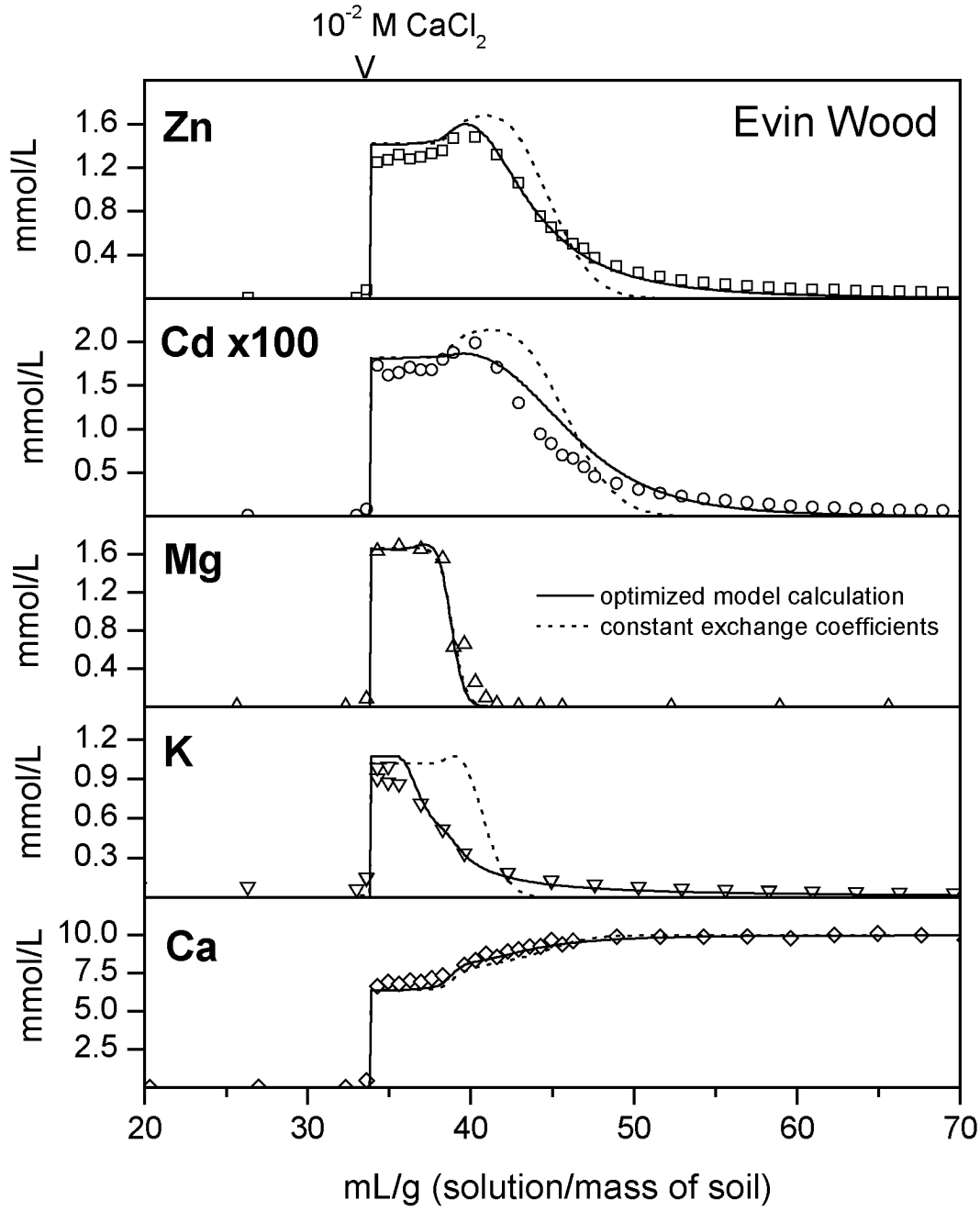

Figure 6.8: Optimized model calculation of cation release from Evin Wood soil (solid lines) using scaled exchange coefficients and comparison to a model calculation based on constant exchange coefficients (thin dashed lines). The optimized model calculation was obtained by decreasing $\log K_{CdCa,0}$ by 0.2 log units, adjusting the amount of adsorbed K, and adjusting a variable exchange coefficient K_{KCa} (Eq. 6.10) by trial-and-error. By using scaled exchange coefficients with generalized parmeters n_M, a more accurate description of the desorption tailings of Cd and Zn is attained than by using constant exchange coefficients.

predicts metal leaching at a constant concentration level, a steady decrease of effluent Zn and Cd concentrations is observed in the experiment (Figure 6.6). Also in the soil Worksop, the Zn and Cd desorption curves exhibit a clear tailing after the initial release peak. These tailings are partly caused by the high heterogeneity of the sorbent phase, but are also influenced by desorption and diffusion kinetics and the spatial heterogeneity of the soil materials. Such effects obviously can not be modeled based on the local equilibrium assumption using scaled exchange coefficients. Further parameter adjustment in order to obtain a better data description therefore would have been questionable. Nevertheless, based on bulk soil properties, on Ca^{2+} mobilizable amounts estimated from F1+F2, and on generalized model parameters, the scaled exchange model gave a reasonable prediction of the observed Zn and Cd effluent concentrations in two soil materials of highly different composition, pH, and contamination history (Table 6.2).

In contrast to soils Worksop and Dornach, desorption of Zn and Cd in Evin Wood soil is obviously dominated by fast and reversible exchange processes (Figure 6.4). Further optimization of the data modeling therefore was justified. While the Zn desorption curve was already excellently predicted, the effluent concentration of Cd was underestimated by approximately 40%. To obtain a more accurate description of Cd elution, an additional model calculation was performed, where the parameter $\log K_{CdCa,0}$ (Table 6.3) was decreased by 0.2 log units (to -1.661). In addition, the exchangeable adsorbed K was adjusted to the cumulative amount extracted by Ca^{2+} in the column experiment (7.42 mol/kg), and a variable exchange coefficient K_{KCa} was obtained by trial-and-error adjustment to the desorption curve:

$$\log K_{KCa} = -3 - 1.3 \log a_K \qquad (6.10)$$

where a_K is the activity of K^+ in solution. All other model parameters remained the same as in the prediction based on the fractions F1 and F2. The resulting model calculations together with the experimental data are shown in Figure 6.8 (solid lines). Overall, an excellent description of the coupled elution patterns of Zn, Cd, Mg, K and Cain the Evin Wood soil was attained. The example of K demonstrates that by scaling an exchange coefficient to the activity of the adsorbing cation, a more pronounced tailing is obtained

in the transport calculation. This reflects the dependence of the modeled tailing from the respective adsorption isotherm slope (Appelo, 1994). In the case of the scaled exchange coefficients for Cd and Zn, the isotherm slope is given by n_M+1. It is therefore the scaling parameter n_M, which determines the modeled desorption tailing. The lower the slope of an adsorption isotherm, i.e., the higher the heterogeneity of the sorbent material and hence the parameter n_M, the more pronounced is the tailing observed in desorption experiments. Hence, by adjusting the parameter n_M to adsorption data in a specific soil material, an improved prediction of the desorption tailing is obtained. Because further factors such as physical heterogeneity of the sorbent, diffusion processes, and reaction kinetics contribute to the observed tailing, the parameter n_M can not be determined from transport data. To demonstrate the effect of the parameters n_M on the modeled desorption curves, an additional transport calculation was carried out based on constant exchange coefficients. These were adjusted in order to obtain the same plateau concentrations after the initial normality front as obtained from the scaled exchange coefficients. The modeling results (thin dashed lines) demonstrate that by using the scaled exchange coefficients with generalized parameters n_M, a better description of the Zn and Cd desorption tailings was achieved than would have been possible with an approach based on conventional constant exchange coefficients.

6.4.5 Model Performance

With an adsorption model based on scaled exchange coefficients, Cd and Zn adsorption to a wide variety of soil materials and over a wide range of solution composition could be correctly described with a single generalized parameter set. As the model yields a charge-balanced description of heavy metal adsorption, it can also correctly reproduce chromatographic patterns observed in column heavy metal transport experiments. Effluent concentrations of Cd and Zn resulting from Ca^{2+} leaching of contaminated soil materials could correctly be predicted using the generalized model parameters and estimating the adsorbed amounts of Cd and Zn from sequential batch extraction data. In the most acidic soil material, an excellent prediction of the coupled effluent concentration patterns of Zn^{2+}, Cd^{2+}, Mg^{2+}, and Ca^{2+} was attained. In conclusion, the model presented in this study represents a promising tool for the prediction and description of heavy metal behavior in the soil environment.

References

Abd-Elfattah, A., Wada, K., *Adsorption of lead, copper, zinc, cobalt, and cadmium by soils that differ in cation-exchange materials*. Journal of Soil Science 32, 271-283, **1981**.

Alloway, B.J., ed., *Heavy Metals in Soils*. Chapman & Hall, London, **1995**.

Appelo, C.A.J., *Some calculations on multicomponent transport with cation exchange in aquifers*. Ground Water 32, 968-975, **1994**.

Axe, L., Anderson, P.R., *Intraparticle diffusion of metal contaminants in amorphous oxide minerals*. In: *Adsorption of Metals by Geomedia*. Jenne, E.A., ed., Academic Press, 427-443, **1998.**

Baeyens, B., Bradbury, M.H., *A mechanistic description of Ni and Zn sorption on Na-montmorillonite, Part I:Titration and sorption measurements*. Journal of Contaminant Hydrology 27, 199-222, **1997**.

Boekhold, A.E., Temminghoff, E.J.M., van der Zee, S.E.A.T.M., *Influence of electrolyte composition and pH on cadmium sorption by acid sandy soil*. Journal of Soil Science 44, 85-96, **1993**.

Boekhold, A.E., van der Zee, S.E.A.T.M., *A scaled sorption model validated at the column scale to predict cadmium contents in a spatially variable field soil*. Soil Science 154, 105-112, **1992**.

Borkovec, M., Bürgisser, C.S., Cernik, M., Glättli, U., Sticher, H., *Quantitive description of multi-component reactive transport in porous media: an empirical approach*. Transport in Porous Media 25, 193-204, **1996**.

Bradbury, M.H., Bayens, B., *A mechanistic description of Ni and Zn sorption on Na-montmorillonite, Part II: modelling*. Journal of Contaminant Hydrology 27, 223-248, **1996**.

Bruggenwert, M.G.M., Kamphorst, A., *Survey of experimental information on cation exchange in soil systems*. In: *Soil Chemistry B. Physico-Chemical Models*. Bolt, G.H., ed., Elsevier, Amsterdam, 141-203, **1979.**

Brümmer, G., Tiller, K.G., Herms, U., Clayton, P.M., *Adsorption-desorption and/or precipitation/dissolution processes of zinc in soils*. Geoderma 31, 337-354, **1983**.

Buchter, B., Davidoff, B., Amacher, M.C., Hinz, C., Iskandar, I.K., Selim, H.M., *Correlation of Freundlich Kd and n retention parameters with soils and elements*. Soil Science 148, 370-379, **1989**.

Christensen, T.H., *Cadmium soil sorption at low concentrations: I. Effect of time, cadmium load, pH, and calcium*. Water, Air, and Soil Pollution 21, 105-114, **1984a**.

Christensen, T.H., *Cadmium soil sorption at low concentrations: II. Reversibility, effect of changes in solute composition, and effect of soil aging*. Water, Air, and Soil Pollution 21, 115-125, **1984b**.

Christensen, T.H., *Cadmium soil sorption at low concentrations: VI. A model for zinc competition*. Water, Air, and Soil Pollution 34, 305-314, **1987**.

Christensen, T.H., Lehmann, N., Jackson, T., Holm, P.E., *Cadmium and nickel distribution coefficients for sandy aquifer materials*. Journal of Contaminant Hydrology 24, 75-84, **1996**.

Curtin, D., Rostad, H.P.W., *Cation exchange and buffer potential of Saskatchewan soils estimated from texture, organic matter and pH*. Canadian Journal of Soil Science 77, 621-626, **1997**.

Davis, J.A., Coston, D.B., Fuller, C.C., *Application of the surface complexation concept on complex mineral assemblages*. Environmental Science and Technology 32, 2820-2828, **1998**.

Dzombak, D.A., Morel, F.M.M., *Surface Complexation Modeling, Hydrous Ferric Oxide*. Wiley, New York, **1990**.

Elrashidi, M.A., O'Connor, G.A., *Influence of solution composition on sorption of zinc by soils*. Soil Science Society of America Journal 46, 1153-1158, **1982**.

Elzinga, E.J., van Grinsven, J.J.M., Swartjes, F.A., *General purpose Freundlich isotherms for cadmium, copper and zinc in soils*. European Journal of Soil Science 50, 139-149, **1999**.

Filius, A., Streck, T., Richter, J., *Cadmium sorption and desorption in limed topsoils as influenced by pH: Isotherms and simulated leaching*. Journal of Environmental Quality 27, 12-18, **1998**.

Fletcher, P., Sposito, G., *The chemical modelling of clay/electrolyte interactions for montmorillonite*. Clay Minerals 24, 375-391, **1989**.

Goldberg, S., *Use of surface complexation models in soil chemical systems*. Advances in Agronomy 47, 233-329, **1992**.

Gray, C.W., McLaren, R.G., Roberts, A.H.C., Condron, L.M., *Sorption and desorption of cadmium from some New Zealand soils: effect of pH and contact time*. Australian Jounal of Soil Research 36, 199-216, **1998**.

Gray, C.W., McLaren, R.G., Roberts, A.H.C., Condron, L.M., *Solubility, sorption and desorption of native and added cadmium in relation to properties of soils in New Zealand*. European Journal of Soil Science 50, 127-137, **1999**.

Harter, R.D., *Competitive sorption of cobalt, copper, and nickel ions by a calcium-saturated soil*. Soil Science Society of America Journal 56, 444-449, **1992**.

Helling, C.S., Chesters, G., Corey, R.B., *Contribution of organic matter and clay to soil cation-exchange capacity as affected by the pH of the saturating solution*. Soil Science Society of America Proceedings 28, 517-520, **1964**.

Hendrickson, L.L., Corey, R.B., *Effect of equilibrium metal concentrations on apparent selectivity coefficients of soil complexes*. Soil Science 131, 163-171, **1981**.

Hooda, P.S., Alloway, B.J., *Cadmium and lead sorption behaviour of selected English and Indian soils*. Geoderma 84, 121-134, **1998**.

Jenne, E.A., *Adsorption of metals by geomedia: data analysis, modeling, controlling factors, and related issues*. In: *Adsorption of Metals by Geomedia*. Jenne, E.A., ed., Academic Press, 427-443, **1998.**

Kinniburgh, D.G., van Riemsdijk, W.H., Koopal, L.K., Borkovec, M., Benedetti, M.F., Avena, M.J., *Ion binding to natural organic matter: competition, heterogeneity, stoichiometry and thermodynamic consistency*. Colloids and Surfaces A-physicochemical and engineering aspects 151, 147-166, **1999**.

Kurdi, F., Doner, H.E., *Zinc and copper sorption and interaction in soil*. Soil Science Society of America Journal 47, 873-876, **1983**.

Langmuir, D., *The power exchange function: A general model for metal adsorption onto geological materials*. In: *Adsorption From Aqueous Solutions*. Tewari, P.H., ed., Plenum Press, New york, 1-18, **1981.**

Lee, S.-Z., Allen, H.E., Huang, C.P., Sparks, D.L., Sanders, P.F., Peijnenburg, W.J.G.M., *Predicting soil-water partition coefficients for cadmium*. Environmental Science and Technology 30, 3418-3424, **1996**.

Manceau, A., Lanson, B., Schlegel, M.L., Harge, J.C., Musso, M., Eybert-Berard, L., Hazemann, J.-L., Chateigner, D., Lamble, G.M., *Quantitative Zn speciation in smelter-contaminated soils by EXAFS spectroscopy*. American Journal of Science 300, 289-343, **2000**.

Martell, A.E., Smith, R.M., *Critical Stability Constants, Vol. 5*. Plenum Press, New York, **1982**.

McBride, M., Sauvé, S., Hendershot, W., *Solubility control of Cu, Zn, Cd, and Pb in contaminated soils*. European Journal of Soil Science 48, 337-346, **1997**.

McBride, M.B., *Reactions Controlling Heavy Metal Solubility in Soils*. Advances in Soil Science 10, 1-56, **1989**.

McBride, M.B., *Environmental Chemistry of Soils*. Oxford University Press, New York, **1994**.

McBride, M.B., *Chemisorption and precipitation reactions*. In: *Handbook of Soil Science*. Sumner, M.E., ed., CRC Press, Boca Raton, B/265-B/302, **1999.**

Milne, C.J. , *Measurement and modelling of ion binding by humic substances*. PhD thesis, University of Reading, Reading, **2000.**

Parkhurst, D.L., Appelo, C.A.J., *User's guide to PHREEQC (Version 2) -- a computer program for speciation, batch-reaction, one-dimensional transport, and inverse geochemical calculations*. Rep. No. 99-4259, U.S. Geological Survey, Denver, **1999.**

Plette, A.C.C., Nederlof, M.M., Temminghoff, E.J.M., van Riemsdijk, W.H., *Bioavailability of heavy metals in terrestrial and aquatic systems: A quantitative approach*. Environmental Toxicology and Chemistry 18, 1882-1890, **1999**.

Rothmund, V., Kornfeld, G., *Der Basenaustausch im Permutit I.* Zeitschrift für anorganische und allgemeine Chemie 103, 129-163, **1918**.

SAS, *SAS System for Windows 8.01*, SAS Institute Inc., Cary, http://www.sas.com/, **1999.**

Sauve, S., Hendershot, W., Allen, H.E., *Solid-solution partitioning of metals in contaminated soils: dependence on pH, total metal burden, and organic matter*. Environmental Science and Technology 34, 1125-1131, **2000**.

Schwartz, A., Wilcke, W., Stýk, J., Zech, W., *Heavy metal release from soil in batch pHstat experiments*. Soil Science Society of America Journal 63, 290-296, **1999**.

Smith, R.M., Martell, A.E., *Critical Stability Constants, Vol. 4.* Plenum Press, New York, **1976**.

Smith, R.M., Martell, A.E., *Critical Stability Constants, Vol. 6.* Plenum Press, New York, **1989**.

Soon, Y.K., *Solubility and sorption of cadmium in soils amended with sewage sludge.* Journal of Soil Science 32, 85-95, **1981**.

Sparks, D.L., *Environmental Soil Chemistry.* Academic Press, San Diego, **1995**.

Stevenson, F.J., *Humus Chemistry - Genesis, Composition, Reactions.* John Wiley and Sons, Inc., New York, **1994**.

Streck, T., Richter, J., *Heavy metal displacement in a sandy soil at the field scale: I. Measurements and parameterization of sorption.* Journal of Environmental Quality 26, 49-56, **1997**.

Temminghoff, E.J.M., van der Zee, S.E.A.T.M., de Haan, F.A.M., *Speciation and Calcium competition effects on Cadmium sorption by sandy soils at various pH levels.* European Journal of Soil Science 46, 649-655, **1995**.

Venema, P., Hiemstra, T., van Riemsdijk, W.H., *Comparison of different site binding models for cation sorption: Description of pH dependency, salt dependency, and cation -proton exchange.* Journal of Colloid and Interface Science 181, 45-49, **1996**.

Voegelin, A., Kretzschmar, R., *Competitive sorption and transport of Cd(II) and Ni(II) in soil columns: Application of a cation exchange equilibrium model.* submitted, **2001a**.

Voegelin, A., Kretzschmar, R., *Evaluating heavy metal mobilization potential from contaminated soils using column leaching experiments.* in preparation, **2001b**.

Voegelin, A., Vulava, V.M., Kretzschmar, R., *Reaction-based model describing sorption and transport of Cd, Zn, and Ni in an acidic soil.* Environmental Science and Technology 35, 1651-1657, **2001**.

Wilkens, B.J., Brummel, N., Loch, J.P.G., *Influence of pH and zinc concentration on cadmium sorption in acidic, sandy soils.* Water, Air, and Soil Pollution 101, 349-362, **1998**.

Yuan, G., Lavkulich, L.M., *Sorption behavior of copper, zinc, and cadmium in response to simulated changes in soil properties.* Communications in Soil Science and Plant Analysis 28, 571-587, **1997**.

Zachara, J.M., Smith, S.C., McKinley, J.P., Resch, C.T., *Cadmium sorption on specimen and soil smectites in sodium and calcium electrolytes.* Soil Science Society of America Journal 57, 1491-1501, **1993**.

Zachara, J.M., Westall, J.C., *Chemical modeling of ion adsorption in soils.* In: *Soil Physical Chemistry.* Sparks, D.L., ed., CRC Press, Boca Raton, 47-95, **1998.**

Zeien, H., Bruemmer, G.W., *Chemische Extraktion zur Bestimmung von Schwermetallbindungsformen in Boeden.* Mitteilungen der Deutschen Bodenkundlichen Gesellschaft 59/I, 505-510, **1989**.

CONCLUSIONS

This work was concerned with the reactivity of heavy metal cations in soil materials, and adsorption models were developed to describe adsorption in these systems.

Regarding the reactivity of heavy metal cations in soils, this work was focussed on Cd^{2+} and Zn^{2+}, which compared to strongly adsorbing cations such as Pb^{2+} and Cu^{2+}, are considered to be rather mobile in the soil environment. The results from adsorption and transport experiments in uncontaminated soil materials indicate similar adsorption behavior for both Cd and Zn (Chapters 3 and 6). However, in column experiments on Cd and Zn retention in a soil material at slightly acidic pH (6.4), Zn in addition to being adsorbed was also slowly incorporated into a newly forming solid phase. Cd retention, in contrast, was still dominated by fast and reversible adsorption reactions. No significant precipitation of Cd was observed. These findings compare to the results from the release experiments with contaminated soil materials (Chapter 5). While Cd and Zn exhibited similar desorption behavior in the acidic Evin Wood soil, the higher pH of the limed Evin Field soil, which was contaminated from the same source, lead to a much more drastic decrease in the mobility of Zn as compared to Cd, which could be due to the formation of Zn bearing solid phases. Liming of soils hence might effectively immobilize Zn by promoting the formation of Zn bearing precipitates, whereas in the case of Cd, mainly the adsorption affinity will be increased. However, once liming is stopped or if arable land is reforested, soil acidification processes will continue. Assuming that Cd is predominantly retained by adsorption, it will mainly be desorption processes that control its remobilization, and therefore require more detailed investigation. In the case of Zn, depending on the extent of precipitate formation, both desorption of adsorbed Zn and dissolution of Zn bearing precipitates will determine its fate. The leaching experiments indicate that such phases might readily dissolve at lower pH (Chapters 4 and 5). However, further studies are required to assess the formation of Zn (and Ni) bearing precipitates and their long-term stability. The combination of column studies with X-ray absorption spectroscopy applied in this work (Chapter 4) proved to be useful to study such processes in soil materials, as it allows to relate the

macroscopically observed metal reactivity with the spectroscopically determined binding mechanism.

To describe the adsorption and transport of the major cations Ca^{2+}, Mg^{2+}, and Na^{+} in the Riedhof soil material, a one-site exchange model was found to be appropriate (Chapter 1). On this basis, a reaction-based model describing Cd^{2+} and Zn^{2+} adsorption to the same soil material was developed (Chapter 3). To account for specific adsorption reactions of Cd^{2+} and Zn^{2+}, a second type of sorption sites was introduced. This combined cation exchange-specific adsorption model proved capable of describing Cd and Zn adsorption to the Riedhof soil material over wide ranges of solution composition. However, to generalize this model to a wide range of soil materials is difficult, as specific sorption sites may be located on a variety of sorbent phases. Therefore, parameter adjustment is required to obtain a correct description metal adsorption in other soil materials. For model application to contaminated soil materials, this would mean that model parameters for the respective soil material and the fractions of the total metal contents, that can be attributed to exchange and specific sorption sites would have to be determined simultaneously. This, however, is in most cases not feasible. In order to obtain an adsorption model that can easily be adjusted to data from contaminated soil materials, a different approach was therefore chosen (Chapter 6). To account for the variability of apparent exchange coefficients with soil and solution composition, scaled exchange coefficients were introduced. Generalized model parameters were obtained by calibration to a wide set of Cd and Zn adsorption data compiled from the literature. The approach was shown to correctly reproduce the main features of Cd and Zn adsorption and transport data, and could also be applied to contaminated soil materials.

Empirical models of cation sorption in soils necessarily represent a compromise between a chemically realistic process description and what is feasible based on the usually available information and the heterogeneity of soils. Studies on metal behavior in idealized model systems help to identify and characterize fundamental sorption reactions. More research, however, is also required to show how knowledge obtained from such model systems can conceptually and quantitatively be applied to soil materials and finally to soils.

ACKNOWLEDGEMENTS

I am deeply indebted to Professor Ruben Kretzschmar who supervised this work with sustained and constructive support. I greatly enjoyed the stimulating and motivating atmosphere he created.

I am indebted to Professor Willem H. van Riemsdijk and Professor Rainer Schulin for taking on the co-examiners position.

I want to thank all members of the FAMEST project for their hospitality during our meetings and for stimulating discussions and namely David G. Kinniburgh for coordinating the EU project.

I gratefully acknowledge the Swiss Ministry of Science and Education for financial support.

I thank Bernhard Buchter for providing his experimental raw data.

I am grateful to Vijay M. Vulava who provided an extensive set of experimental data that were the initial basis of my modeling efforts.

I am very grateful to Kurt Barmettler for helping with numerous experiments and for tips and tricks regarding laboratory practice.

I would like to thank Andreas C. Scheinost for conducting XAS analysis and Karin Bühlmann for the good experimental work during her diploma thesis.

I want to thank Florian Kuhnen for calculating some of the transport experiments and for helping with computer problems.

Furthermore, I would like to thank all members of the soil chemistry group and colleagues at the institute. This work would not have been possible without their support. Special thanks to: Charlotte Wüstholz for keeping the group running and for minimizing paperwork. Achim Kayser for helping with the review and for patiently answering all my questions. Annette Hofmann and Stephan Kraemer for reviewing parts of my thesis. Heike Leyer for putting up with me in our office during the last few months. Christoph Jung for mountaineering shop talk during coffee breaks.

Last but not least, I want to thank my family for their great support and all my friends outside the institute with whom I shared many good and bad times.

Andreas Voegelin, February 2001

CURRICULUM VITAE

Andreas Voegelin
born on June 10, 1971 in Niederdorf (BL), Switzerland
citizen of Reigoldswil (BL)

1978-1983	Primary School in Niederdorf.
1983-1987	Secondary School in Oberdorf.
1987-1990	Gymnasium in Liestal. *Matura Type B*
1991-1997	Studies of Environmental Natural Sciences at the Swiss Federal Institute of Technology (ETH) Zürich. Specialization in Environmental Chemistry and Terrestrial Ecosystems. Diploma thesis under guidance of Prof. R. P. Schwarzenbach. *Dipl. Natw. ETH*
1997	Research assistant at the Swiss Federal Institute for Environmental Science and Technology (EAWAG), Dübendorf.
1998-2001	Ph.D. studies at the Institute of Terrestrial Ecology, Soil Chemistry Group of Prof. R. Kretzschmar, Swiss Federal Institute of Technology (ETH) Zürich.